A MULTILEVEL STUDY OF DRIVING BEHAVIOR AND SYSTEM PERFORMANCE- HARNESSING LARGE-SCALE NATURALISTIC DRIVING AND CONVENTIONAL SAFETY DATA

A Dissertation Presented for the

Doctor of Philosophy

Degree

The University of Tennessee, Knoxville

Amin Mohammadnazar

December 2021

This dissertation is dedicated to my parents, brothers, and beloved family who constantly encouraged me to pursue my dreams and finish my dissertation

ACKNOWLEDGMENTS

I would like to thank everyone who has directly or indirectly supported, encouraged, and guided me in my quest for knowledge. I wish to express my deep appreciation to Dr. Asad J. Khattak whose valuable insight and knowledge steered me through this research. It has been my honor working under his supervision and I will always be proud of my association with him. A debt of gratitude is extended to my dissertation committee, Dr. Candace Brakewood, Dr. Anahita Khojandi, and Dr. Haileab Hilafu. I am honored to have their tremendous guidance, help, and support in my dissertation. Also, special thanks to Dr. Russell Zaretzki for supervising my M.S. statistics degree.

To my co-authors, Dr. Asad J. Khattak, Dr. Ramin Arvin, Dr. Iman Mahdinia, Dr. Nima Hoseinzadeh, Dr. Numan Ahmad, Dr. Zulqarnain H. Khattak, Dr. Jun Liu, Dr. Candace Brakewood, and Dr. Lee Han, thank you for your valuable knowledge and insights in my research. I also want to thank all my lab mates for their continuous support and memorable experiences. Special thanks to the Department of Civil and Environmental Engineering faculty and staff. My work has been greatly supported through the Tennessee Department of Transportation, Collaborative Sciences Center for Road Safety, and the US Department of Transportation.

My acknowledgment would be incomplete without thanking my parents and family for their valuable supports and precious love for supporting me throughout these years. My Family's involvement, concern, forbearing, and understanding have been the prime support for me throughout these years and without their help, I could not reach this stage in my life.

ABSTRACT

The performance of a transportation system highly depends on the drivers' behavior because driving behavior is one of the main causes of traffic accidents and one of the key factors in fuel consumption and vehicle emissions studies. Specifically, the focus of this dissertation is on aggressive driving who not only put their selves and others at risk but also contribute more to greenhouse gas emissions. Recently, the development of advanced sensors, connected vehicles (CVs), location-based services (LBS) provided unprecedented access to new high-resolution microscopic-level data which can be used to evaluate and monitor instantaneous driving behavior and safety performance of different road types and facilities in a spatio-temporal domain. Therefore, the main objective of this study is to develop a framework to harness the new large-scale data to proactively detect aggressive drivers in different roadways and neighborhoods and investigate the impact of aggressive driving on crash frequency, crash severity, and fuel consumption and emissions. In this study, the concept of "driving volatility" which is a surrogate safety measure of unsafe and aggressive driving behavior is used. As a rigorous measure of micro-driving behavior, driving volatility shows the degree of deviation from the norm which can help us to predict driving behavior in the short term. This dissertation explores driving aggressiveness and transportation system performance at different levels: 1) Driver level; 2) Location level; 3) Roadway level; 4) Network level. In summary, the main contribution of this dissertation is to evaluate transportation system performance in correlation with driving behavior at different levels by harnessing big data from real-world driving conditions and integrating them with conventional data. This dissertation includes a variety of topics such as crash frequency/severity analysis, driving

style classification, fuel consumption, and emission. The findings of this study provide new insight into the field of transportation at different levels. The methodology of this study can be used for monitoring driving behavior and detecting risky drivers on different roadways. This study also helps the practitioners to identify critical locations and facilities with high risky driving behaviors, fuel consumption, and emission for safety and fuel efficiency improvements.

TABLE OF CONTENTS

LIST OF TABLES

LIST OF FIGURES

CHAPTER 1 : INTRODUCTION

SUMMARY

Driving behavior is one of the most important factors in transportation system performance that is measured through road safety, crash frequency/severity analysis, network monitoring, energy consumption, and vehicle emissions. However, due to the complexity of driving behavior and lack of naturalistic driving data, driving behavior has not been sufficiently studied in the literature, and instead, researchers are more focused on infrastructure and vehicle factors. However, the development of advanced sensors, connected vehicles (CVs), location-based services (LBS), video and radar surveillance provides unprecedented access to new high-resolution microscopic-level data on driver's location, maneuver, speed, travel time, and crash/near-crash events in real-world driving conditions. Such reach data enable us to evaluate and monitor instantaneous driving behavior and safety performance of different road types and facilities in a spatio-temporal domain. Therefore, the main question is how we can harness the emerging data to improve our understanding of driving behavior which is the key to implementing transportation improvement strategies. Specifically, this study focuses on aggressive drivers who not only put their selves and others at risk but also contribute more to greenhouse gas emissions. Aggressive driving refers to any behavior that can increase the risk of collision. Some of these behaviors include:

- Speeding (exceeding the speed limit)
- Tailgating (following too closely behind another vehicle)
- Sudden and abrupt lane changing
- Running stop signs and red lights
- Passing on the right of another vehicle

- Weaving in traffic (moving from one lane to another repeatedly)

Hence, this dissertation aims to propose a framework to harness the new large-scale data to comprehensively study driving behavior with a focus on aggressive drivers under naturalistic driving conditions in different road types and facilities. Specifically, this dissertation creates a unique database by assembling and combining big data generated by connected and automated vehicles (CAVs), Naturalistic Driving Study (NDS) data, and conventional traffic and crash data. Rigorous statistical techniques such as Geographically and Temporally weighted regressions, Bayesian Conditional Autoregressive models, and machine learning methods are utilized in order to extract useful information from the data to better understand the driving behavior in naturalistic and connected vehicles environments.

One of the innovative ideas explored in the dissertation is the concept of "driving volatility" which is a surrogate safety measure of unsafe and aggressive driving behavior. As a rigorous measure of micro-driving behavior, driving volatility shows the degree of deviation from the norm. Therefore, higher driving volatilities indicate higher fluctuation in speed, acceleration, deceleration in both the lateral and longitudinal directions, and as a result, higher driver instability. Driving volatility helps us to predict what drivers will do in the short term. Especially, this dissertation employs the concept of "temporal driving volatility" which captures alterations in instantaneous driving behavior by creating a time-series stream of data at the driver level. This provides us with the opportunity to capture driving behavior as a time-dependent variable.

This dissertation aims to explore driving behavior and system performance at different levels of transportation systems: (1) Driver level; (2) Location level; (3) Roadway level; (4) Network level. Figure 1-1 shows the hierarchy of these levels and how they are going to be evaluated in this dissertation. At the **driver level**, this study tracks individual drivers to evaluate differences in their driving styles on different roadways. One advantage of this approach is detecting risky drivers who continuously drive aggressively during the observation period or drivers who always drive calmly. Also, a driving score is proposed to assess drivers' performance on different roadways. It can have an application in Driving Assistance Systems (DAS) for monitoring driving behavior and giving feedback about their driving performance. Furthermore, the study evaluates the effects of truck drivers' physical condition and driving errors on the injury severity of fixed-object large truck crashes. At the **location level,** this study analyzes emissions and fuel consumption of vehicles within work zones and curves which are critical scenarios in transportation systems since they cause flow disruption and create significant variation in vehicle operation. Using the naturalistic driving data, the Vehicle Specific Power (VSP) model and Autonomie model are used to compare emissions and fuel consumption of drivers with different driving styles at these locations. At the **roadway level**, the study uses the CAV data to investigate how the perception of an aggressive, normal, and calm driving style varies across different road types. Also, the proportion and distribution of different driving styles on different roadways are investigated in order to see how frequent risky driving behaviors are on different roadways. Crash frequency of rural multilane highways is another topic investigated at the roadway level. A rigorous methodological framework is applied to incorporate spatio-temporal instability of road crashes by allowing the effects of explanatory variables to vary across space and time.

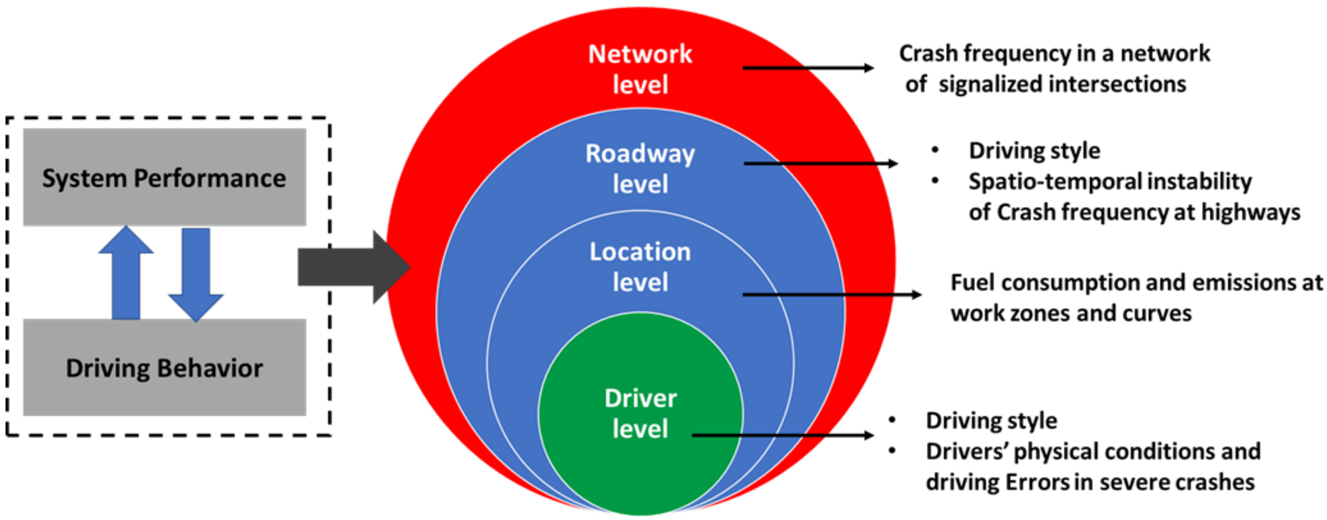

Figure 1-1 Hierarchy of different levels of system performance in association with drivers' behavior in the system

The Geographically and Temporally Weighted Negative Binomial Regression (GTWNBR) model is used to investigate the variation of Safety performance functions (SPF) parameters on divided multilane rural highways across space and time simultaneously. At the **network level**, the dissertation incorporates driving behavior factors in the estimation of SPFs using temporal volatility measures. To this aim, the CAV data from the Safety Pilot Model Deployment study are combined with traditional data (e.g. roadway geometry, traffic volume) to predict crash frequency in a network of four-leg signalized intersections in Ann Arbor, MI. Figure 1-2 presents the infographic of the data collection process and contents provided in different chapters of the dissertation. In summary, the main contribution of this dissertation is to evaluate driving behavior at different levels by harnessing big data from real-world driving conditions and integrating them with conventional data. This dissertation includes a variety of topics such as crash frequency/severity analysis, driving style classification, fuel consumption, and emission. The findings of this study provide new insight into the field of transportation at different levels. This study helps the researchers and practitioners follow the spatio-temporal trend of critical safety factors, locations, and facilities with high risky driving behaviors, fuel consumption, and emission to identify sites and roadways for safety and fuel efficiency improvements. Also, the methodology of this study can be used for monitoring driving behavior and detecting risky drivers on different roadways.

Figure 1-3 shows the outline of the proposal. The main objective of the study is to develop a framework to harness new large-scale data to evaluate driving behavior under a naturalistic driving behavior in different levels of the transportation system.

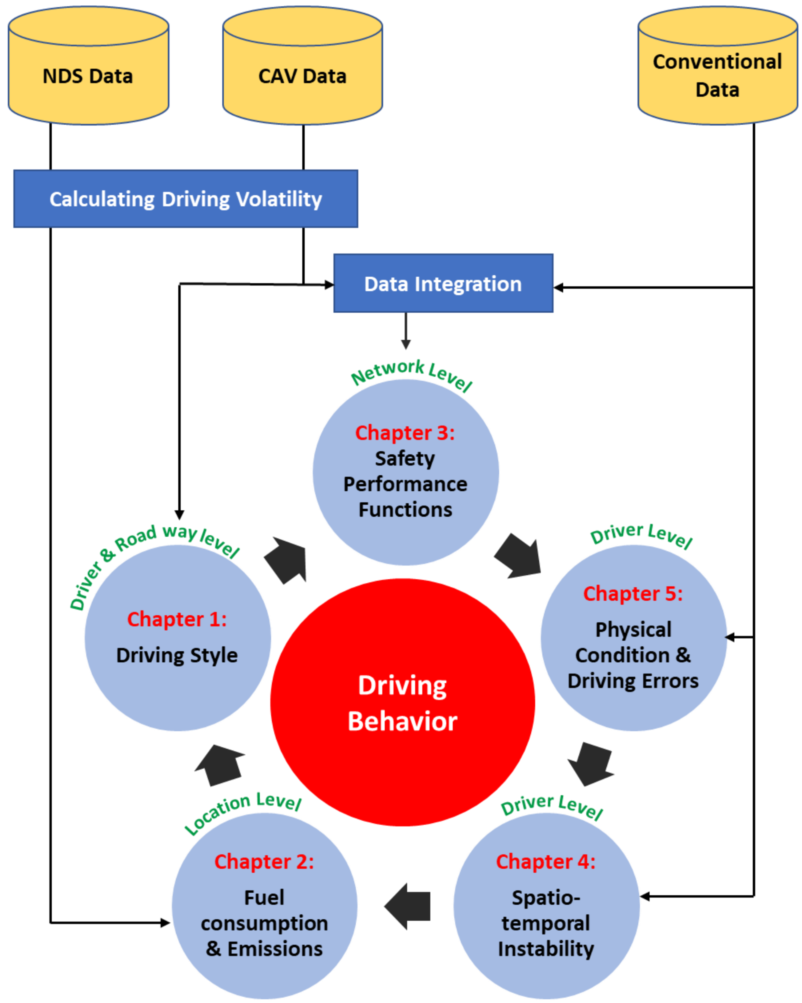

Figure 1-2 Info-graphic of the data collection and different levels of driving behavior analysis

It is expected that under this dissertation, at least 5 papers in top transportation journals be published:

1. Mohammadnazar, A., Arvin, R., & Khattak, A. J. (2021), *Classifying travelers' driving style using basic safety messages generated by connected vehicles: application of unsupervised machine learning.*
    - Journal article: Published in *Transportation Research Part C: Emerging Technologies.*
    - Peer-review conference paper: Presented at the 99th Transportation Research Board Annual Meeting 2020, Washington DC.
2. Mohammadnazar, A., Khattak, Z. H., & Khattak, A. J. *Analyzing the impact of instantaneous driving in work zones and curves on emissions and fuel efficiency using naturalistic driving data.* Accepted for presentation at the 101th Transportation Research Board Annual Meeting 2022, Washington DC.
3. Mohammadnazar, A., Arvin, R., & Khattak, A. J. (2021). *Incorporating Driving Volatility Measures in the Development of Safety Performance Functions for Intersections: Application of Bayesian Conditional Autoregressive Models.* Accepted for presentation at the 101th Transportation Research Board Annual Meeting.
4. Mohammadnazar, A., Mahdinia, I., Ahmad, N., Liu, J., & Khattak, A. J. (2021). *Understanding How Relationships Between Crash Frequency and Correlates Vary for Multilane Rural Highways: Estimating Geographically and Temporally Weighted Regression Models.*
    - Journal article: Published in the journal of *Accident Analysis & Prevention*

- Peer-review conference paper: Presented at the 99th Transportation Research Board Annual Meeting 2020, Washington DC.

5. Mohammadnazar, A., Mahdinia, I., Arvin, R., & Khattak, A. J. (2021). *How are physical conditions and driving errors of commercial large truck drivers associated with injury severity in fixed-object collisions?*
    - Under review in the *Journal of Transportation Safety & Security*
    - Peer-review conference paper: Presented at the 100th Transportation

To this end, a unique database is created by integrating emerging data sources such as CAV data (with more than 2.2 billion seconds of observations) and naturalistic driving data (with more than 2 million seconds of observations), with conventional data such as crash, traffic, and roadway inventory. After applying pre-processing techniques, driving volatility measures are calculated to capture instability in driving. These measures are utilized to analyze driving behavior at different levels. In terms of methodological approach, innovative and rigorous statistical methods such as GTWNBR model and Bayesian Conditional Autoregressive models along with machine learning methods such as clustering methods are utilized in order to extract useful information from the data.

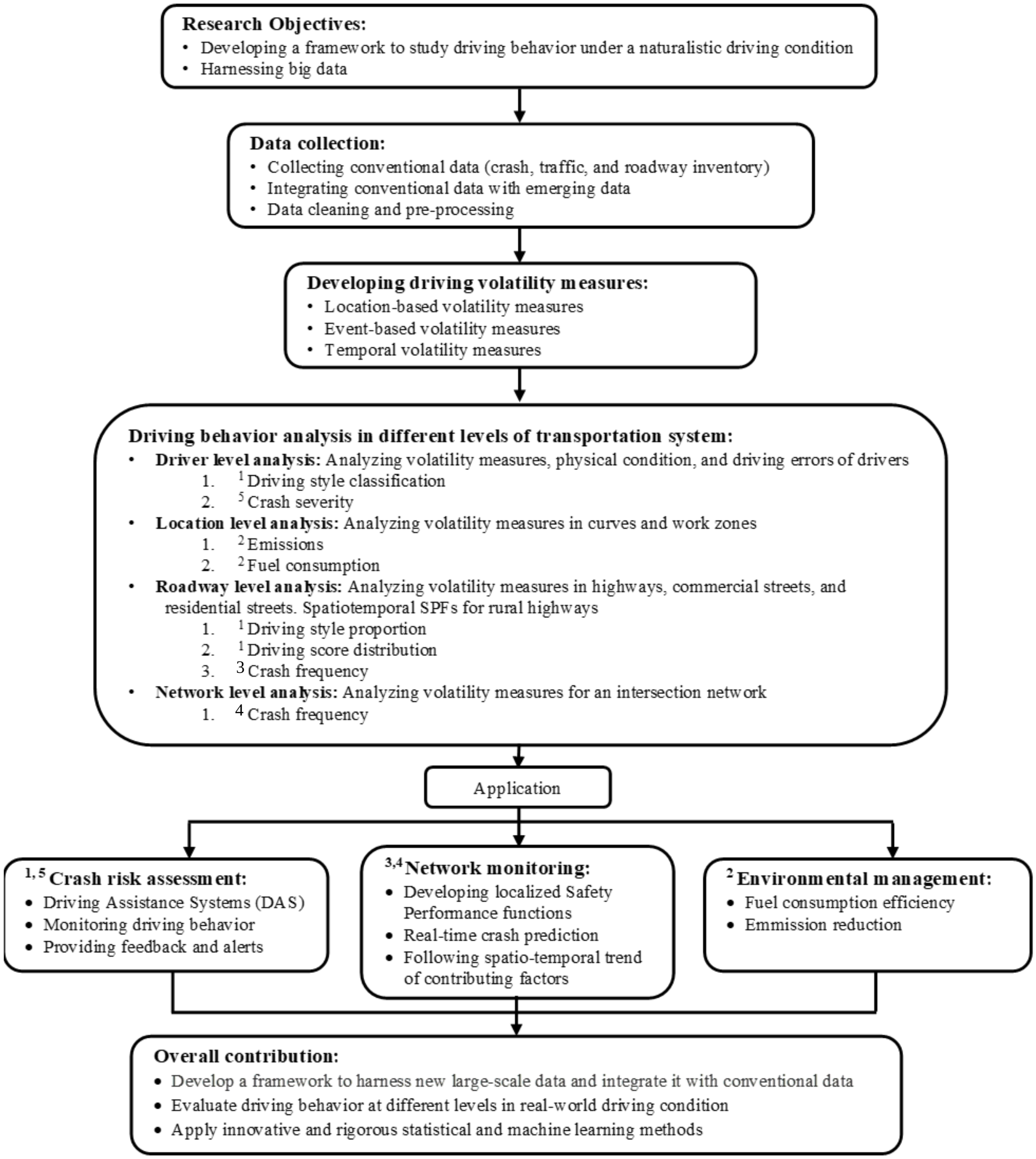

Figure 1-3 Outline of the proposal

Note:
[1] Chapter 1: Relevant paper published in *Transportation Research Part C: Emerging Technology*
[2] Chapter 2: Relevant paper accepted for presentation at the 101th Transportation Research Board Annual Meeting 2022, Washington DC.
[4] Chapter 3: Relevant paper accepted for presentation at the 101th Transportation Research Board Annual Meeting 2022, Washington DC.
[3] Chapter 4: Relevant paper published in the journal of *Accident Analysis & Prevention*
[5] Chapter 5: Relevant paper under review in the *Journal of Transportation Safety & Security*

CHAPTER 2 : CLASSIFYING TRAVELERS' DRIVING STYLE USING BASIC SAFETY MESSAGES GENERATED BY CONNECTED VEHICLES

A version of this chapter is published in the journal of *Transportation research part C: emerging technologies.*

> Mohammadnazar, A., Arvin, R., & Khattak, A. J. (2021). Classifying travelers' driving style using basic safety messages generated by connected vehicles: Application of unsupervised machine learning. Transportation research part C: emerging technologies, 122, 102917.

ABSTRACT

Driving style can substantially impact mobility, safety, energy consumption, and vehicle emissions. While a range of methods has been used in the past for driving style classification, the emergence of connected vehicles equipped with communication devices provides a new opportunity to classify driving style using high-resolution (10 hertz) microscopic real-world data. In this study, location-based big data and machine learning are used to classify driving styles ranging from aggressive to calm. This classification can be used to customize driver assistance systems, assess mobility, crash risk, fuel consumption, and emissions. This study's main objective is to develop a framework that harnesses Basic Safety Messages (BSMs) generated by connected vehicles to quantify instantaneous driving behavior and classify driving styles in different spatial contexts using unsupervised machine learning methods. To this end, a subset of the Safety Pilot Model Deployment (SPMD) with more than 27 million BSM observations generated by more than 1300 individuals making trips on diverse roadways and through several neighborhoods in Ann Arbor, Michigan, were processed and analyzed. To

quantify driving style, the concept of temporal driving volatility, as a surrogate safety measure of unsafe driving behavior, was utilized and applied to vehicle kinematics, i.e., observed speeds and longitudinal/lateral accelerations. Specifically, six volatility measures are extracted and used for classifying drivers. K-means and K-medoids methods are applied for grouping drivers in aggressive, normal, and calm clusters. Clustering results indicate that not only does driving style vary among drivers, but the thresholds for aggressive and calm driving vary across different roadway types due to variations in environment and road conditions. The proportion of aggressive driving styles was also higher on commercial streets than on highways and residential streets. Notably, we propose a Driving Score to measure driving performance consistently across drivers.

INTRODUCTION

Driving behavior is a broad concept that can be a function of a considerable number of variables and factors including driving performance, environmental awareness, willingness to take risks, and reasoning abilities. Due to the large number of variables that influence driving behavior, it can be difficult to numerically analyze it. Therefore, although drivers develop their distinct driving habits (*1*), previous studies found similarities in driving styles of drivers which enabled the authors to classify drivers into distinct groups (*2-6*). Driving style is a personal way of driving that can be either habitual or an act of instantaneous preference. The data used for driving style recognition can be obtained either from questionnaires (*7-10*) or traceable driving information including position, speed, and acceleration of vehicles (*2; 4; 6; 11*). Driving style recognition could be a very useful application in several different fields. For example, Driver Assistance Systems (DAS) can be programmed to detect different driving behavior in real-time and provide feedback to the drivers, even warning them of risks on the roadway (*12*). Furthermore, insurance companies are interested in adopting DAS as a way to profile drivers and offer attractive insurance premiums to their clientele. Driving style classification can also be adapted for fuel consumption (*13*), energy efficiency (*14; 15*), and emission reduction (*16*).

The development of connected vehicles (CVs) and location-based services (LBS) provide unprecedented access to information about a driver's maneuvers, steering status, location, and heading in real-world driving conditions (*17; 18*). LBS data are categorized into two major groups based on their location acquisition mechanism: 1) data collection via user-end hardware, e.g. smartphones and GPS receivers; 2) data collection via onboard sensors and vehicle-to-infrastructure (V2I) communication, e.g. connected vehicles (*19*). Such rich data that are available from advanced sensors capable of sending and receiving Basic Safety Messages (BSMs) is ideal for monitoring traffic conditions and driver behavior.

This study explores variations in driving styles under different roadway contexts using connected vehicle data. Driving styles can vary across different road types, as aggressive driving styles on highways could be perceived as normal behavior on commercial streets and vice versa. To this end, three road types (highways, commercial streets, and residential streets) are considered to be representatives of road types where driving style can be inherently different based on roadway context, and individual driving styles are evaluated separately in these types.

LITERATURE REVIEW

Driving style refers to the way drivers choose to drive as an act of instantaneous preference or habitual act. Driving style is reflected in drivers' actions, decisions, and maneuvers (*1; 20*). Generally, studies about driving style can be categorized into two major groups: survey studies and studies based on vehicle motion information. In the former group, driving style is determined based on self-reported driving behavior which can be obtained through questionnaires. These studies investigate the relation between driving style and driving behavior and personality of drivers (*7-10*). The latter group of studies, including this study, uses the motion information of vehicles to classify driving styles of drivers. These studies usually classify driving style into three categories: Aggressive style, Normal style, and Calm (conservative) style (*2; 4; 6; 11; 21-24*). Among them, particular attention has been devoted to aggressive driving styles as unsafe driving behavior that increases collision risk. For example, a study carried out by the American Automobile Association Foundation for Traffic Safety revealed that aggressive driving was associated with 56 percent of fatal crashes in the United States (*25*). An aggressive driving style is generally associated with higher speeds, sudden acceleration and deceleration, abrupt changes in vehicle steering wheel angle, and harsh lateral and longitudinal maneuvers (*5; 11; 26; 27*), whereas a calm driving style is associated with relatively lower speeds, gradual acceleration, and deceleration, smooth lateral and longitudinal maneuvers, and mild changes in a vehicle steering wheel (*11; 26*). A moderate or normal driving style is positioned between these two styles (*5; 11; 27*).

A diverse range of methods and algorithms have been used to classify different driving styles. Generally, these methods can be categorized into two groups: machine learning-based methods and rule-based methods. In rule-based methods, a set of rules are defined for different driving features to detect different driving styles. Several studies used fuzzy logic as a rule-based method for driving style detection (*5; 6; 26; 28-30*), namely in (*6*), where an online system using fuzzy logic detected driver styles in real-time. Machine learning methods used in the literature include both supervised and unsupervised methods. The Artificial Neural Network (ANN), the Support Vector Machine (SVM), and the Random Forest Decision method are among the most commonly applied methods in driving style classification. MacAdam et al. (*31*) used ANN to analyze the aggressiveness levels of 36 drivers by measuring their preference for passing, chasing, or being passed by other vehicles. They found that younger drivers usually drive more aggressively than middle-aged and older drivers. In another study, Brombacher et al. (*3*) used ANN to classify and score driving styles based on lateral and longitudinal maneuvers. They categorized driving styles into “very sporty”, “sporty”, “normal”, “defensive”, and “very defensive” with an accuracy of 81 percent. Wang et al. (*27*) used a semi-supervised approach for driving style classification integrating the K-means method with the SVM method. After labeling the driving data of 20 drivers using the K-means method, they applied the SVM method to classify driving styles into aggressive and normal styles. Their results showed that this method could improve the accuracy of classification by 10 percent (*27*). Li et al. (*32*) considered the transition between different maneuvers as a measure of driving style. They used a Random Forest Decision technique to classify driving behavior into low, moderate, and high-risk styles. The authors found that maneuver transition probabilities are more accurate measures than maneuver frequencies for driving style classification. Combining different machine learning techniques is another approach adopted in (*33*) where a Fusion technique was applied to aggregate SVM, K-nearest Neighbors, and Multi-Layer Perception for driving style recognition using smartphone data. One drawback of applying supervised learning methods for driving style classification is that these methods require labeled data as ground truth to train the algorithm, which is mostly not the case for data used in driving style detection. Therefore, unsupervised learning techniques such as clustering methods can be used for labeling different driving styles. The K-means clustering, the hierarchical clustering, the Support Vector Clustering, and the Mixture-based Clustering are among the Unsupervised methods applied in previous studies. For instance, Mantouka et al. (*34*) applied a two-stage K-means clustering approach to detect unsafe trips based on acceleration profiles, speeding, and mobile usage obtained from smartphones. They found that the driving styles of drivers mostly change over time. Higgs et al. (*35*) used the K-means method to evaluate the variation of driving styles within car-following periods. The authors found that drivers showed different driving styles within a car-following period. In another study, Yao et al. (*36*) applied dynamic time wrapping and hierarchical clustering to investigate driver behavior patterns of taxi drivers based on the lateral and longitudinal position of the vehicles on curves. Then, driving behavior of the drivers were evaluated form safety and ecological point of view.

Data used for driving style classification can be collected in several ways such as driving simulators (*6; 22; 27*), test vehicles (*4; 31; 32; 37*), and smartphones (*26; 33; 34*). Although driving simulators are safe, low-cost, and easy to set up, they are not fully representative of real-world conditions (*38-40*) since it is hard to simulate real-world traffic conditions with all their complexity and variety. Also, drivers might lose their spontaneity when they know their driving is being monitored. Data that comes from test vehicles more closely resemble real-world driving conditions. However, due to the high cost of field tests and the difficulty of data collection, the scope of these studies is limited in terms of the number of distinguished drivers, the number of trips, different types of roads driven on, different types of vehicles driven by the drivers, and the area covered by the tests. Data collected from user-end hardware, e.g. smartphones, are more comprehensive than test vehicle data as they contain information from a diverse population of drivers covering various types of roadways and neighborhoods. However, depending on the service a location-based application is providing to users, data might be biased (e.g. drive-safe apps offered by the insurance companies). Furthermore, different factors such as weather conditions, satellite signal blockage, and receiver quality can decrease a GPS's speed measurement accuracy (*41*). This study, however, benefits from large-scale high-resolution BSM data generated by connected vehicles equipped with vehicle-to-vehicle (V2V) and vehicle-to-infrastructure (V2I) technologies. The sampled data used in the study contains trajectories from more than 1300 unique drivers over two months. This is a high-resolution comprehensive database that represents real-world naturalistic driving conditions. Therefore, many limitations in previous studies are addressed to a large extent. Note that here the connectivity between vehicles does not affect driving style but the instrumented vehicles provide useful data about vehicle motion information. Furthermore, a notable gap in previous studies was a lack of driving style comparisons in roadways with different contexts. This paper classifies driving style in different road types to show how the perception of an aggressive or calm driving style can vary across different roadways. Therefore, this study contributes to the field in three ways:

1. Developed a framework for harnessing BSMs generated by CVs to comprehensively study driving style under a naturalistic driving condition in different road types considering that perception of an aggressive or calm driving style can vary across different road types.
2. Proposed an approach to evaluate variations in instantaneous driving behavior and style over space by developing several temporal volatility measures.
3. Proposed an approach for calculating driving score as a measure of driver performance.

DATA

This paper used BSMs collected from connected vehicles participating in the Safety Pilot Model Deployment (SPMD) program in Ann Arbor, Michigan. The main goal of this program was to deploy connected vehicle technology in the real-world and evaluate the feasibility of dedicated short-range communication for safety benefits (Bezzina & Sayer, 2014). This one-year program, run by the US Department of Transportation, started in August 2012 with vehicles that were equipped with V2V and V2I technologies to transmit BSMs with a frequency of 10 Hz. Containing information from 2836 vehicles equipped with V2V technology and 30 roadside equipment (RSE) covering more than 73 lane-miles on public streets, the SPMD is one of the largest real-world data collection programs ever undertaken in the field (Bezzina & Sayer, 2014). Considering the so-called four Vs of big data - Volume, Velocity, Variety, and Veracity (Yang et al., 2017)- the SPMD data can be considered as big data because they satisfy at least two of the Vs, namely Volume and Veracity. Overall, the SPMD data collection effort consists of light vehicle drivers with comprehensive data collection on the surrounding environment (63 vehicles), light vehicle drivers (2836 drivers), heavy vehicle fleet (3 vehicles), and a transit vehicle fleet (3 vehicles). This study focuses on a sample of 2836 drivers from Ann Arbor community drivers and employees of the University of Michigan. The participants had a valid driver license and drove on average more than 32 miles/day mostly in the model deployment geographic area. After recruiting more than 2500 drivers and vehicles, the vehicles were equipped with four main sensors including a DSRC antenna, an onboard unit (OBU), a GPS antenna (installed on the roof), and a power supply. The data collection was performed for 6 months, and 2 months of the data collected in October 2012 and April

2013 is publicly available through the Research Data Exchange (RDE) website (https://www.its.dot.gov/data/). This dataset contains high-resolution records (N~225 million BSMs) of vehicles' position (latitudinal, longitudinal, altitudinal) and motion (speed and acceleration). Figure 2-1 plots the BSMs generated by the CVs in the study area. This figure demonstrates the spread of trajectories over the study area with high resolution.

METHODOLOGY

The key objectives of this study are to develop a framework to harness big data generated by CVs, quantify instantaneous drivers' behavior in different roadway contexts, and classify individuals' driving styles using unsupervised machine learning (Figure 2-2). The proposed framework consists of several steps: 1- Data acquisition, 2- Data pre-processing and integration, 3- Quantifying driving volatility, and 4- Driving style classification. The initial hypothesis is that driving styles on highways is different from local streets due to the differences in complexity and driving environmental variation we expect on these roadways since the context of these roadways is different such as land use, built environment, development patterns, access points, and road users. In addition to the comparison of driving styles on highways and local streets, this study further tests the hypothesis that driving styles also vary on different local streets. To do so, the Urban Street Design Guide classification was used, which classifies local streets into two major groups: commercial streets (commercial strip corridors and downtown streets) and residential streets (*42*). In order to quantify driving behavior of drivers the concept of driving volatility, as a surrogate safety measure of unsafe driving behavior was used.

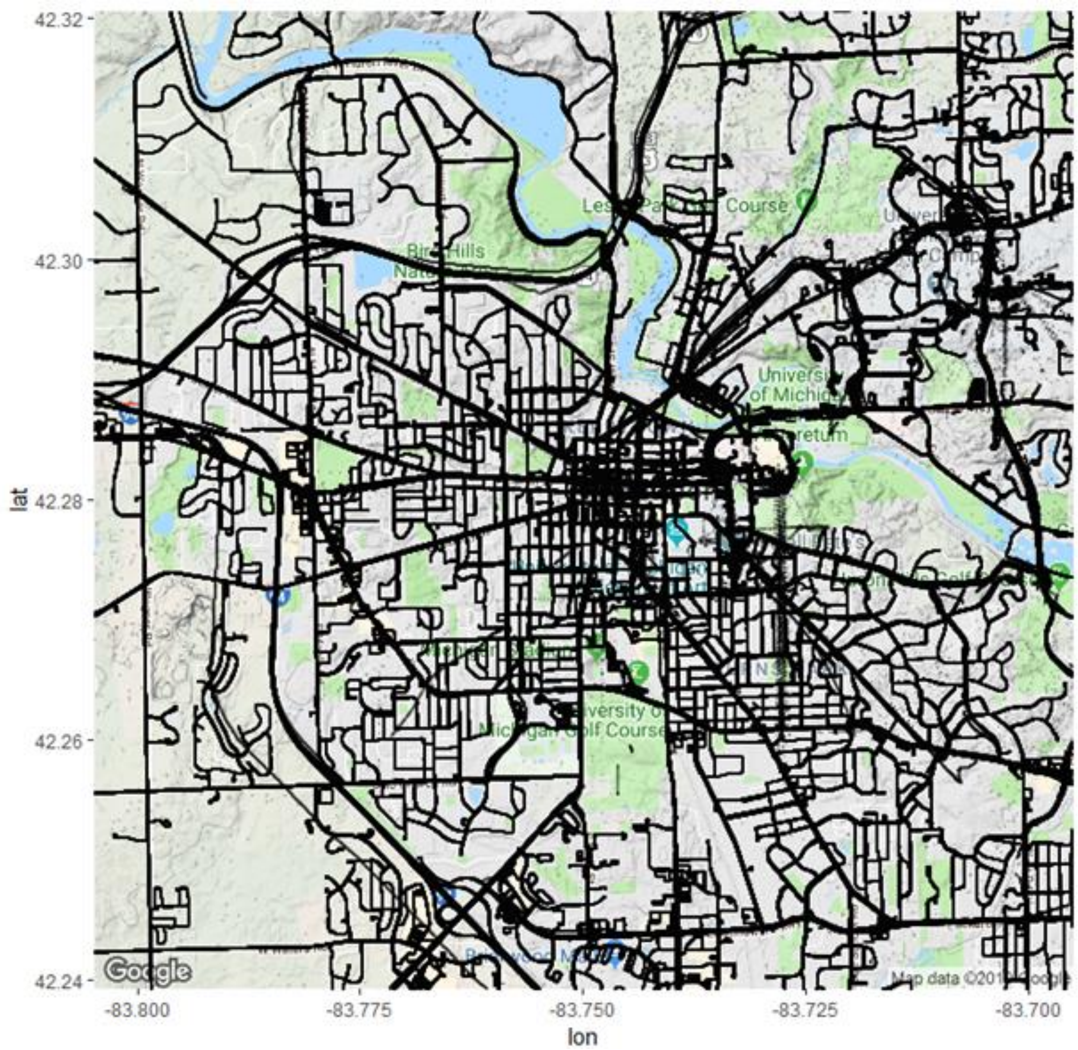

Figure 2-1 Study area and generated map by connected vehicles

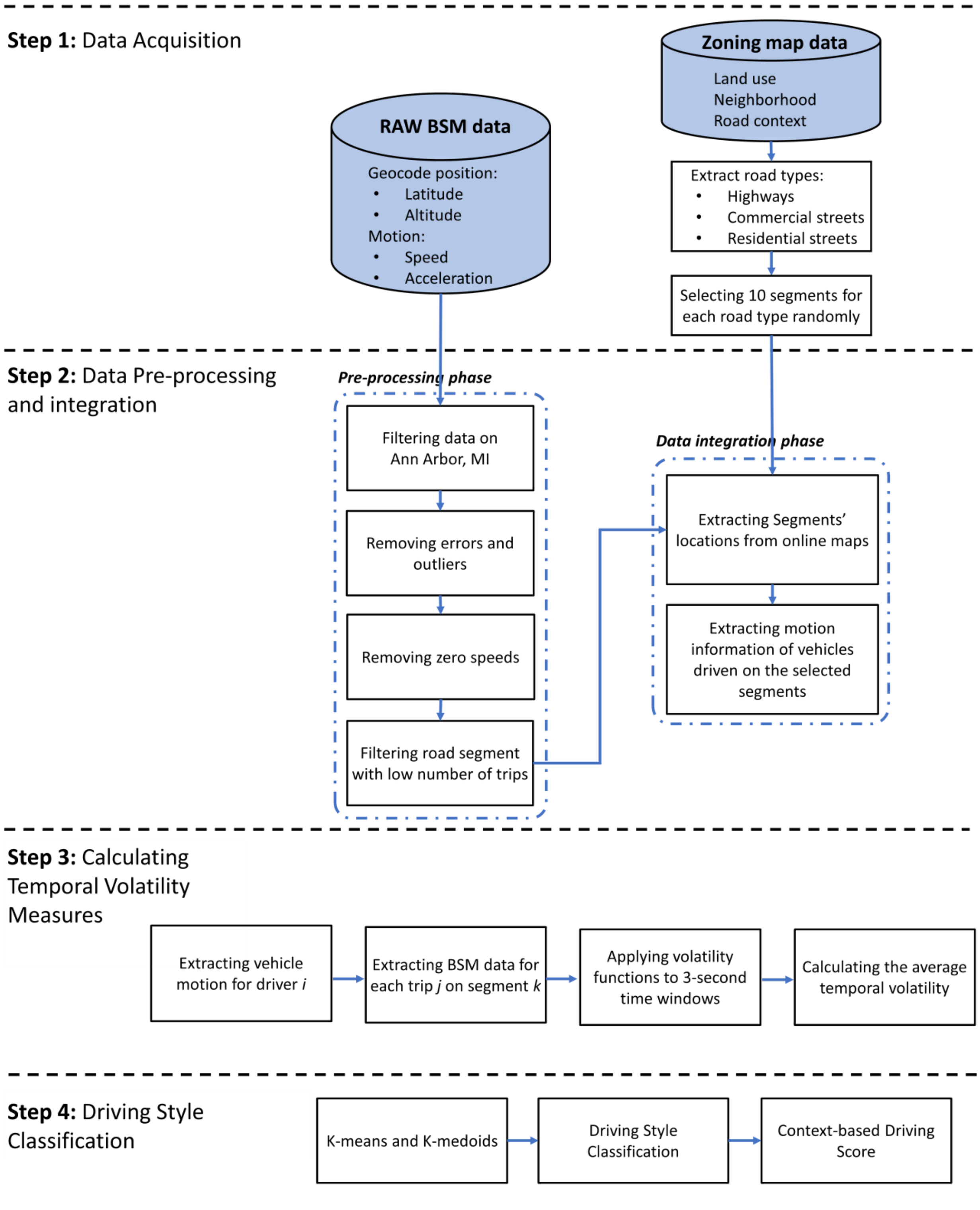

Figure 2-2 The methodological approach of the study

The concept of driving volatility has been explored in several studies (*43-45*). Driving volatility shows the degree of deviation from the norm. Therefore, higher driving volatilities indicate higher fluctuation in speed, acceleration, deceleration in both the lateral and longitudinal directions, and as a result, higher driver instability. It has been found that aggressive driving has a positive correlation with driving volatility (*46*). Also, previous studies show that driving volatility has a strong positive association with crash frequency (*43*) and severity (*46*). Therefore, it can be concluded that volatile driving is aggressive behavior that can significantly increase crash risk. Although SPMD data provides us with trajectory and motion information, the threshold values for different driving styles have not been determined. In other words, although variations in drivers' acceleration in a period can be captured, the amount of variation in a driver's acceleration or speed which represents an aggressive, normal, or calm driving style cannot be determined. Therefore, in such cases of dealing with unlabeled data, it is best to use unsupervised learning methods. In this study, K-means and K-medoids are performed to aid in driving style classification, which is discussed in detail in the clustering approach section. Driving volatility measures defined by Kamrani et al. (*43*) and temporal driving volatility were calculated and used as classification features. After driving style classification, driving style events belonging to each driver were aggregated to score his or her driving. Therefore, the final product of the study is the driving score of drivers in different road types both separately and overall. As mentioned previously, this study uses connected vehicle data only to access vehicle motion information. Therefore, evaluating the impact of connectivity (e.g., for collision avoidance) between vehicles on the driving style is not within the scope of this analysis. The next sections first explain the pre-processing procedure applied to the SPMD data. Next, the calculations of temporal driving volatility measures as classification features are described in detail. Finally, the clustering approach used for driving style classification is described.

Data acquisition

The raw BSM data were obtained from the online SPMD database. Then, to prepare the data for further analysis, pre-processing and data integration steps were applied. First, the data was filtered on the study area, Ann Arbor city, MI. Then, outliers and errors were removed from the dataset based on the recorded speed, longitudinal and lateral acceleration of CVs. The main issue with the dataset is a coding error in acceleration values, which were coded as ±g, made by developers when transferring data from DSRC to CSV files. These errors are removed in the pre-processing step. Finally, zero speeds values were omitted from the data set because they had the potential to affect driving volatility measures substantially.

Online maps were used to distinguish highway segments from local streets using geometric characteristics of the segments (e.g. shoulder width, median width, and level of accessibility). Also, to identify commercial and residential streets, we first need to identify neighborhoods with commercial and residential land use. For this purpose, zoning codes provided on the Ann Arbor zoning map were used (*47*). Then, after identifying segments in each area, those segments with a low number of trips were removed from the database. Finally, 10 different segments for each road type were selected randomly from the remaining segments, and their coordinates were extracted from online maps. Figure 2-3 illustrates these segments' locations on a map of Ann Arbor.

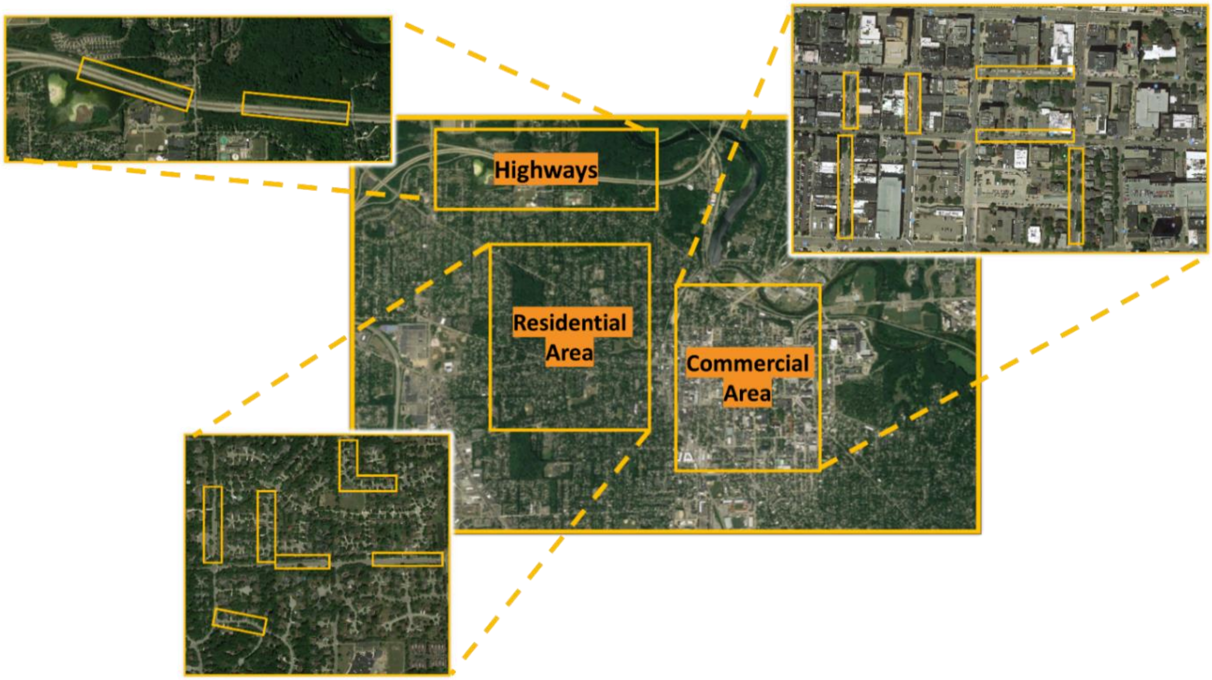

Figure 2-3 Location of segments selected in Ann Arbor, MI

Finally, vehicle kinematic information on the selected segments was extracted from the SPMD data. Therefore, after following these steps, three subsets (highways, commercial streets, and residential streets) were prepared for the classification.

Calculating temporal driving volatility

In this study, in order to classify travelers' driving style, the concept of temporal driving volatility is utilized. In the following, the volatility functions used for the calculation of driving volatility measures and the concept of temporal driving volatility are presented.

Measures of driving volatility

Previous studies have developed several volatility functions which have been applied to speed (*43; 46; 48; 49*), lateral acceleration (*48*), longitudinal acceleration (*43; 46; 48; 49*), and vehicular jerk (*43*) to evaluate alteration in driving movement. This paper applies several mathematical functions on CV data to develop three groups of driving volatilities:

1- Speed-based volatility
2- Longitudinal acceleration-based volatility
3- Lateral acceleration-based volatility

Volatility functions applied to speed, lateral, and longitudinal acceleration are discussed as follows (*43*).

Coefficient of Variation (C_v): This measure takes into account the standard deviation and the mean value to capture the dispersion using the following equation:

$$C_v = \frac{S_{dev}}{\overline{|x|}} * 100 \tag{1}$$

where S_{dev} is the standard deviation, and $\bar{x}$ is the mean. It can be used for speed, acceleration, and deceleration separately.

Mean Absolute Deviation (D_{mean}): This measure calculates the average distance between the observation of a variable and the mean of the variable:

$$D_{mean} = \frac{1}{n}\sum_{i=1}^{n}|x_i - \bar{x}| \tag{2}$$

where D_{mean} is the mean absolute deviation, n the number of observations, and $\bar{x}$ is the mean. It can be used for speed, acceleration, and deceleration.

Quartile Coefficient of Variation (Q_{cv}): This measure considers the spreading of a dataset as follows:

$$Q_{cv} = \frac{Q_3 - Q_1}{Q_3 + Q_1} * 100 \tag{3}$$

where Q_3 is the third quartile of a variable, and Q_1 is the first quartile.

Time-Varying Stochastic Volatility (V_f): This measure requires observations with a positive time series. Therefore, it can only be applied to vehicular speed which only contains positive values. This measure can be calculated as below:

$$V_f = \sqrt{\frac{1}{n-1}\sum_{i=1}^{n}(r_i - \bar{r})^2} \tag{4}$$

$$r_i = \ln\left(\frac{x_i}{x_i - 1}\right) * 100 \tag{5}$$

where x_{i-1} is the previous observation regarding the observation x_i, and $\bar{r}$ is the mean value of parameter "r".

Temporal driving volatility

This study employs the concept of temporal driving volatility developed by Arvin et al. (*50*), which captures alterations in instantaneous driving behavior by creating a time-series stream of data at the driver level. This provides us with the opportunity to capture driving behavior as a time-dependent variable. To calculate temporal driving volatility, a 3-second time interval is used, and the measures are allocated to the subject time. It was found that using a 3-second time-frame for the calculation of volatility measures brings about the strongest association of volatility measures with crash risk compared to 1, 2, and 5 second time windows (*51*). Figure 2-4 depicts the calculation of temporal driving volatility using the moving window. Finally, the average temporal volatility is used as a measure of driving style classification.

Clustering Approach

K-means

K-means is an unsupervised method for partitioning objects into *k* clusters with *k* mean values called centroids so that each object clusters around the nearest centroid (*52*). The final output of the K-means method is a set of clusters with their centroids, which minimizes the error function defined below (*53*):

$$E = \sum_{i=1}^{k} \sum_{x \in C_i} d(x, \mu(C_i)) \tag{6}$$

where $C_1, C_2, \dots, C_k$ are the *k* clusters, $\mu(C_i)$ is the centroid of cluster C_i, and $d(x, \mu(C_i))$ represents the distance between the observation *x* and $\mu(C_i)$.

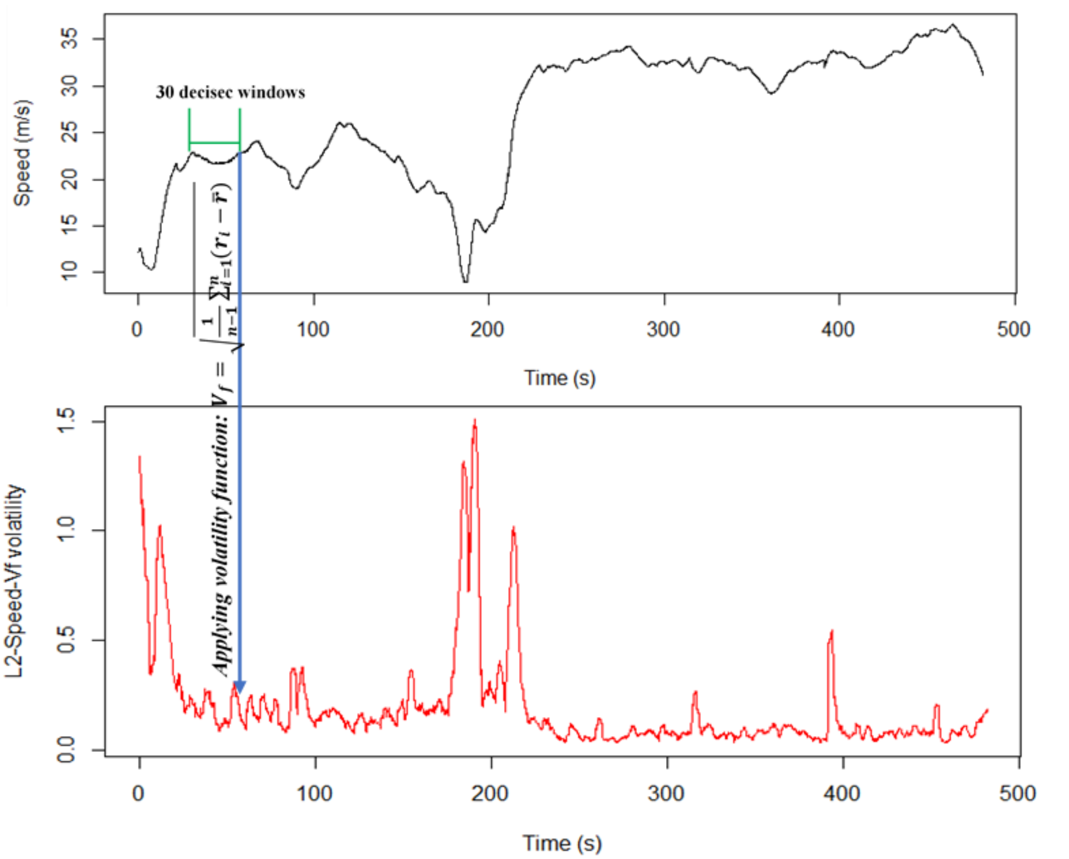

Figure 2-4 Calculation of temporal driving volatility

There are several formulas for the distance calculation. However, in this paper, Euclidean distance is used. If $x = \{x_1, x_2, \dots, x_n\}$ and $\mu = \{\mu_1, \mu_2, \dots, \mu_n\}$ are a point and a centroid of a cluster respectively, then the Euclidean Distance from *x* to *μ* is calculated using the equation below:

$$d = \sqrt{\sum_{k=1}^{n} (x_k - \mu_k)^2} \tag{7}$$

Assuming *D* as the data set, and *k* is the number of clusters, the steps of the K-means algorithm are:

Step 1: Randomly choose sets of centroids $(C_1, C_2, \dots, C_k)$ from D

Step 2: Assign the remaining data points to the clusters with the closest centroids (min d)

Step 3: Recompute the cluster centroids of the changed clusters above based on the mean value of the data points in each cluster

Step 4: Reassign the data points to the closest clusters based on the new centroids calculated in the last step

Step 5: Repeat steps 3 and 4 until no changes happen in the clusters' membership (no change in the error function)

Step 6: Report the results

K-medoids approach

In the K-medoids method, instead of centroids, objects cluster around representative objects called medoids (*54*). The error function of the K-medoids algorithm calculates the sum of the dissimilarities between each data point and its corresponding medoid:

$$E = \sum_{i=1}^{k} \sum_{x \in C_i} (x - m(C_i)) \tag{8}$$

where $C_1, C_2, \ldots, C_k$ are the *k* clusters, and $m(C_i)$ is the medoid of the cluster C_i.

Many algorithms have been proposed for K-medoids clustering. However, this paper applies Partitioning Around Medoids (PAM) as it is one of the most widely used K-medoid algorithms, proposed by Kaufman and Rousseeuw (*55*). Assuming *D* as the data set, and *k* as the number of clusters, the steps of the PAM algorithm are:

Step 1: Select *k* data points from the data set randomly as cluster medoids

Step 2: Assign the remaining data points to the clusters with the closest medoids

Step 3: Calculate the error function in equation (8)

Step 4: Select a non-medoid data point from *D* randomly and each time compute the error function assuming that one of the current medoids are swapped for the selected non-medoid data

Step 5: If the error function calculated in the last step is lower than the one calculated in step 4, then swap the old medoid with the new one

Step 6: Repeat steps 2 to 5 until no changes happen in the clusters' membership (no change in the error function)

Cluster number and clustering method selection criterion

From the perspective of driving style classification, each cluster represents a driving style. A cluster's number is usually selected based on either the subjective judgment of the researcher or clustering quality measures. In this study, using the former approach, 3-

cluster classification is considered because the authors believe it is more consistent with previous studies conducted on driving style classification (*2; 4; 6; 11; 21-24; 32*).

In this paper, the average silhouette width criterion (*ASWC*) was used for the selection of the clustering method. Generally, ranging from -1 to +1, (*ASWC*) demonstrates how well the objects are classified in the clusters. Higher ASWC values indicate a higher quality of clusters in terms of within-cluster homogeneity and between-cluster separation (*55*). Assuming that the data has been clustered in *k* clusters, for each data point x_i in cluster C_i, the silhouette coefficient of datapoint x_i is calculated as follows (*55*):

$$S_{x_i} = \frac{b_{x_i} - a_{x_i}}{\max(a_{x_i}, b_{x_i})} \tag{9}$$

where S_{x_i} is the silhouette coefficient of the datapoint x_i, a_{x_i} is the average distance between x_i and other data points in the same cluster, and b_{x_i} is the minimum average distance between datapoint x_i and data points in any other clusters. Then, the silhouette average of each cluster and the silhouette average of all clusters can be calculated using equations (10) and (11):

$$SWC_j = \frac{1}{n}\sum_{i=1}^{n} S_{x_i} \tag{10}$$

$$ASWC = \frac{1}{k}\sum_{j=1}^{k} S_j \tag{11}$$

where *n* is the number of data points in the same cluster, and *k* is the number of all clusters.

RESULTS AND DISCUSSION

Descriptive Statistics

Table 2-1 shows the descriptive statistics of the driving volatility measures at the driver-level in different road types. Based on the results, driving volatility measures have higher values in commercial streets compared to residential streets and highways, indicating that driving in commercial streets is more volatile than in other roadways. For example, the mean values of time-varying stochastic volatility (*Speed*-V_f) for the drivers in highways, commercial streets, and residential streets are 0.044, 0.155, and 0.053, respectively. The higher values of driving volatility in commercial streets are expected because of the higher variation in environment and road conditions in commercial districts, e.g. traffic signals, access points, and commercial establishments, and more complex interaction with other road users (pedestrian and bicyclists). Similarly, driving in residential streets is more volatile than in highways given the fact that driving environments in residential streets are more complex and variable. This evidence indicates that the idea of classifying the driving style separately for different road classes is logical.

Although the SPMD data is limited in terms of providing traffic volume data for different roadway segments, the hourly distribution of BSMs generated by CVs can give a rough sense of traffic volume variation during a day. In this regard, Figure 2-5 illustrates the distribution of BSMs generated by CVs at different times of the day over two months on different road types. As expected, a higher number of BSMs have been generated on highways compared to residential and commercial streets which is consistent with the higher traffic volumes on these roads. Also, based on the figures, the BSM generation frequency reaches its maximum at two times of a day which is consistent with the morning (7:30-9:30 am) and evening (3:30 pm-6:30 pm) rush hours in Ann Arbor. It is expected that traffic congestion can result in more driving volatilities in different roadways. Generally, the figure indicates that the BSM data used in this study covers a wide range of traffic conditions at different times of the day.

Clustering method selection

Each observation in the dataset represents a driving event that will be classified in the nearest cluster. The data was standardized to make the classification features comparable. Then, the "*cluster*" and "*factoextra*" packages in *R* software were utilized to perform K-means and K-medoids clustering (*56; 57*). Figure 2-6 shows the chart of *ASWC* values for different numbers of clusters on highways, commercial streets, and residential streets using K-means and K-medoids methods. From the figure, the K-means method has higher *ASWC* values meaning that it provides more quality clusters (in terms of within-cluster homogeneity and between-cluster separation) compared to the K-medoids method. Particularly, for 3-cluster classification, *ASWC* values for the K-means method provide better results, and therefore, the K-means method was selected over the K-medoids method.

Classification results

When performing K-means clustering on the dataset, each event was assigned a number (1, 2, or 3) to represent the number of the cluster in which the driving event has been placed.

Table 2-1 Descriptive statistics of the temporal volatility measures at driver-level

Volatility Measures	Highway Drivers N = 1302				Commercial Street Drivers N = 975				Residential Street Drivers N = 840			
	Min	Max	Mean	SD	Min	Max	Mean	SD	Min	Max	Mean	SD
Speed-V_f	0.03	35.98	0.18	0.59	0.00	138.11	3.74	7.56	0.08	27.69	0.67	1.15
Speed-D_{mean}	0.02	5.935	0.30	0.27	0.00	9.96	0.87	0.55	0.06	15.91	0.71	0.51
Speed-C_v	0.00	0.72	0.01	0.01	0.00	1.11	0.12	0.10	0.00	0.56	0.03	0.03
Speed-Q_{CV}	0.00	0.69	0.01	0.01	0.00	0.85	0.10	0.08	0.00	0.45	0.03	0.02
$Accl_x$-D_{mean}	0.02	0.71	0.13	0.04	0.00	1.51	0.35	0.10	0.06	0.88	0.23	0.08
$Accl_y$-D_{mean}	0.00	0.75	0.08	0.04	0.00	1.94	0.09	0.08	0.00	2.70	0.09	0.08

Note: V_f: Time-Varying Stochastic Volatility C_v: Coefficient of variation; Q_{cv}: Quartile coefficient of variation; D_{mean}: Mean absolute deviation; $Accl_y$: Lateral acceleration; $Accl_x$: Longitudinal acceleration

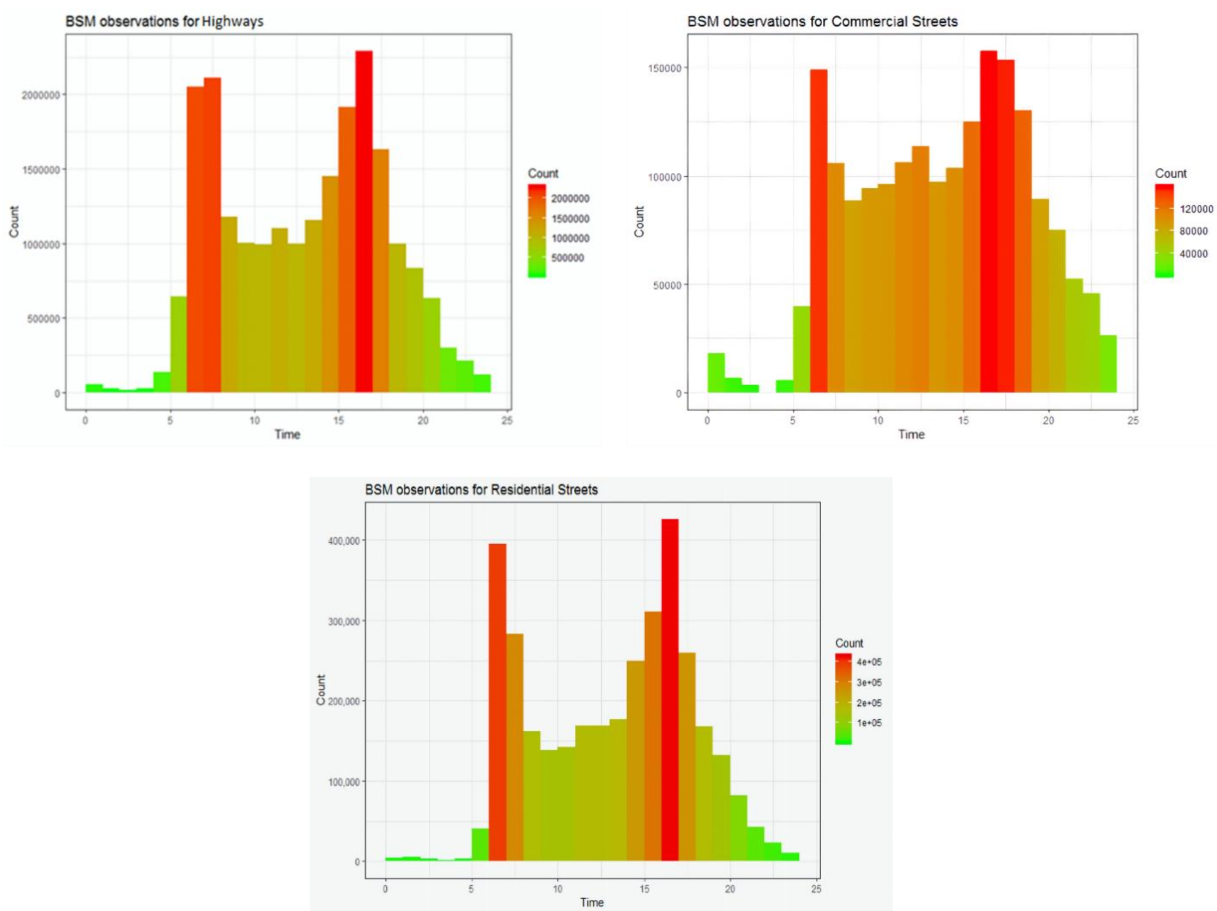

Figure 2-5 Histograms of BSM observations over time for highways, commercial streets, and residential streets

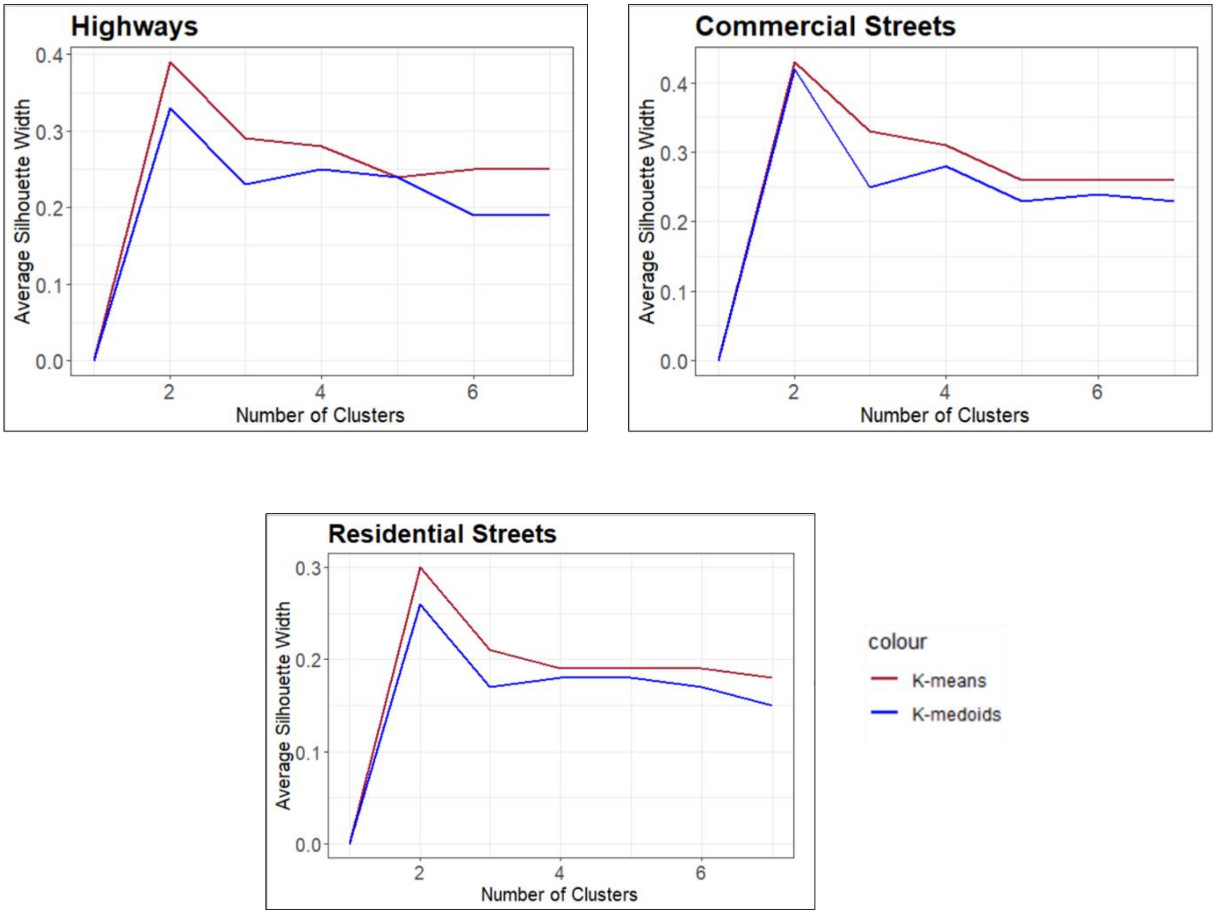

Figure 2-6 Comparison of K-means and K-medoids performance using ASWC

Deciding which driving style is represented by each cluster was based on the researcher's judgment. The mean values of classification features for each cluster were used to determine the driving style that was being represented. Table 2-2 shows the scaled mean values of classification features for highways, commercial streets, and residential streets. This table shows that for highways and residential streets, clusters 1, 2, and 3 have the highest driving volatility measures, respectively. Also, for commercial streets, except for Mean Absolute Value of Speed (*Speed*-D_{mean}) and Mean Absolute Value of Lateral acceleration ($Accl_y$-D_{mean}), the clusters follow the same order. This has been depicted more clearly in Figure 2-7 using radar charts of cluster centers. In these charts, classification features are illustrated on axels starting from the same point in which the length of each spoke shows the magnitude of the corresponding feature in the cluster. Drawing a line to connect these values creates a blue region in which a larger size indicates the higher a features' mean values are in the cluster. Given the fact that high values of driving volatilities represent aggressive and risky driving (*46*), it is logical to allocate the large, medium, and small regions (clusters 1, 2, and 3) to aggressive, normal, and calm driving styles respectively. Table 2-3 shows the results of classifying driving style events for each road type. Results show that of the 7537 events recorded from 1302 drivers on highways, 11.85, 44.13, and 44.02 percent were classified as aggressive, normal, and calm driving, respectively. This indicates that aggressive driving is not a recurring behavior on highways. Instead, the majority of drivers have normal and calm driving styles on highways. In residential streets, the proportion of aggressive events is smaller than highways (7.96 percent), and calm driving accounts for the majority of events (56 percent).

Table 2-2 The scaled cluster centers for highways, commercial streets, and residential streets

Cluster	**Speed-** V_f	**Speed-** D_{mean}	**Speed-** C_v	**Speed-** Q_{CV}	$Accl_x$**-** D_{mean}	$Accl_y$**-** D_{mean}
Highways						
Cluster 1 (Aggressive)	1.572	1.705	1.971	1.940	1.096	0.654
Cluster 2 (Normal)	0.147	0.316	0.186	0.187	0.334	0.337
Cluster 3 (Calm)	-0.570	-0.775	-0.717	-0.710	-0.630	-0.514
Commercial streets						
Cluster 1 (Aggressive)	1.486	0.669	1.500	1.500	0.505	-0.245
Cluster 2 (Normal)	-0.182	0.712	-0.079	-0.073	0.761	0.818
Cluster 3 (Calm)	-0.569	-0.584	-0.617	-0.620	-0.533	-0.231
Residential streets						
Cluster 1 (Aggressive)	2.209	1.803	2.356	2.338	1.789	1.297
Cluster 2 (Normal)	0.399	0.607	0.494	0.493	0.332	0.151
Cluster 3 (Calm)	-0.558	-0.636	-0.639	-0.636	-0.458	-0.274

Table 2-3 Number of trips classified in each driving style cluster

Type of road	Total num. of events	Total num. of drivers	Driving style					
			Aggressive		Normal		Calm	
			Number of events	%	Number of events	%	Number of events	%
Highways	7537	1302	893	11.85	3326	44.13	3318	44.02
Commercial streets	3387	975	795	23.47	757	22.35	1835	54.18
Residential streets	1912	840	147	7.96	690	36.09	1075	56.22

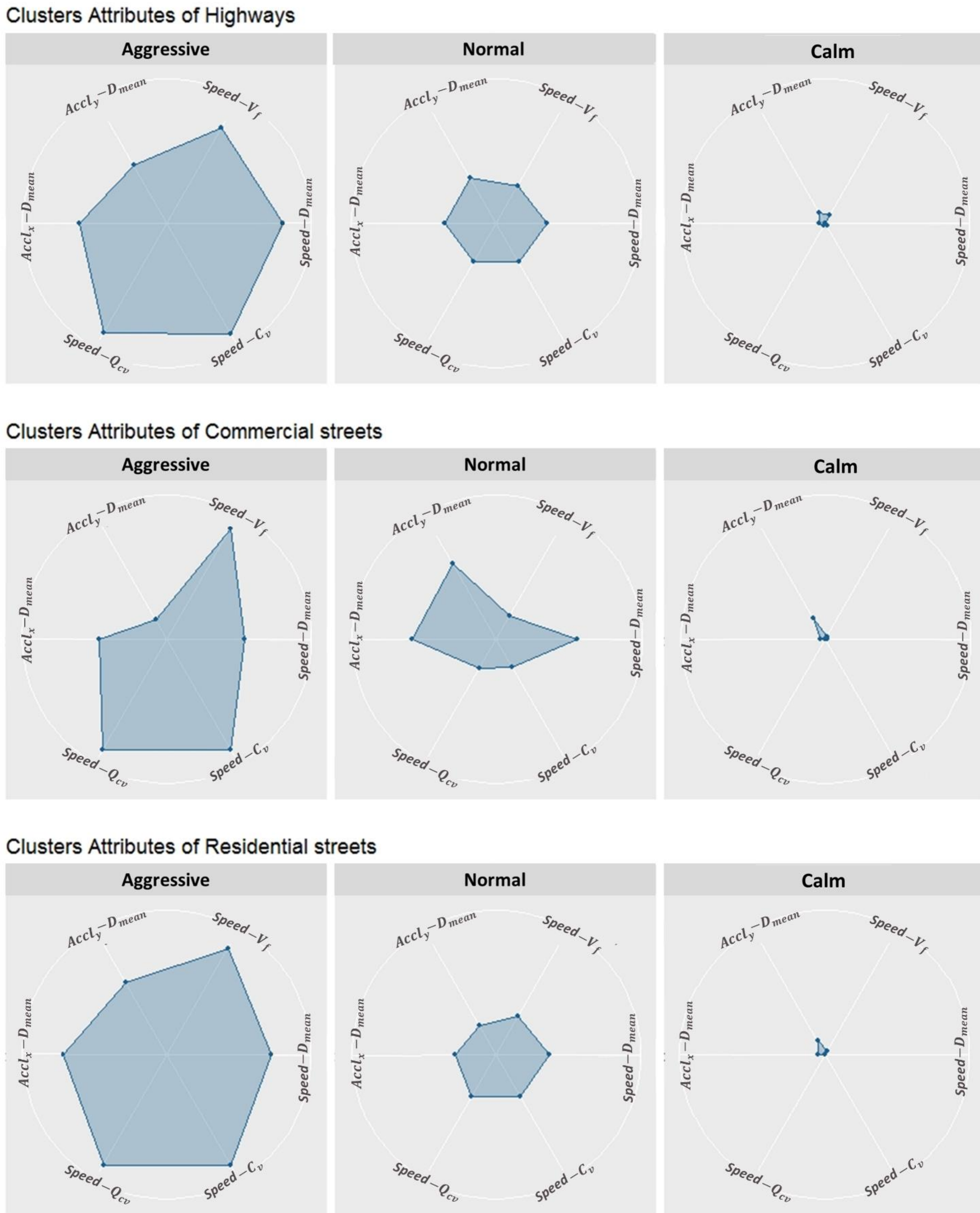

Figure 2-7 Radar charts of classification features mean values in the clusters for highways, commercial, and residential streets

These values indicate that overall driving behavior on residential streets is consistent with the nature of this neighborhood, which requires cautious and slow driving. Although the proportion of aggressive driving is higher in commercial streets than in highways and residential streets (23.47 percent), calm driving events are still the most frequent style in this road type (54.18 percent). A higher number of aggressive events in commercial streets could be because of the more complex and various environments in these segments, which makes drivers have sharp acceleration and deceleration more frequently.

By performing Principal Component Analysis (PCA), the number of features was reduced from a 6-dimensional space to a 2-dimensional space to visualize the clusters. Table 2-4 shows the contribution percentage of the classification features in the first two principal components and the percentage of variance explained by each principal component. From the table, it can be found that the first two principal components explain 78.61, 82.29, and 81.93 percent of the variance in highways, commercial, and residential streets, respectively. Also, the contribution percent values indicate that the first principal component (PC_1) in all three road types is largely influenced by the variables which capture speed variation (*Speed*-C_v, *Speed*-Q_{CV}, *Speed*-D_{mean} and *Speed*-V_f*)*, while the second principal component (PC_2) is mostly influenced by the variables which capture acceleration variation ($Accleration_x$-D_{mean} and $Accleration_y$-D_{mean}).

Table 2-4 PCA loadings and percentage of variance explained with each component for the two first principal components

Classification Features	Highways		Commercial Streets		Residential Streets	
	PC_1	PC_2	PC_1	PC_2	PC_1	PC_2
	(63.92 %) *	(14.69 %)	(59.60 %)	(22.69 %)	(66.98 %)	(14.95 %)
Speed-V_f	14.39**	3.06	22.71	5.60	17.43	0.33
Speed-D_{mean}	21.67	3.00	15.25	12.40	19.24	6.52
Speed-C_v	24-61	5.37	25.51	4.34	22.77	6.32
Speed-Q_{CV}	23.10	6.33	25.56	4.08	22.57	6.62
$Accl_x$-D_{mean}	11.73	1.15	10.66	18.91	11.96	14.37
$Accl_y$-D_{mean}	5.50	81.09	0.30	54.66	6.02	65.85
* Percentages of variance explained by the component						
**Percentage of the feature contribution in the principal component						

Figure 2-8 illustrates the labeled clusters in a 2-dimensional area. As depicted in the figure, the clusters for calm and normal driving styles on highways are more compact, containing a higher number of events. However, for commercial and residential streets, the majority of the events are clustered in the blue cluster, showing that most of the driving events in these roadways are classified as a calm driving style. This figure is consistent with the results presented in table 2-3. The significant lower proportion of aggressive driving events could be the result of several factors.

Driver tracking and driving score

Now that driving events are classified on different roads, we are able to track drivers in different roadways by aggregating the driving events corresponding to each individual. Table 2-5 shows the proportion of drivers who had a constant driving style. For instance, on highways, 23 drivers always possessed an aggressive driving style, 1.76 percent of the whole population. Similarly, in commercial streets, 4.31, 8.72, and 28.00 percent of the drivers always exhibited aggressive, normal, and calm driving, respectively. Remarkably, in residential streets, 40.71 percent of the drivers always drove calmly on the streets. Overall, considering all the segments, 1.73, 6.35, and 3.46 percent of the 1385 drivers in the dataset always had an aggressive, normal, and calm driving style, while 88.59 percent of the individuals had various behavior at different locations.

In the next step, individual drivers were tracked and profiled to evaluate their driving performance in different road types. In order to quantify driving styles, values of 1, 2, or 3 were assigned to aggressive, normal, and calm driving, respectively.

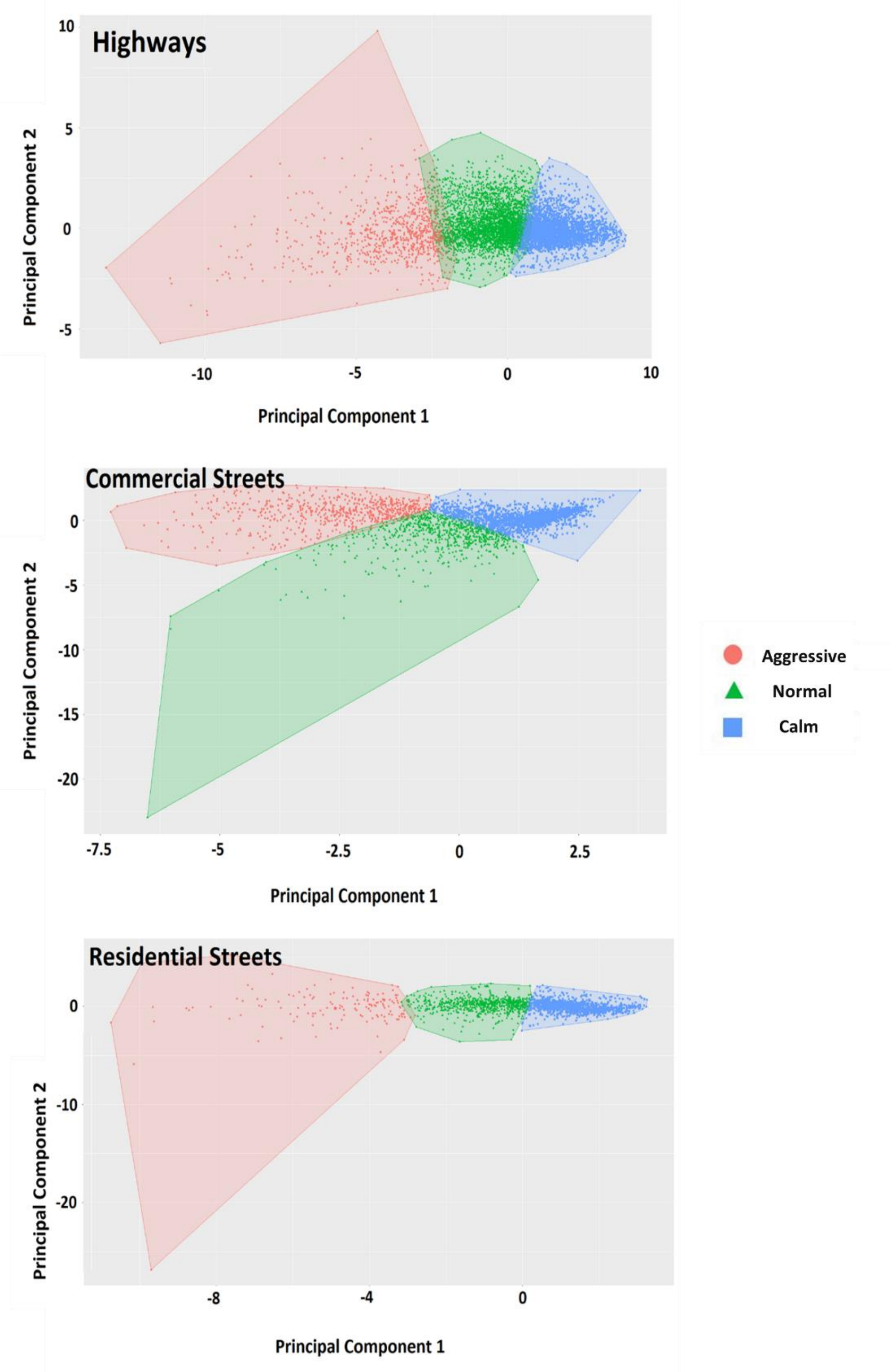

Figure 2-8 Visualization of clusters in 2-dimensional space

Table 2-5 Numbers and proportion of drivers with a constant driving style in different roads

Type of road	Number of drivers	Aggressive drivers		Normal drivers		Calm drivers		Drivers with various behavior	
		Count	Percent %	Count	%	Count	%	Count	%
Highways	1302	23	1.76	126	9.67	91	6.98	1062	81.56
Commercial streets	975	42	4.31	85	8.72	273	28.00	575	58.97
Residential streets	840	15	1.79	107	12.74	342	40.71	376	44.76
Overall	1385	11	0.79	80	5.78	67	4.84	1227	88.59

Therefore, driving style is a discrete variable that takes on values from 1 to 3. As discussed, there can be different values of driving style for a driver as he/she can have different driving behavior on different road segments. Therefore, to have a single value as a measure of driving performance, we define “Driving Score” which is the average of these values for each road type. To this end, driving events were aggregated based on drivers' ID in highways, commercial streets, and residential streets. Therefore, for each driver, there are three Driving Scores ranging between 1 and 3 which reflect the driver’s performance on different roads. Unlike driving style, Driving Score is a continuous variable that can take on any values between 1 and 3 which gives us more flexibility in assessing drivers’ performance. Figure 2-9 illustrates the schematics of the Driving Score as a measure of an excellent, good, or bad driver, and the histogram charts of the Driving Score in all road types. A Driving Score of 3 represents calm and low-risk driving whereas a driving score of 1 represents aggressive driving which increases collision risk. The Driving Score is a variable measure that changes by drivers’ performance, meaning that a driver with a low score can drive more calmly in order to improve his or her score and vice versa. In Figure 2-9, the right-skewed histograms of Driving Scores on all three road types indicate that there is a higher quantity of drivers with good and excellent performance than the number of drivers with poor and very poor performance. This is confirmed by the shape of the ‘overall’ histogram.

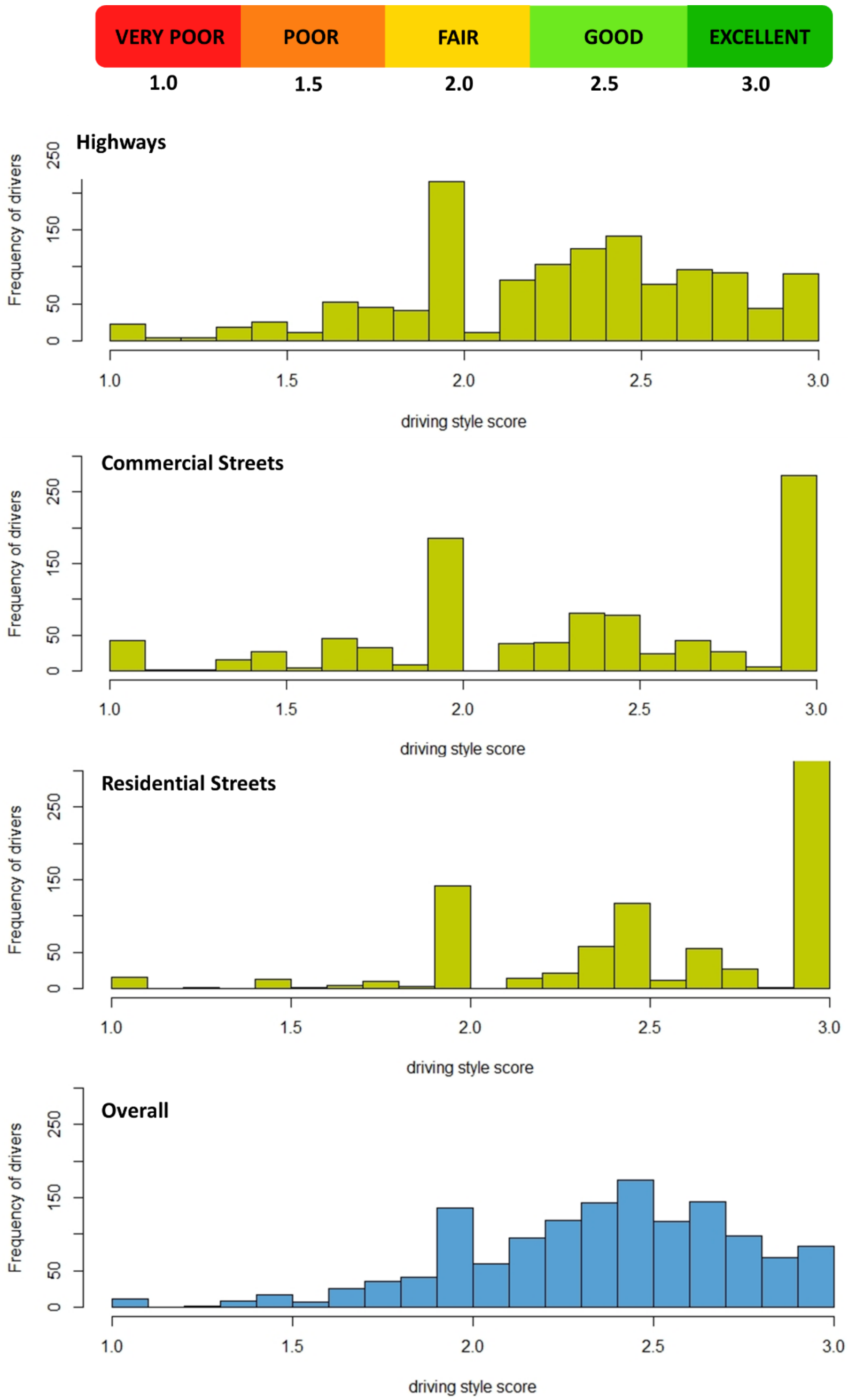

Figure 2-9 Range of Driving Score criterion and histogram of driving scores both separately and overall

Discussion

Previous studies proved that not only does driving style vary among drivers (*5; 11; 26; 27*), but that a driver can change his or her driving style over time (*6; 35; 37; 58*). Harnessing BSMs generated by connected vehicles, this study extends the understanding of driving style by showing that driving styles vary among different roadway types. Different thresholds obtained for aggressive, normal, and calm driving styles on freeways, commercial, and residential streets indicate that the perception of an aggressive or calm driving style varies across different road types. This is because of the differences in complexity, environmental variation, number of access points, traffic conditions, and interactions with other road users (pedestrian and bicyclists) among these roadways. Given the fact that traffic flow on highways is more uniform than commercial and residential streets, sudden acceleration and deceleration, abrupt changes in vehicle steering wheel angle, and harsh lateral and longitudinal maneuvers are more likely to be conceived as aggressive driving style on these roads. This study also provides new insight into driving styles at both microscopic and macroscopic scales. At the macroscopic scale, this study shows the proportions of different driving styles on different roadways. For example, it was found that the majority of the driving style events on highways, commercial streets, and residential streets were classified as normal and calm driving styles. In other words, an aggressive driving event is not always a recurrent behavior on roadways segments analyzed in this study. This finding is in line with the results of the 2008 AAA Foundation’s Traffic Safety Culture Index survey where most of the drivers reported that they had engaged in risky driving behaviors only a few times in the past 30 days (*59*). At a microscopic scale, however, this study tracks individual drivers to evaluate differences in their driving styles on different roadways. One advantage of this approach is detecting risky drivers who continuously drive aggressively during the observation period or drivers who always drive calmly. The results show that a significant proportion of the drivers had various driving styles while driving on different roadways, e.g. normal drivers who sometimes drive aggressively. It is consistent with the result of previous studies that found that the driving style of individual drivers changes over time (*6; 37; 58*). Furthermore, this study proposes a driving score that assesses drivers' performance on different roadways. Ranging from 1 to 3, the driving score converts the driving style as a discrete variable to a continuous variable that can change by drivers' performance. Another advantage of using driving scores is to find the distribution of driving performance on different roadways. Right-skewed histograms of driving scores on a roadway indicate that on average drivers had good performances on the roadway.

LIMITATIONS

While the connected vehicles in the SPMD study collect information of subject vehicles using OBU, the data does not include information on the surrounding environment and traffic conditions of roadways for the trips undertaken by drivers. We acknowledge that variation in traffic conditions of roadways may affect driving behaviors. However, this limitation is mitigated to some extent by evaluating the driving style on highways, commercial streets, and residential streets separately. Also, this study takes into account the overall performance of the drivers on roadways over two months. Therefore, the driving performance of drivers is the aggregate under different traffic conditions that can happen during this period. Furthermore, in this study, 10 segments on highways, commercial and residential streets were selected as representative segments for the driving classification of each road type. Although a significant proportion of the drivers who participated in the SPMD program drove on these segments, they may not be representative of the whole population of segments for a type of road. If a larger sample size was used, the classification would likely be more accurate. Also, this paper only takes into account variations in longitudinal and lateral vehicle movements. However, other measures can represent driving styles such as lane change behavior, tailgating behavior, and time to collision. However, the calculation of these measures requires information regarding the surrounding environment which is not collected in this dataset. With higher market penetration of CVs in the future, this information will be available to the researchers for future studies.

CONCLUSION

With the emergence of connected vehicles, researchers have unprecedented access to location-based data, which can be coupled with big data analytics and machine learning methods, to extract valuable information and get new insights about micro and macro level transportation performance. This research benefits from a sample of the SPMD data as a large-scale real-world database containing the BSMs generated by connected vehicles. This dataset includes the position and motion information of more than 1300 vehicles making trips on diverse roadways and through several neighborhoods in Ann Arbor. Focusing on driver behavior, the main objective of this study is to develop a framework to harness BSM data to study and quantify instantaneous driving behavior in order to classify driving styles. The main contribution of this study is to quantify volatility in driving behavior using high-volume real-world CV data and classify driving styles in different road types using unsupervised machine learning methods. Finally, an approach was proposed for scoring drivers' aggressiveness which can be used as a measure of driving performance on different road types.

The results show that the proposed method in this study could successfully extract the driving volatility features from raw BSM data to quantify driving behavior at different road types. The clustering results indicate that the K-means method provides more accurate classification results compared to the K-medoids method. It was found that there was a significant difference between the three groups of drivers in terms of temporal driving volatilities which helped the authors classify drivers based on these measures. Clustering results show that perception and thresholds of aggressive, normal, and calm driving vary in different road types. In other words, an aggressive style in highways can be perceived as normal driving in commercial streets and vice versa. Moreover, the analysis indicates that aggressive driving, as one of the most important contributing factors in motor vehicle crashes, is not a recurrent behavior on roads. The results show that the proportion of aggressive driving events is highest in commercial streets (4.31 percent) and lowest in highways (1.76 percent). Also, the histograms of the driving scores in different roadways demonstrate that drivers showed good performance overall. This study uses one of the most high-resolution datasets for driving style classification, containing driving information from more than 1300 unique drivers. Therefore, the methodology and results of this study can be generalized to a high extent in other areas.

The findings of the study can be used in location-based services to improve the safety of vehicles on different types of roadways. For example, it can have an application in Driving Assistance Systems (DAS) for monitoring driving behavior and giving feedback about their driving performance. The driving score proposed in this study can be a good measure of driving performance of the drivers. If the driving score of a driver indicates that he or she is driving aggressively, the driver could be alerted/advised to drive more calmly. This methodology can also be applied to individual CVs which could then be submitted by the car owners to the insurance companies as a record of driving style history. Another application of the study is in fuel consumption and emission studies. Because aggressive driving styles increase fuel consumption and emissions (*13*), air pollution hot spots could be identified with high accuracy.

Future studies could integrate crash data with CV data to evaluate the association of crash frequency/severity with driving styles on different road types. Also, temporal evaluation of driving style can be considered in future studies to assess the variation of driving styles over time (e.g. variation of driving style at different hours of a day). Furthermore, although this study uses criteria such as the number of trips and number of connected vehicles passing through the segments for selecting the representative segments, considering additional selection criteria such as safety conditions (i.e., segments with high crash rates) and traffic conditions (e.g. segments with high traffic volumes) can be studied in future research.

CHAPTER 3 : ANALYZING THE IMPACT OF INSTANTANEOUS DRIVING IN WORK ZONES AND CURVES ON EMISSIONS AND FUEL EFFICIENCY USING NATURALISTIC DRIVING DATA

A version of this chapter is accepted for presentation at the 101th Transportation Research Board Annual Meeting.

ABSTRACT

Consumption of fossil fuel-based energy for vehicle propulsion and associated emissions are a global concern. A key question is how can reductions in energy and emissions be realized? One pathway is to examine situations where high-energy consumption on roadways occurs, e.g., speed volatility at work zones, or on sharp curves. Driving behavior in such situations can substantially impact energy consumption and emissions, which are lightly researched. Can reductions in aggressive (versus calm) driving in such situations impact energy consumption and emissions? Harnessing second-by-second data from the naturalistic driving study (over 1580 drivers) and using the concept of driving volatility, as a surrogate for risky driving behavior, this paper explores driving styles in work zones and curves. The data are combined with real powertrain drive cycle simulations using the Autonomie model. Results of driving style classification show that aggressive driving events account for 12.2% and 15.4% of events that occurred in work zones and on curves. Furthermore, Aggressive driving revealed an average of 23% increase in fuel consumption and an 18.8% increase in total emissions on curves, while these values were 59.2% and 39.9% in work zones respectively. Through rigorous analysis, this research identifies high-volatility locations where reductions in energy and emissions are possible. The results have implications for transportation agencies in terms of improving work zone configurations and providing signage or technology on curves to

reduce fuel consumption and emissions. Moreover, automated and connected vehicles can smooth out traffic flow with advanced advisories and warnings.

INTRODUCTION

Global warming is one of the biggest threats the world is facing today. Under the Paris agreement on climate change countries agreed to reduce the use of fossil fuels and greenhouse gas emissions (*60*). The united states, as one of the biggest contributors to greenhouse gas emissions, has set a target of lowering its greenhouse gas emissions by 50-52% below 2005 levels in 2030 (*61*). Transportation is one of the largest sources of energy consumption and emissions in the United States. With an average of 250 million registered light-duty vehicles in the U.S. in 2018, personal vehicles are one of the greatest sources of pollution. This fact strengthens the relevance of working toward the development of energy-efficient mobility systems aimed at reducing energy, emissions, fuel consumption, and improving safety. While most technological advancements focus on improving roadway safety and congestion, improvement in energy and vehicular efficiency has not been as widely emphasized although both are linked together. Reducing congestion has a direct impact on fuel consumption and emissions reduction. Thus, congestion mitigation projects should also consider reduction, which is dependent on a multitude of factors including driver behavior, vehicle and roadway types, and traffic conditions.

A typical trip involves a combination of acceleration, idling, cruising, and deceleration maneuvers. The time spent in each of these maneuvers depends on a variety of factors such as driving behavior, road type, and level of congestion. Thus, driving styles such as aggressive, normal, and calm behavior contribute significantly to an increase or decrease in fuel economy and emissions. Road blockages or work zones are common sources of congestion, increasing fuel consumption and emissions. On the other hand, driving on curves involves variations in driving regimes and requires higher vehicle power to overcome vehicle inertia which also results in increased emissions. The driving style and behavior within these curves are expected to influence the level of fuel economy and emissions. However, it is practically not feasible to monitor driving styles and fuel consumption or emissions from everyday road driving data sources. For increased accuracy of monitoring driving styles and resulting fuel and emission estimates, disaggregate second by second driving profiles are required. The availability of advanced sensor technologies in recent years has enabled the collection of countless terabytes of such second-by-second vehicle trajectory data. In this regard, the naturalistic driving data serves as a potential source for identifying driving styles and assessing how the variation of driving styles influence the vehicular fuel economy and emissions on various types of roadway scenarios. Thus, due to the relevance of work zones and curves, this study will focus on these scenario types.

LITERATURE REVIEW

The section describes existing literature on driving style classification and studies estimating fuel efficiency and consumption benefits.

Driving style classification studies

Previous studies found that driving style is strongly associated with energy efficiency (*14; 62*), fuel economy (*13*), and emissions (*16*). Driving style is defined as the way a driver chooses to drive as a habitual behavior or an instantaneous decision making. Driving style might be perceived from drivers' decisions, maneuvers, and actions (*1*). Usually, past research conducted on driving style classification mainly utilizes vehicles' kinematics to categorize driving styles. These studies mostly consider three categories for classifying driving styles: Aggressive, Normal, and Calm style (*2; 4; 6; 23; 24; 63*). Generally, past research applied two groups of algorithms for driving style classification: supervised machine learning methods and unsupervised machine learning methods. The Artificial Neural Network (ANN) (*3; 31*), the Support Vector Machine (SVM) (*27*), and the Random Forest Decision method (*32*) are the most common supervised learning algorithms in driving style detection. Labeled data (i.e., ground truth data) are the vital part of training a supervised learning algorithm. However, mostly, labeled data are not available to the researchers. Hence, unsupervised learning methods (e.g., clustering algorithms) may be applied to label different driving styles (*63*). The K-means (*35; 64*), the K-medoids (*63*), and the hierarchical clustering are among the unsupervised learning algorithms used in the literature.

Fuel consumption and emissions studies

Various studies have examined the impact of traffic conditions on emissions levels while a few recent studies have utilized SHRP 2 naturalistic driving data. A study (*65*) conducted in Ann Arbor, Michigan, analyzed free flow and congested traffic conditions to estimate emissions on a freeway segment. The high-level congestion experienced due to work zones resulted in a high level of emissions. Salem et al. (*66*) studied the effectiveness of lean construction tools in improving operating conditions at work zones. The improved conditions resulted in reduced emissions. Further, improvements in traffic conditions resulting from the use of wireless communication technologies have also been studied to address their impact on vehicular emissions (*67; 68*). These technologies have the ability to adapt driver behavior to existing traffic conditions. In another study, Li et al. (*69*) used a simulation environment to introduce a smart advisory system where a pedestrian crossing was present. The system enhanced driver behavior in hazardous conditions, which resulted in the reduction of emissions. Likewise, Zhou et al. (*70*) used simulation to assess the emission impacts on a large-scale network in North Carolina. The study used a baseline case with no disruption and two other scenarios with congestion and diversion patterns under work zones. An increase in emissions for no diversion traffic was observed when vehicles formed a queue upstream of work zones.

Another study (*71*) analyzed the impact of shifting construction activities from daytime to nighttime on emission levels. They observed lower emission levels due to lower volumes at night however, pollutants worsened at night. Thomas (*72*) studied emissions resulting from recurring and non-recurring congestion. The study measured the impact of non-recurring incidents on emission levels using a stochastic model. Barth and Boriboonsomsin (*73*) studied speed as a function of congestion level to estimate emission levels. Freeway emissions were characterized using traffic speed, capacity, and travel demand (*74*). Likewise, Qi et al. (*75*) estimated emissions on freeways and arterials under varying congestion levels. Results showed an increase in emissions with poor traffic conditions. Papson et al. (*76*) studied emissions on signalized intersections under congested and non-congested conditions using time-in-mode methodology.

A few studies have utilized SHRP 2 data to analyze emissions impacts. A study by Sun et al. (*77*) established optimized drive schedules from SHRP2 NDS, which are a series of vehicle-speed trajectory points. Drive schedules are used in chassis dynamometer tests to measure tailpipe fuel economy and emissions (*71*). Another study (*68*) developed synthesized drive cycles for pickup trucks capturing the principles of naturalistic driving. These optimize the design of the powertrain in pickup trucks using federal fuel consumption and emission standards. Another study (*78*) designed NDS in Michigan by instrumenting 117 vehicles and collected over 210,000 mi of data. The NDS data was used to quantify the fuel consumption rates of different drivers. Likewise, Tanvir et al. (*79*) conducted a small-scale NDS study in North Carolina and collected high-resolution data for thirty-five drivers. The study developed eco-driving metrics for different driving styles and measured their impact on fuel consumption with different confounding factors. While past studies have utilized simulation environments and aggregate data to analyze the impact of various communication technologies on emissions, the impact of monitoring fuel consumption and emissions from everyday road travel and specific activities is unclear. This study fills this gap in the literature by utilizing, disaggregating second by second driving profiles from naturalistic driving data to estimate fuel consumption and emissions resulting from driving under work zones and curves for increased accuracy.

Literature gap and Contributions

While past studies have classified driving styles using aggregate sources of data, however, measures of driving volatility from second-by-second naturalistic data have not been used for such classification within work zones and curves. Likewise, there is a lack of literature on assessing how aggressive driving behavior influence fuel consumption and emissions within work zones and curves using disaggregate driving profiles. This study leverages second by second driving profiles from naturalistic driving data to classify driving styles to aggressive, normal, and calm behavior and analyze the influence of these driving styles on fuel consumption and emissions. The study is going to answer the following questions:

- How can we better utilize second by second disaggregate naturalistic driving data to detect aggressive driving events via classifying driving styles into aggressive, normal, and calm within work zones and curves?
- How driving aggressiveness can affect fuel efficiency and emissions in work zones and curves on different road types?
- How do transitions from roadway scenarios, i.e., from the freeway to arterials, impact fuel and emission estimates in work zones and curves?

To answer these questions, machine learning algorithms were utilized to classify driving styles using second by second driving profiles from naturalistic driving data. Further, real drive cycle simulations from Autonomie model were used to estimate the influence of these driving styles on fuel economy and emissions within curves and work zones.

DATA DESCRIPTION

The study utilizes Naturalistic Driving Study (NDS) data which was from Strategic Highway Research Program (SHRP 2) (*80*). Including over 3500 participants from multiple states, the NDS project is one of the largest and most comprehensive naturalistic driving studies conducted in the US. The data were collected over four years from 2010-

2013 having 4300 naturalistic driving years. The high-resolution data on kinematics, steering, and vehicular offsets were collected using various types of sensors, cameras, and data acquisition systems. (*80*).

The data used in the study is a subset of NDS data consisting of kinematics and roadway features belonging to 1580 drivers. The kinematics data includes 30-seconds of lateral and longitudinal speeds and acceleration/deceleration profiles for driving events categorized as unsafe. This results in two different behaviors from the driver; one prior to the unsafe event that reflects the true behavior of aggressive driving irrespective of the outcome, and the second component represents the driver adjustment or driver's reaction to the unsafe event. Since this study is going to evaluate the impact of driving style, as an instantaneous behavior, on the fuel composition and emissions, the latter part of the trajectories which was as a result of drivers' reaction to an unsafe event was excluded from the analysis. Also, error checking was performed via descriptive analysis to remove errors and outliers such as driving events with zero speed from the data set. The data relevant to roadway features were used to identify driving traces within work zones and curves. A subset of event traces from videos was also reviewed. The reaction time or impact time was used to distinguish these two sequences within the driving profile. Work zones and curves were classified into two categories; a) area before entering work zones and curves, b) an activity area where the vehicle is traversing work zones and curves. These three classifications were categorized to identify changes in driving behavior. Since behavior may differ as drivers transition towards these activity areas, thus these were categorized to study the true effects of changes in fuel efficiency and emissions as drivers enter these activity areas. Likewise, roadway facility types including freeways and arterials were also used to study differences in fuel and emissions estimates since traffic conditions differ between the two facilities resulting in different driving styles and behavior.

METHODOLOGY

Figure 3-1 presents the methodological approach of the study. As discussed in the last section, the NDS data contain information regarding geocode position, motion information, and roadway features of driving events. For further analysis, the raw data were pre-processed by removing errors and outliers (e.g., driving events with zero speeds) and excluding the near-crash trajectories. Then, two subsets of events that occurred at curves, and work zones were selected from the data using the roadway features such as roadway locality and roadway alignment. Next, roadway features such as traffic condition and traffic flow information were used to identify those work zones and curve events that occurred in freeways and arterials. In the next step, driving volatility measures, as explained in the next section, are calculated as measures of driving style classification. Then, K-means, K-medoids, and hierarchical clustering methods are applied to classify driving events in different locations. The results of driving style classification are used as input to the Autonomie simulation model to quantify fuel economy and emissions for the specific driving styles. After assessing the overall impact of driving styles within work zones and curves on fuel economy and emissions, these measures were further analyzed for different facility types such as freeways and arterials. The following sections first explain the formulations of driving volatility measures. Then, the clustering approach and algorithms applied in the paper are discussed. Finally, a brief description of the Autonomie simulation model is provided.

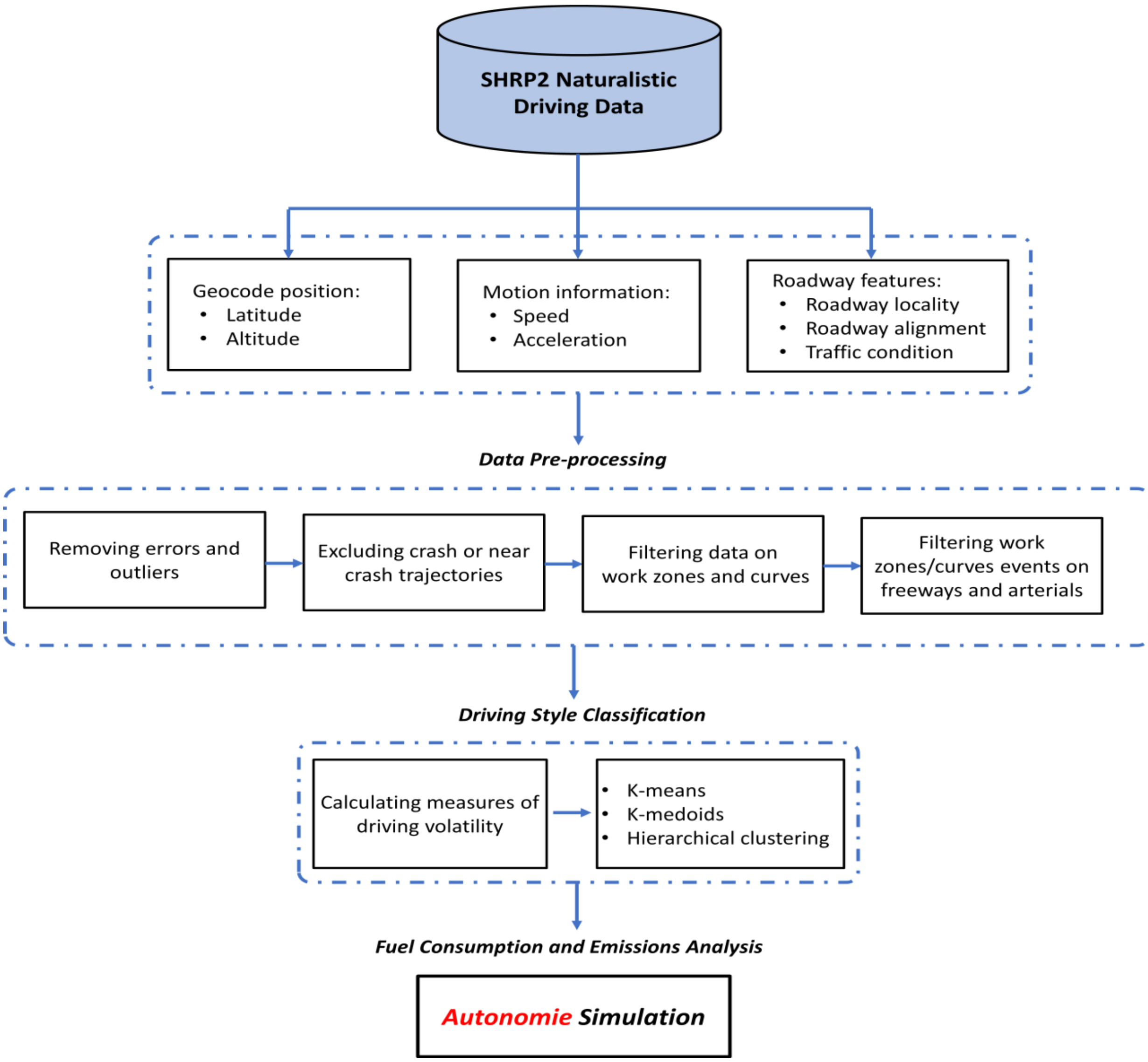

Figure 3-1 The methodological approach of the study

Driving classification approach

Calculating driving volatility measures

The study applies the concept of using driving volatility as a surrogate for risky driving behavior to detect driving styles in different locations and road classes. (*43; 48; 63; 81*). Driving volatility measures indicate how much the individuals deviate from normal driving. Hence, larger values of driving volatilities are correlated with higher variations in speed, deceleration, and acceleration, and as a result, higher instability in driving. Past research found that driving volatility is positively correlated with the crash count (*43*) and severity (*46*). Thus, volatile driving might be considered as a sign of aggressive driving behavior which can meaningfully increase the risk of crashes. Past research has applied several volatility functions to speed, longitudinal acceleration, and lateral acceleration, and vehicular jerk (*43; 45; 48; 82; 83*) to explore variation in the kinematics of vehicles. Likewise, this study uses three categories of driving volatility measures:

1. Volatility measures applied to speed
2. Volatility measures applied to longitudinal acceleration
3. Volatility measures applied to lateral acceleration

The following section presents the volatility functions used for speed, lateral acceleration, and longitudinal acceleration.

Standard Deviation (SD): This measure, which is one of the most commonly used volatility measures, captures the variation of observations from the mean:

$$SD = \sqrt{\frac{1}{n-1}\sum_{i=1}^{n}(x_i - \bar{x})^2} \tag{1}$$

where SD is the standard deviation, $\bar{x}$ is the mean, and *n* is the number of observations in the data. This measure can be applied to speed, deceleration, and acceleration.

Coefficient of Variation (C_v): This volatility measure, which is independent of units, captures the variation around the mean with respect to the mean:

$$C_v = \frac{SD}{\overline{|x|}} * 100 \tag{2}$$

where C_v is the coefficient of variation, $\bar{x}$ is the mean, and SD is the standard deviation.

Mean Absolute Deviation (D_{mean}): It measures the average distance from the mean to the observations:

$$D_{mean} = \frac{1}{n}\sum_{i=1}^{n}|x_i - \bar{x}| \tag{3}$$

This measure is applied to the vehicular speed, deceleration, and acceleration.

Quartile Coefficient of Variation (Q_{cv}): It is only used for vehicular speed:

$$Q_{cv} = \frac{Q_3 - Q_1}{Q_3 + Q_1} * 100 \tag{4}$$

where Q_{cv} is the quartile coefficient of variation, Q_1 is the first quartile of a variable, and Q_3 is the third quartile.

Clustering approach

Several clustering approaches have been applied in the literature among which k-means, k-medoid, and hierarchical clustering are among the most commonly used algorithms (*84; 85*). In this study, these methods were employed and results were compared based on the goodness of clustering measures. The following presents a brief explanation of the algorithms and the approach to the clustering method selection and determining the number of clusters for the classification of driving events.

K-means clustering

K-means is a partitioning algorithm for grouping data points into *k* clusters with *k* centroids in a way that each data point is grouped in the closest centroid (*52*). The objective function in K-means algorithms is to minimize the error presented below (*53*):

$$E = \sum_{i=1}^{k} \sum_{x \in C_i} d(x, \mu(C_i)) \tag{5}$$

where $C_1, C_2, \ldots, C_k$ are the *k* clusters, $\mu(C_i)$ is the centroid of cluster C_i, and $d(x, \mu(C_i))$ is the function for calculating distance between the observation *x* and centroid $\mu(C_i)$.

Although several formulas have been suggested in the literature for calculating the distance, in this study, Euclidean distance is used. The Euclidean distance between objects and centroids are calculated using the equation presented below:

$$d_i = \sqrt{\sum_{k=1}^{n} ({x_k}^{(i)} - \mu_i)^2} \tag{6}$$

where $x_1, x_2, \dots, x_k$ are objects clustered in cluster i and μ_i is the centroid of cluster *i*.

Assuming *k* as the number of clusters, the K-means algorithm includes the following steps:

1st Step: Select a random set of centroids $(C_1, C_2, \dots, C_k)$ from the data set

2nd Step: Assign the remaining objects to the nearest cluster

3rd Step: Update the clusters' centroids by recalculating the mean value of the objects in clusters

4th Step: Reassign the objects to the nearest cluster with updated centroids in the 3rd step

5th Step: Repeat the *3rd* and 4th steps until the position of centroids do not change

K-medoids clustering

Unlike K-means in which data points are clustered around the centroids, the K-medoids algorithm clusters the objects around representative data points called medoids (*54*). K-medoids algorithm minimizes the following error function:

$$E = \sum_{i=1}^{k} \sum_{x \in C_i} (x - m(C_i)) \tag{7}$$

where $C_1, C_2, \dots, C_k$ are the clusters, and $m(C_1), m(C_2), \dots, m(C_k)$ are the corresponding medoids of the clusters.

Although previous studies applied several methods for K-medoids clustering, this study uses Partitioning Around Medoids (PAM) as a commonly-used algorithm proposed by (*55*). Assume that *k* is the number of clusters, the PAM algorithm includes the following steps:

1st Step: Randomly choose *k* objects as initial cluster medoids from the data set

2nd Step: Assign the remaining objects in the data set to the nearest medoids

3rd Step: Compute the error in equation (7)

4th Step: Randomly choose a non-medoid object from the data set

5th Step: Assume that one of the existing medoids is replaced with the chosen objects in the *4th* step: and compute the error

6th Step: Replace the old medoid with the medoid if the calculated error in step 5 is lower than the error in the *3rd* Step

7th Step: Repeat the steps 2 to 6 until the position of medoids do not change

Hierarchical clustering

Hierarchical clustering is an unsupervised learning method that clusters the objects by forming a hierarchy of clusters which can be visualized as a dendrogram. Generally, two major approaches have been proposed for hierarchical clustering: agglomerative (bottom-up) and divisive (top-down). In this study, the agglomerative method which is the most common approach (*86*) was used for driving style classification. The steps of the agglomerative hierarchical clustering are as follows:

1st Step: Assume every object as a cluster

2nd Step: Calculate the distance between every pair of clusters

3rd Step: Find the two closest clusters and merge them into one single cluster

4th Step: Repeat steps 3 and 4 until only one cluster remains

Selecting number of clusters and clustering method

Each cluster in driving style classification represents a driving style. Although several studies have proposed different methods (e.g., clustering quality measures), there is still no certain solution for determining the number of clusters (*85*). Therefore, deciding about the number of clusters is typically based on the judgment of the researchers. In this study, 3-cluster classification is considered because first, it better presents the variation between different groups, and second, it is more in line with the past research carried out on the topic (*2; 4; 11; 21-24; 32; 63*).

The clustering method in the study is selected using the average silhouette width criterion (*ASWC*) which indicates how properly the data points are grouped in the clusters. *ASWC* ranges between -1 to +1, and larger values of ASWC show better quality clustering concerning between-cluster heterogeneity and within-cluster homogeneity (*55*). Suppose that the objects are grouped in *k* clusters. Therefore, the silhouette coefficient of data point x_i in cluster C_i is calculated using the following equation (*55*):

$$S_{x_i} = \frac{b_{x_i} - a_{x_i}}{\max(a_{x_i}, b_{x_i})} \tag{8}$$

where S_{x_i} is the silhouette coefficient of the object x_i, b_{x_i} is the minimum average distance from object x_i and objects in other clusters, and a_{x_i} is the average distance from x_i and other objects in the same cluster. Therefore, the silhouette width of cluster *j* and the average silhouette width of all clusters is computed using the following two equations:

$$\mathrm{SWC_j} = \frac{1}{\mathrm{n}} \sum_{\mathrm{i=1}}^{\mathrm{n}} \mathrm{S_{x_i}} \tag{9}$$

$$ASWC = \frac{1}{k}\sum_{j=1}^{k} S_j \tag{10}$$

where *k* is the number of clusters, and *n* is the number of objects grouped in the same cluster.

Fuel consumption and emission models

Autonomie software

Autonomie (*87*) provides a high fidelity simulation framework to realistically assess fuel consumption, emissions, and the overall performance of vehicles. The Simulink-based vehicle models within Autonomie actuate virtual pedals to follow a drive cycle–speed trajectory as a function of time. Autonomie is a forward-looking command-based simulation package that uses real commands to simulate fuel consumption in real-world conditions. For example, given a desired speed, the wheel torque needed for achieving the speed is estimated by the driver model. Then, the power controller module in the vehicle sends real commands to other components to achieve the desired wheel torque. Thus, Autonomie enables the development of fuel consumption and emission models which are based on the physics of the vehicles instead of lookup tables and generalized equations. Autonomie includes a large number of predefined powertrain configurations and component technologies. This provides flexibility to estimate fuel efficiency and emissions at a vehicle level for different powertrains such as internal combustion engines, hybrid, and electric.

The architecture of Autonomie® and a flow diagram for processing the vehicle trajectories are shown in Figure 3-2. Within Autonomie®, the propulsion and braking demand for vehicle level components for a given vehicle model and driving cycle are allocated by the Vehicle Propulsion Controller (VPC). Within the low-level controls, the component tasks including clutch, engine, motor, and gearbox are coordinated by a combination of VPC and powertrain components during transient processes. The engine model uses torque at a certain speed to estimate fuel rate by requesting torque from a powertrain controller. The assumptions for efficiency and power density (Islam et al., 2018) are based on Department of Energy assumptions for 2019 vehicles. Each of the vehicles is considered as a midsize vehicle with power and mass sized to meet 0-70 mph performance requirement. The vehicle models have 5% prediction error under most test cases as verified by the US Department of Energy (Jeong et al., 2019).

VSP model

The three conventional techniques for describing vehicle activity include the use of speed, driving schedule, and operating mode distribution. This technique captures all driving behavior and vehicular activity while modeling emissions and is thus, considered more accurate. Vehicle emissions and engine load are directly correlated while VSP serves as a proxy for the engine load. VSP microscopic model has been used to estimate emissions regarding vehicle second-by-second speed, acceleration, and terrain gradient (*88-90*). Speeds estimated at 1s activity by averaging ten consecutive points within 1Hz were used as inputs for the model. The VSP for second by second data is calculated using equation 11.

$$VSP = v\left(\frac{A}{M}\right) + \left(\frac{B}{M}\right)v^2 + \left(\frac{C}{M}\right)v^3 + (a + g(Arctan(grade)))v \tag{11}$$

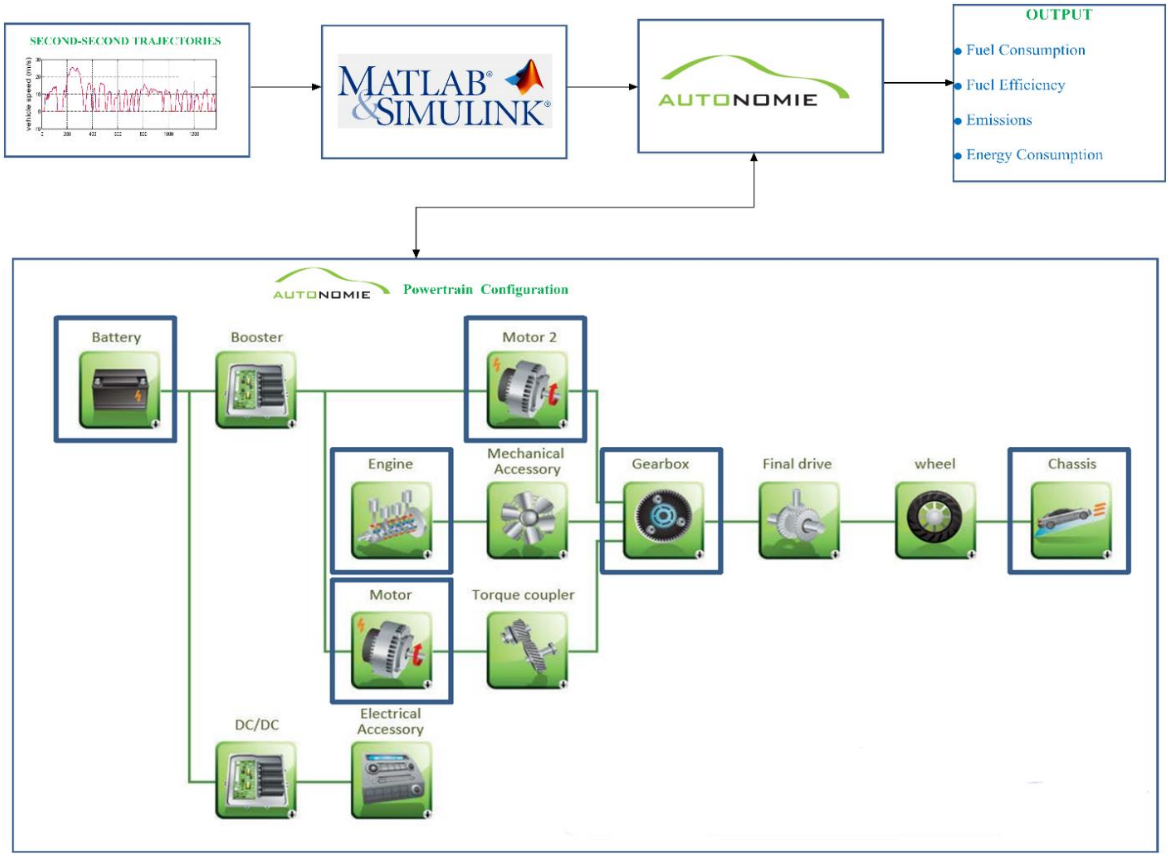

Figure 3-2 Architecture for Autonomie model simulations

where *VSP* is vehicle specific power [kW/metric ton]; *v* is vehicle velocity [m/s]; *a* is acceleration (positive or negative) [m/s^2]; and grade is the slope of terrain [±%]. A is the rolling resistance coefficient, B is the rotational resistance coefficient. C is the aerodynamic drag coefficient. The grade was assumed based on guidelines (*91*) from the Highway Capacity manual that suggest a maximum grade of 5% for arterials and 3% for freeways based on design speed. The simplified form with coefficients is provided in equation 12.

$$VSP = v[1.1a + 9.81\left(Arctan(grade)\right) + 0.132] + 0.000302v^3 \quad (12)$$

The total emissions for a vehicle can be calculated as shown in equation 14; *t* is the time vehicle drives in the VSP-Mode; CO_2 is carbon dioxide (g/s); *NOx* is oxides of nitrogen (g/s); *CO* is carbon monoxide (g/s); *HC* is hydrocarbons (g/s).

$$Total\ Emissions = CO_2^{VSP\text{-}Mode} * t + CO^{VSP\text{-}Mode} * t + NO_x^{VSP\text{-}Mode} * t + HC^{VSP\text{-}Mode} * t \quad (13)$$

VSP operating mode bins were derived based on MOVES matrix as provided in Table 3-1. The derived operating modes bins were correlated to pollutants and green-house gas emissions based on vehicle activity within MOVES matrix. The total emissions were estimated by summing the calculated emissions for each operating mode bin as a function of time spent in those operating mode bins.

Likewise, the fuel consumption rate was calculated as a function of emission rates within MOVES operating bins shown in equation 4 (*88; 89*). The emission rates are calculated by taking its ratio over time spent in operating bins.

$$FR = 1.154(ER_{HC} * \frac{12}{13} + ER_{CO} * \frac{12}{28} + ER_{CO2} * \frac{12}{44}) \tag{14}$$

where ER_{HC} represents the emission rate for HC, ER_{CO} represents the emission rate for CO and ER_{CO2} represents the emission rate for $CO2$.

RESULTS AND DISCUSSION

In this section, first, the descriptive statistics of the volatility measures used for the classification are provided. Then, the driving classification results in work zones and curves located on freeways and arterials are presented. Next, the VSP and Autonomie models are used to estimate the emissions and fuel consumption of vehicles with different driving styles driving through work zones and curves, using the naturalistic driving data from SHRP2.

Descriptive Statistics

Tables 3-2 and 2.3 show the descriptive statistics of the driving volatility measures. Table 3-2 belongs to the events that occurred at work zones and curves while Table 3-3 presents the statistics of the freeway and arterial events which occurred at work zones or curves. Based on the results, except for *Speed*-C_v and *Speed*-Q_{CV}, volatility measures have larger values in curves than in the work zones, indicating that generally, drivers drive more volatile in curves compared to work zones.

Table 3-1 VSP modes and average emissions rate (88; 89)

VSP-Mode	Definition (kw/t)	CO_2 (g/s)	CO (mg/s)	NO_x (mg/s)	HC (mg/s)
1	VSP < -2	1.671	7.807	0.901	0.450
2	-2 ≤ VSP < 0	1.458	3.908	0.628	0.257
3	0 ≤ VSP < 1	1.135	3.347	0.346	0.406
4	1 ≤ VSP < 4	2.233	8.335	1.173	0.432
5	4 ≤ VSP < 7	2.920	10.959	1.706	0.530
6	7 ≤ VSP < 10	3.525	17.013	2.368	0.705
7	10 ≤ VSP < 13	4.107	20.026	3.103	0.822
8	13 ≤ VSP < 16	4.635	29.222	4.234	0.976
9	16 ≤ VSP < 19	5.161	35.531	5.069	1.112
10	19 ≤ VSP < 23	5.633	55.068	5.865	1.443
11	23 ≤ VSP < 28	6.535	113.824	7.623	2.061
12	28 ≤ VSP < 33	7.585	207.586	12.149	3.373
13	33 ≤ VSP < 39	9.024	441.775	15.456	4.857
14	39 ≤ VSP	10.088	882.300	17.863	10.948

Notes: The average emission rates are for Tier 1 light-duty gas vehicles with engine displacement <3.5L and odometer< 50,000 miles.

Table 3-2 Descriptive statistics of classification features for events that occurred in work zones and curves

Classification features	Work zones				Curves			
	min	max	mean	S.D.	min	max	mean	S.D.
Speed-SD	0.02	31.02	6.03	5.34	0.00	43.54	6.14	5.39
Speed-D_{mean}	0.01	29.95	5.00	4.63	0.00	41.96	5.10	4.62
Speed-C_v	0.31	284.79	18.84	36.08	0.00	265.18	15.62	22.42
Speed-Q_{CV}	0.01	100.00	12.14	19.42	0.00	100.00	11.19	16.11
$Accl_x$-SD	0.00	0.20	0.05	0.03	0.00	0.19	0.05	0.03
$Accl_x$-D_{mean}	0.00	0.15	0.04	0.03	0.00	0.16	0.04	0.03
$Accl_y$-SD	0.00	0.20	0.04	0.03	0.00	0.37	0.06	0.04
$Accl_y$-D_{mean}	0.00	0.15	0.03	0.03	0.00	0.28	0.05	0.03

Table 3-3 Descriptive statistics of classification features for work freeways and arterial events that occurred in work zones and curves

Classification features	Freeways events occurred at work zones or curves				Arterials events occurred at work zones and curves			
	min	max	mean	S.D.	min	max	mean	S.D.
Speed-SD	0.23	43.54	4.53	4.81	0.00	31.02	6.97	5.51
Speed-D_{mean}	0.17	41.96	3.77	4.14	0.00	29.95	5.77	4.74
Speed-C_v	0.23	260.51	7.47	15.45	0.00	284.79	20.99	29.96
Speed-Q_{CV}	0.00	100.00	5.41	10.32	0.00	100.00	14.45	18.80
$Accl_x$-SD	0.01	0.20	0.04	0.03	0.00	0.19	0.06	0.03
$Accl_x$-D_{mean}	0.00	0.14	0.03	0.02	0.00	0.16	0.04	0.03
$Accl_y$-SD	0.01	0.29	0.04	0.04	0.00	0.37	0.07	0.05
$Accl_y$-D_{mean}	0.00	0.25	0.03	0.03	0.00	0.28	0.05	0.04

The larger values of driving volatility measures in curves are expected since driving through a curve requires the drivers to have more variation in the acceleration, deceleration, and vehicle steering wheel angle to keep the vehicle on the road. Similarly, based on Table 3-3, driving in arterials is more volatile than in freeways. This may be attributed to a higher alteration in the road environment and traffic conditions in arterials compared to freeways.

Driving classification results

Selecting the clustering method

Every object in the data belongs to a driving event that can be grouped in clusters. To make the classification features comparable, the data were standardized. K-means, K-medoids, and hierarchical clustering were applied. Figure 3-3 presents the graph of *ASWC* values for different clustering methods with different numbers of clusters on work zones, curves, freeways, and arterials. From the figure, for classification with 3 clusters, the K-means algorithm has larger *ASWC* values showing that it results in better clustering than the hierarchical and K-medoids methods. Thus, in this study, the K-means clustering algorithm was chosen over other methods.

Classification results

The output of K-means clustering assigns a number from 1 to 3 to each event which represents the cluster to which the driving event belongs. Determining which driving style every cluster represents is based on the magnitude of volatility measures in each cluster. Table 3-4 shows the scaled mean values of volatility measures of events that occurred in work zones, curves, freeways, and arterials.

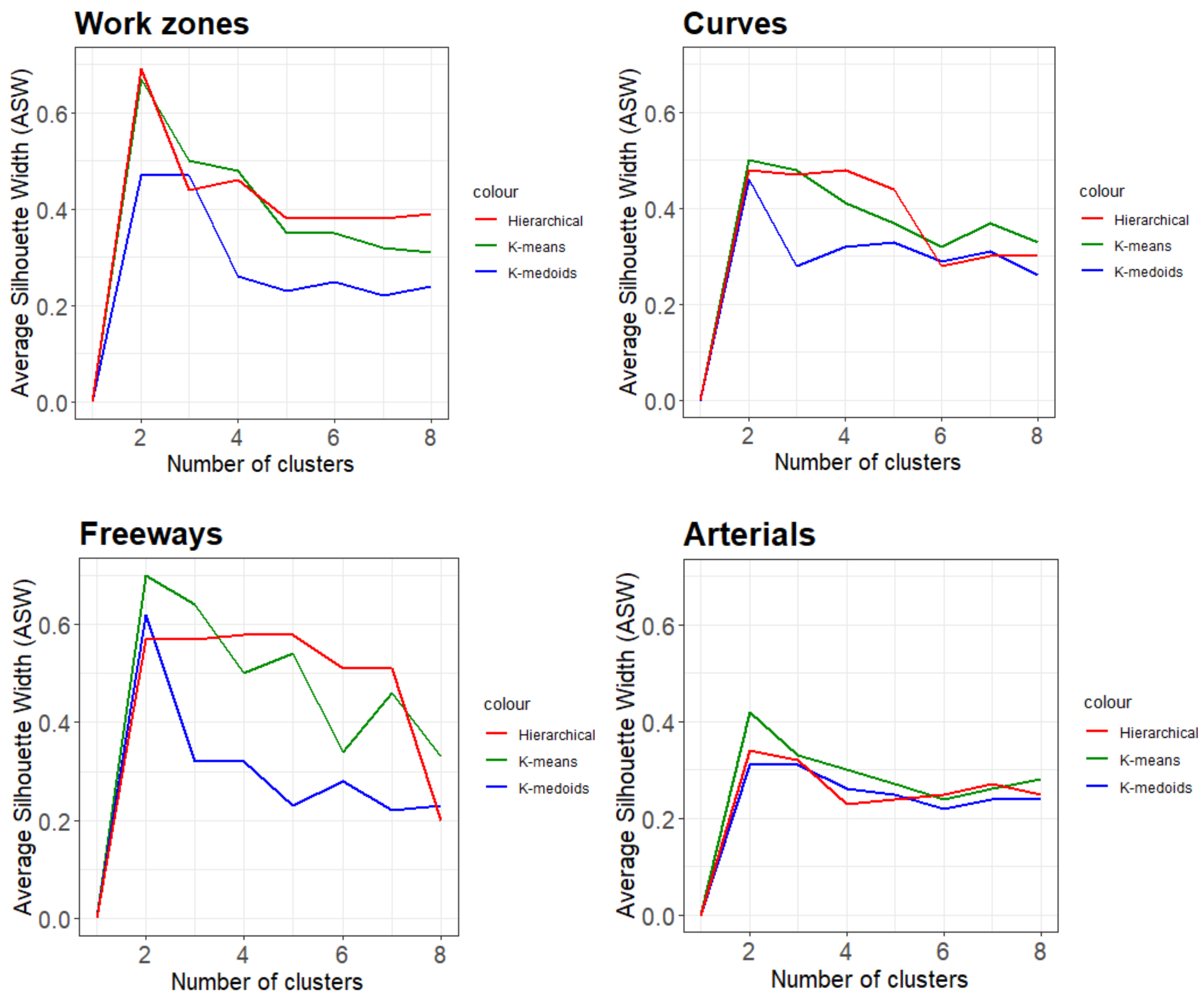

Figure 3-3 Performance of K-means, hierarchical, and K-medoids clustering based on ASWC

Table 3-4 The scaled cluster centers work zones, curves, freeways, and arterials

Location	Driving Style	*Speed*-SD	*Speed*-D_{mean}	*Speed*-C_v	*Speed*-Q_{CV}	$Accl_x$-SD	$Accl_x$-D_{mean}	$Accl_y$-SD	$Accl_y$-D_{mean}
Work zones	Cluster 1 (Aggressive)	1.45	1.44	0.92	1.04	1.26	1.31	2.07	2.04
	Cluster 2 (Normal)	0.72	0.67	0.48	0.58	0.81	0.8	-0.34	-0.36
	Cluster 3 (Calm)	-0.57	-0.55	-0.37	-0.43	-0.57	-0.59	-0.26	-0.25
Curves	Cluster 1 (Aggressive)	1.73	1.75	1.53	1.66	1.38	1.4	0.36	0.29
	Cluster 2 (Normal)	0.2	0.17	0.09	0.04	0.51	0.49	1.03	1.03
	Cluster 3 (Calm)	-0.53	-0.52	-0.43	-0.45	-0.57	-0.57	-0.53	-0.51
Freeways	Cluster 1 (Aggressive)	1.53	1.51	1.136	1.27	1.35	1.37	1.43	1.41
	Cluster 2 (Normal)	0.06	0.05	-0.03	-0.04	0.23	0.25	-0.08	-0.09
	Cluster 3 (Calm)	-0.55	-0.54	-0.36	-0.39	-0.61	-0.62	-0.42	-0.41
Arterials	Cluster 1 (Aggressive)	1.33	1.32	0.99	1.13	1.09	1.12	0.19	0.14
	Cluster 2 (Normal)	-0.13	-0.15	-0.15	-0.19	0.16	0.13	0.86	0.88
	Cluster 3 (Calm)	-0.64	-0.63	-0.44	-0.49	-0.68	-0.67	-0.59	-0.57

This table shows that there is a common trend in the driving volatility of events in different locations in a way that, respectively, the largest values of volatility measures belong to clusters 1, 2, and 3. To better visualize the variation of classification features in different clusters, radar charts were used (Figure 3-4). In radar charts, classification features are represented by axes in which the length of spokes is proportional to the magnitude of the classification features. A line can be drawn through these values to form a polygon that shows how classification features vary along the clusters. Specifically, larger areas of polygons indicate higher means of classification features in the clusters. Therefore, it is rational to respectively assign the small, medium, and large polygons (clusters 3, 2, and 1) to calm, normal, and aggressive driving styles since driving volatility is positively associated with aggressive driving (*46*).

Table 3-5 presents the classification results of driving events in work zones and curves including the number and percentage of different driving styles. Based on the results, respectively, 12.19%, 15.36%, and 14.92% of the total driving events in work zones, curves, and locations other than work zones or curves are categorized into aggressive driving. This finding shows that aggressive driving style is not a common driving behavior among the drivers but most driving events are categorized as calm driving styles in all locations. Especially, the proportion of aggressive driving in work zones is the lowest. In curves, the percentage of aggressive events is larger than in work zones (15.36 %). However, calm driving still constitutes the majority of events (59.37 %). These findings show that overall driving behavior in work zones and curves is consistent with the road condition and traffic rules which require slow and cautious driving.

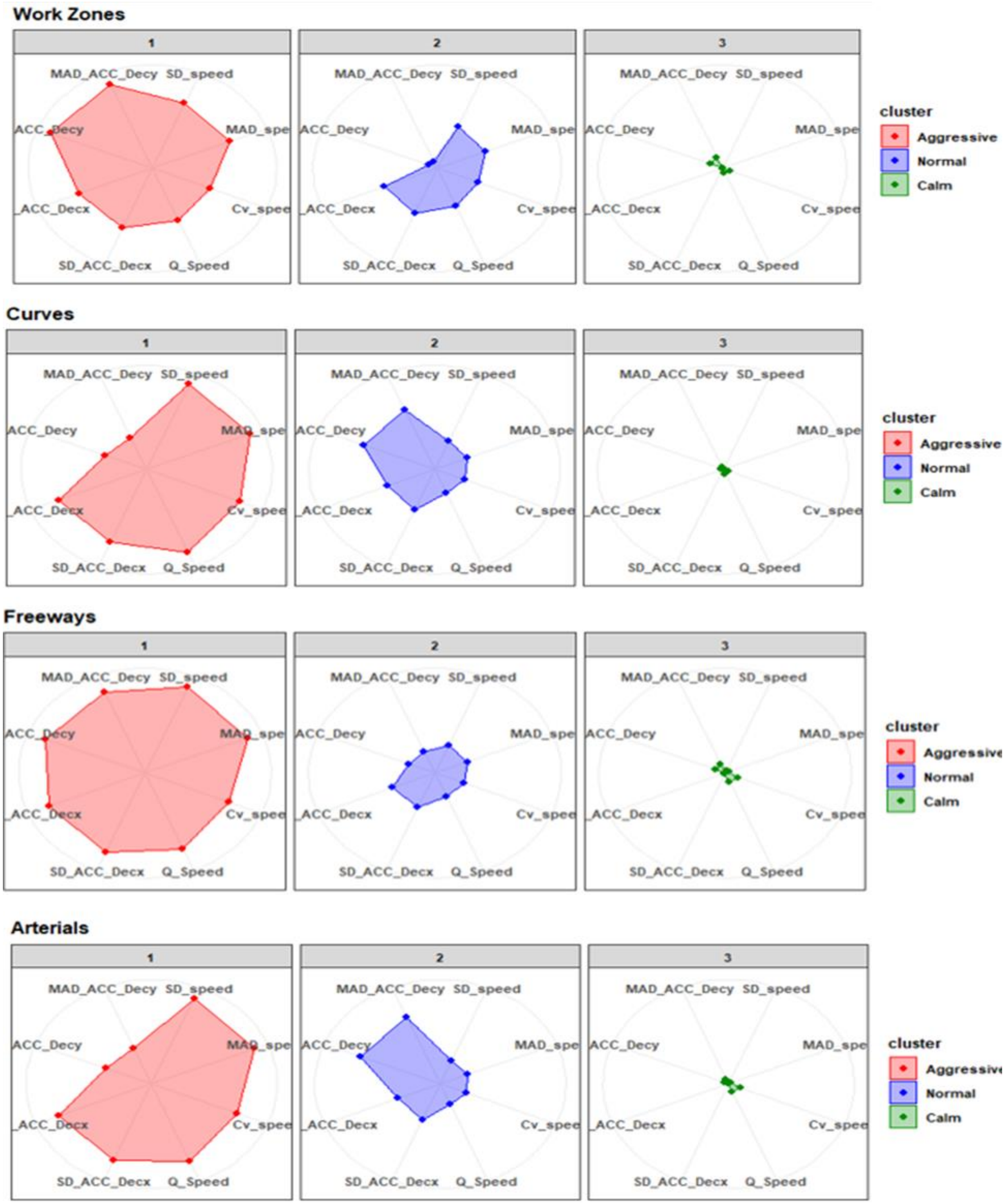

Figure 3-4 Radar charts of mean values of classification features in the clusters for work zones, curves, freeways, and arterials

Table 3-5 Proportion of calm, normal, and aggressive driving styles occurred in work zones, curves, and other locations

Cluster	Work zones		Curves		Other	
	Nom.of events	%	Nom.of events	Percentage	Nom.of events	Percentage
Aggressive	44	12.19%	195	15.36%	1174	14.92%
Normal	91	25.21%	321	25.27%	1632	20.76%
Calm	226	62.60%	754	59.37%	5059	64.32%
Overall	361	100%	1270	100%	7865	100%

Table 3-6 presents the results of driving style classification for freeways and arterials events that occurred in work zones or curves. It was found that the percentage of aggressive driving events on arterials (25.80 %) is higher than on freeways (16.77 %). A larger proportion of aggressive events in arterials compared to freeways could be because of the higher complexity of road environment, higher number of commercial establishments, intersection points, driveways, and more complex interaction with vulnerable road users, which result in rapid acceleration and braking and abrupt speed changes.

The Principal Component Analysis (PCA) was used to decrease the dimensions to visualize the clusters in a two-dimensional space. Figure 3-5 illustrates the labeled clusters in different locations. The figure shows that the clusters of calm driving styles in all locations are denser, indicating that the majority of the driving events in these locations are identified as calm driving styles. These results are in line with the findings presented in Tables 3-5 and 3-6.

Fuel consumption and emissions modeling results

Comparison of work zones and curves with the baseline using VSP model

Table 3-7 summarizes the results for average emissions within work zones and emissions before entering work zones (representing baseline conditions). Work zones and construction areas are expected to have an impact on emissions and the results reveal that as vehicles enter the work zones, they experience higher variations in speeds and accelerations due to capacity drops. This results in higher emission rates by an average of 10.63% for work zones on arterial compared to the baseline case.

Table 3-6 Proportion of calm, normal, and aggressive driving styles in freeways and arterials occurred in work zones and curves

Cluster	Freeway events occurred in work zones/curves		Arterial events occurred in work zones/curves		Other events occurred in work zones/curves	
	Nom.of events	%	Nom.of events	%	Nom.of events	%
Aggressive	101	16.77%	210	25.80%	30	19.23%
Normal	199	33.06%	268	32.92%	44	28.21%
Calm	302	50.17%	336	41.28%	82	52.56%
Overall	602	100%	814	100%	156	100%

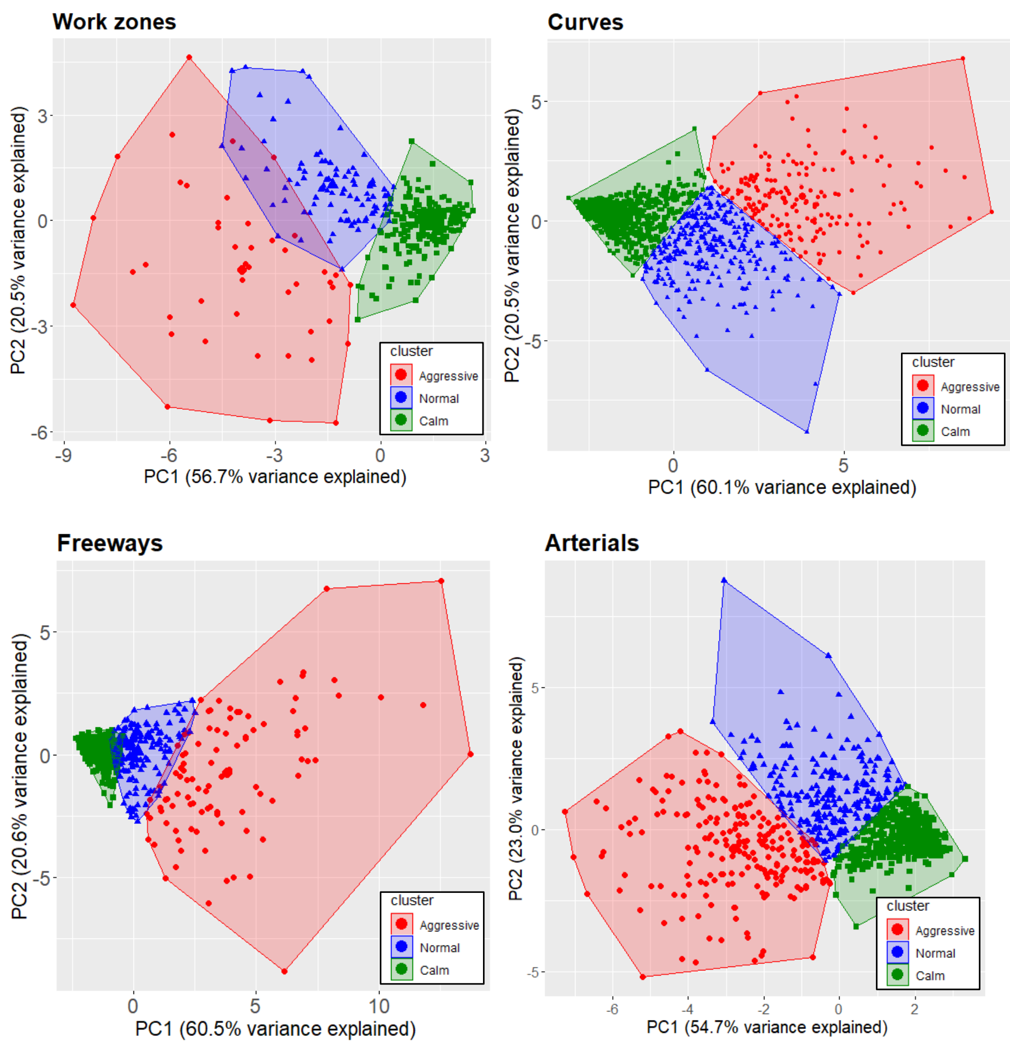

Figure 3-5 Two-dimensional-space visualization of clusters

Table 3-7 Average Emissions resulting from Work zone

Roadway Type	Measure	CO2 (g)	CO (g)	NOx (g)	HC (g)	Total (g)
Freeway	Base	1175.90	98.52	2.04	1.23	1277.68
	Within Work zone	1349.13	110.92	2.31	1.39	1463.75
	% Change	14.73	12.58	13.37	13.37	14.56
	p-value	<0.05	0.056	<0.05	<0.05	<0.05
Arterials	Base	367.53	23.74	0.57	0.31	392.14
	Within Work zone	407.29	25.60	0.61	0.33	433.84
	% Change	10.82	7.85	7.79	7.99	10.63
	p-value	<0.05	0.061	<0.05	0.057	<0.05

On the other hand, an increase of 14.56% with respect to the baseline is found for work zones on freeways. The differences between the emissions results for freeways and arterial are expected due to higher traffic and speed limits of freeways as opposed to arterials. Furthermore, traffic flow and congestion levels play an important role in varying vehicle dynamics, leading to increased emissions. The three analyzed flow regimes show an increase in emissions as traffic conditions transition from free flow to heavily congested. These impacts are shown in Figures 3-6. Figure 3-6 reveals that emissions for work zones on both freeways and arterials increase as the traffic flow conditions deteriorate and change from free flow to stable and unstable conditions. This is expected since queues generated from bottlenecks result in stop-and-go traffic waves that increase exhaust emissions. Likewise, curves are critical segments of the roads in transportation networks, especially when considering emission levels. This is because traveling on curves increases vehicle power consumption that could lead to higher emissions. The results in Table 3-8 reveal a higher rate of variation in acceleration/deceleration leading to higher emissions as vehicles start to navigate the curves. The emissions are higher as opposed to baseline conditions. The difference in emission levels in arterial and freeway is 18.83% and 12.08% respectively, compared to the baseline case. Further, traffic flow conditions reveal a similar trend towards an increase in emission levels. Figure 3-7 shows emission levels for both freeway and arterials under the three flow regimes. As flow transitions from free flow to stable and congested regimes, emissions are observed to increase. Emissions are observed to increase as traffic gets congested and ultimately reached breakdown. Congested flow conditions show the worst emission levels due to unstable flow as vehicles queue together.

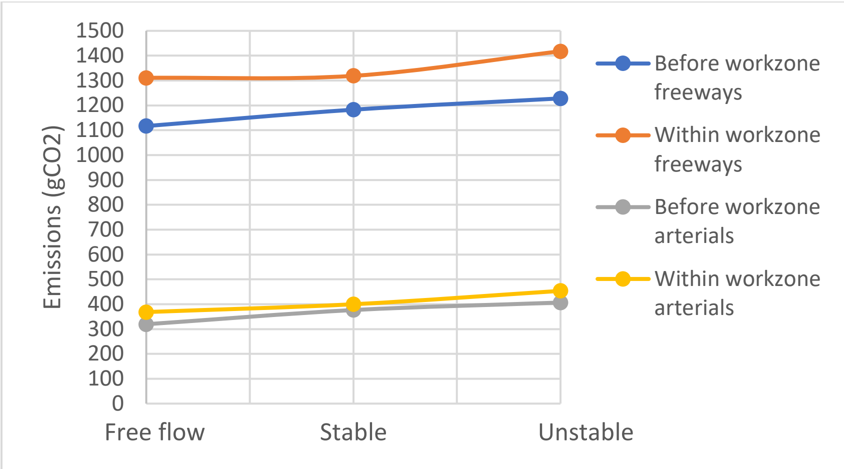

a) CO2 Emissions

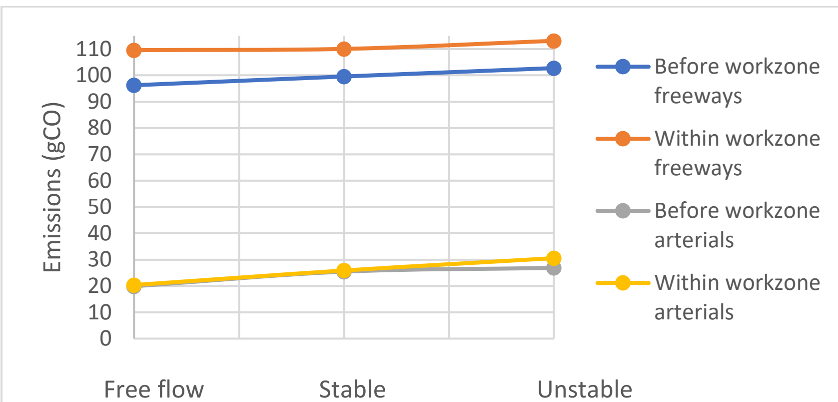

b) CO Emissions

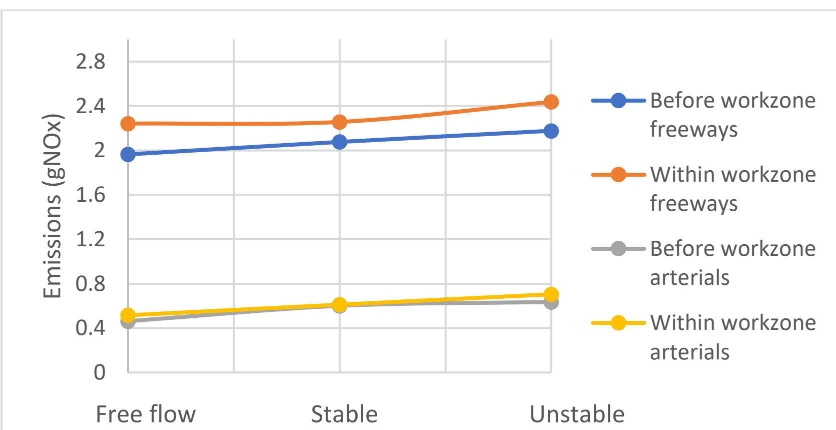

c) NOx Emissions

Figure 3-6 Emissions in work zones under different traffic flow regimes

Table 3-8 Average Emissions resulting from Curves

Roadway Type	Measure	CO2 (g)	CO (g)	NOx (g)	HC (g)	Total (g)
Freeway	**Base**	375.09	33.11	0.65	0.39	409.25
	Within curve	448.87	36.21	0.78	0.45	486.30
	% Change	19.67	9.35	18.73	14.81	18.83
	p-value	<0.05	0.061	<0.05	0.057	<0.05
Arterials	**Base**	322.92	25.20	0.54	0.32	348.98
	Within curve	364.31	25.91	0.59	0.33	391.13
	% Change	12.82	2.80	9.08	3.95	12.08
	p-value	<0.05	0.069	<0.05	0.061	<0.05

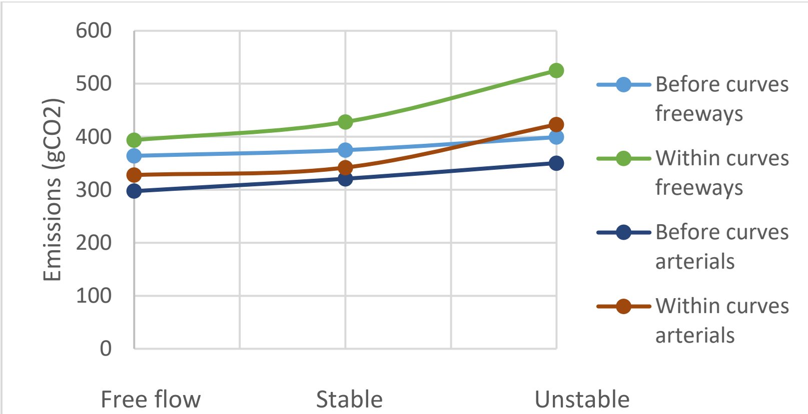

Chapter 1 CO2 Emissions

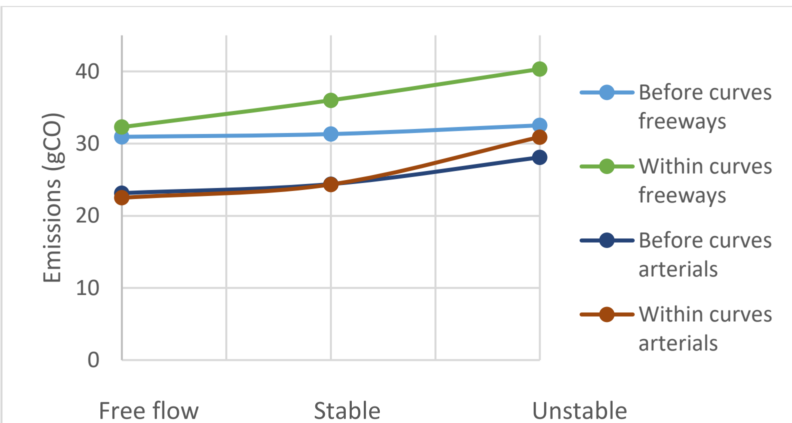

Chapter 2 CO Emissions

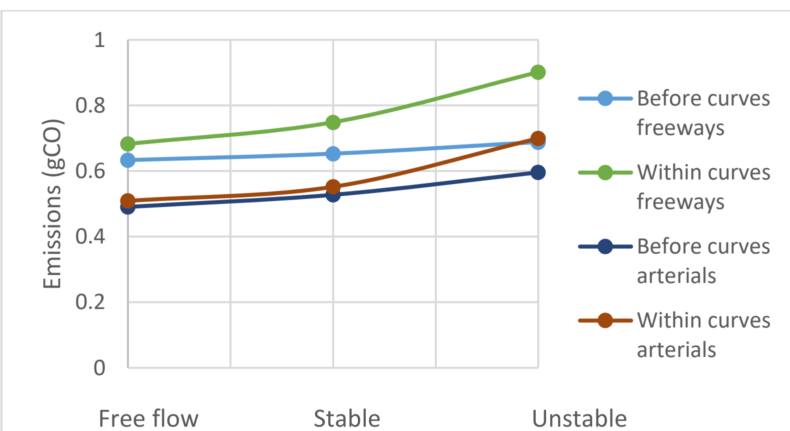

Chapter 3 NOx Emissions

Figure 3-7 Emissions in curves under different traffic flow regimes

Modeling results of fuel consumption show that the change in driving behavior resulting from the transition towards driving within work zones and curves is expected to result in increased fuel consumption. Fuel consumption is sensitive to driving distance thus, instances of driving with similar distance or time were selected for comparison between different categories. Figure 3-8 reveals that fuel consumption on average increases while driving within work zones on freeways under the three different flow regimes. As the flow conditions transition from free flow to stable and unstable, fuel consumption increases. These results are consistent with emissions resulting from similar conditions. Fuel consumption on freeways is observed to be higher compared to arterials due to higher speed limits and traffic on freeways. An average increase of 15.70% and 10.50% is observed in fuel consumption on work zones within freeways and arterials.

Likewise, the results for fuel consumption on curves are provided in Figure 3-9. These results reveal a similar trend compared to work zones. Fuel consumption is observed to increase while driving over curves as opposed to the baseline driving case. Furthermore, fuel consumption increases as flow transitions from free-flow to stable and unstable. Similar to work zones, driving on curves in freeways result in higher fuel consumption compared to driving on arterials. On average, a 19.06% increase in fuel consumption is observed on freeways while an 11.69% increase in fuel consumption is observed on arterials when driving through curves.

Results of Autonomie model

The change in driving behavior resulting from the transition towards driving within work zones and curves is expected to impact the fuel economy.

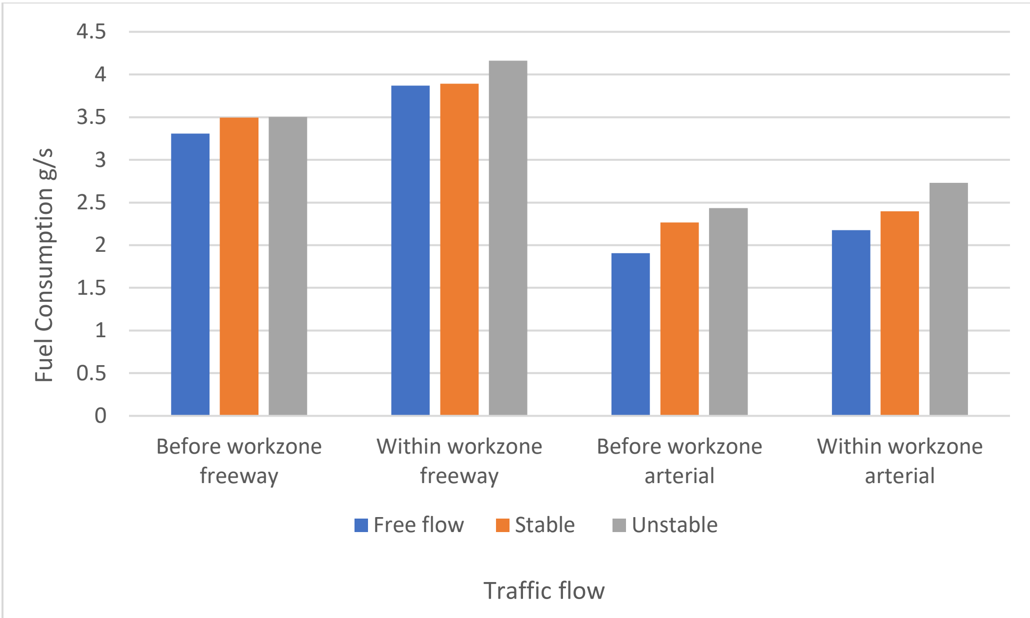

Figure 3-8 Average fuel consumption rate in work zones

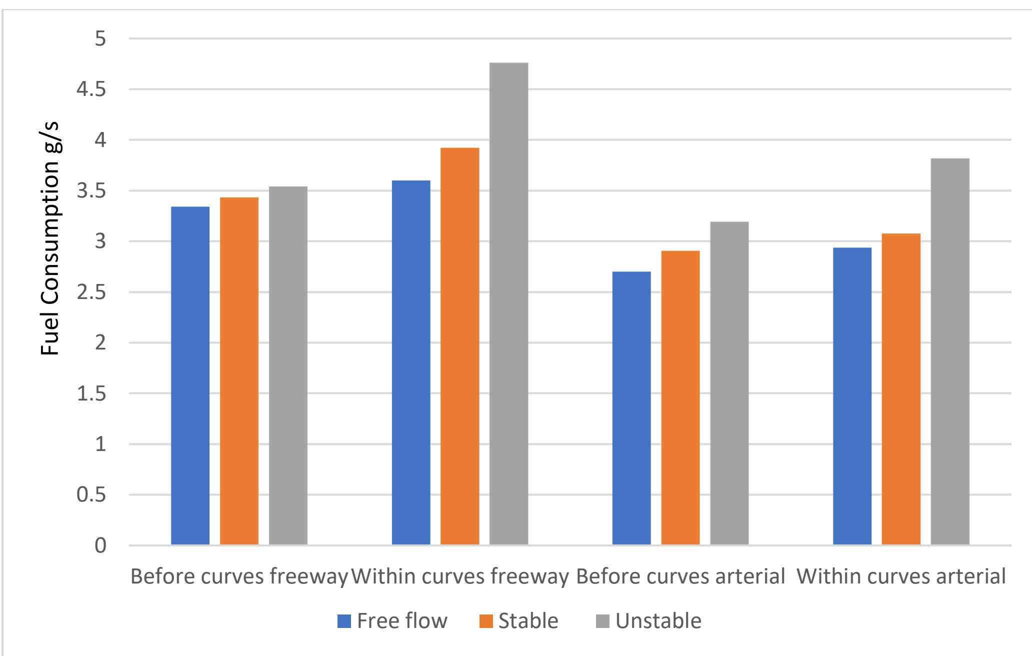

Figure 3-9 Average fuel consumption rate on curves

Fuel economy is sensitive to driving distance thus, instances of driving with similar distance or time were selected for comparison between different categories. The estimates are provided for multiple scenarios of Autonomie drive cycle simulations. Figure 3-10 reveals that fuel economy on average decreases under aggressive driving within both work zones and curves as opposed to calm and normal driving behavior. As the driving behavior transitions from aggressive to normal and calm driving, fuel economy increases. This is expected since aggressive driving involves abrupt stop-and-go waves that influence the flow of traffic resulting in lower fuel economy. An average improvement of 23% and 59.1% in fuel economy is observed with calm driving as opposed to aggressive driving within curves and work zones.

Likewise, the differing dynamics of freeways and arterials are expected to influence the fuel economy differently. Figure 3-11 reveals that aggressive driving on both freeways and arterials within curves and work zones reduces fuel economy. Fuel economy for all three driving styles on freeways is observed to be higher compared to arterials. This may be attributed to higher speed limits and lower stop and go waves due to the absence of traffic control signals on freeways Calm driving style shows the highest improvement in fuel economy within both freeways and arterials. On average, calm driving reveals a 50.4% increase in fuel economy on freeways while a 28.4% increase in fuel economy on arterials compared to aggressive driving.

Work zones are expected to have an impact on emissions and the results reveal that as vehicles enter the work zones, they experience higher variations in speeds and accelerations due to capacity drops.

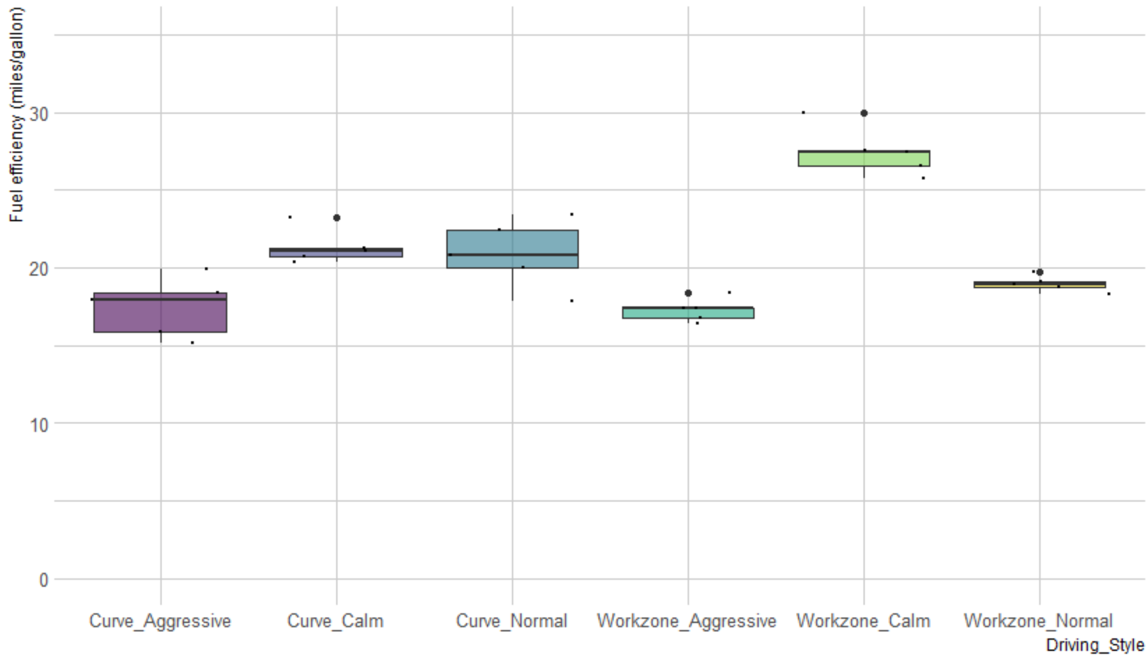

Figure 3-10 Fuel economy estimates for curves and work zones based on driving styles

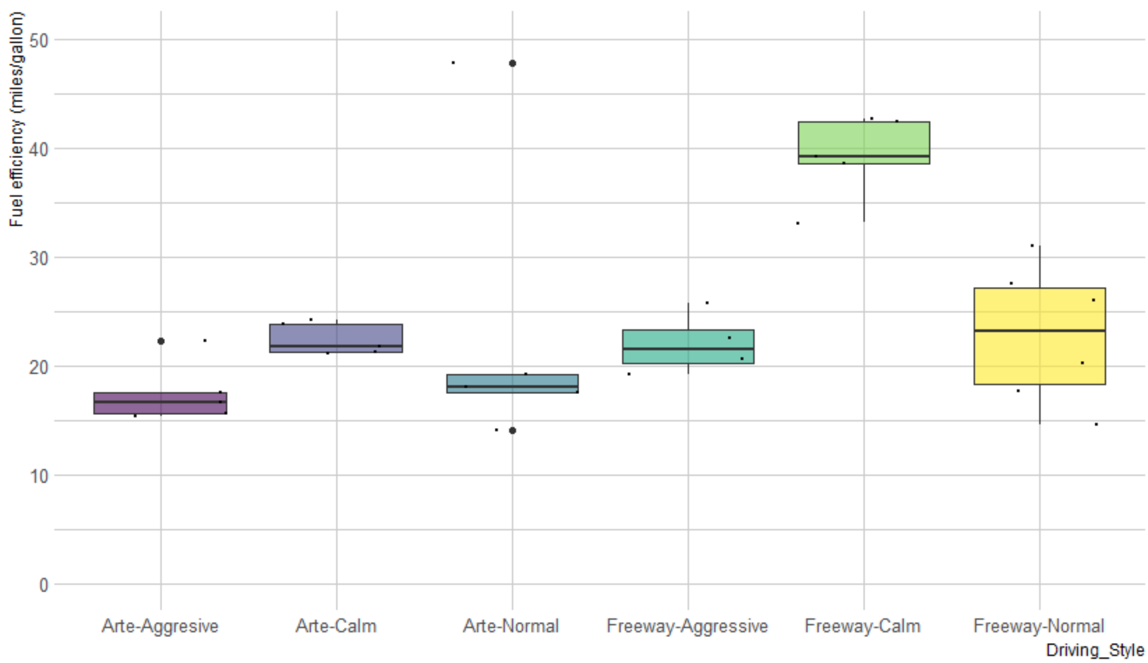

Figure 3-11 Fuel economy estimates for freeways and curves based on driving styles

Likewise, curves are critical segments of the roads, especially when considering emission levels. This is because traveling on curves increases vehicle power consumption that could lead to higher emissions. Further, driving styles and transitions between aggressive, normal, and calm behavior also influence vehicular emissions. As depicted in Figure 3-12, an average decrease of 18.8% is observed for calm driving within curves compared to aggressive driving. On the other hand, a decrease of 39.9% is observed with calm driving within work zones as opposed to aggressive driving. These are intuitive findings since aggressive driving behavior is expected to influence acceleration-deceleration regimes and results are in line with the findings for fuel economy. Further, differences are expected between the emissions estimates for freeways and arterial due to higher traffic and speed limits of freeways as opposed to arterials and lower flow disruption on freeways. Furthermore, traffic flow and congestion levels play an important role in varying vehicle dynamics, leading to increased emissions. The three driving styles in Figure 3-13 show a decrease in emissions as the driving style transitions from aggressive to calm. An average reduction of 24.7% and 41.6% is observed within arterials and freeways. Figure 3.13 reveals that emissions for both freeways and arterials within curves and work zones are increased with aggressive and normal driving styles due to unstable driving conditions. Further, arterials are observed to produce higher emissions compared to freeways for the observed driving styles. This is expected due to excessive queues generated from bottlenecks on arterials that result in stop-and-go traffic waves and increase exhaust emissions.

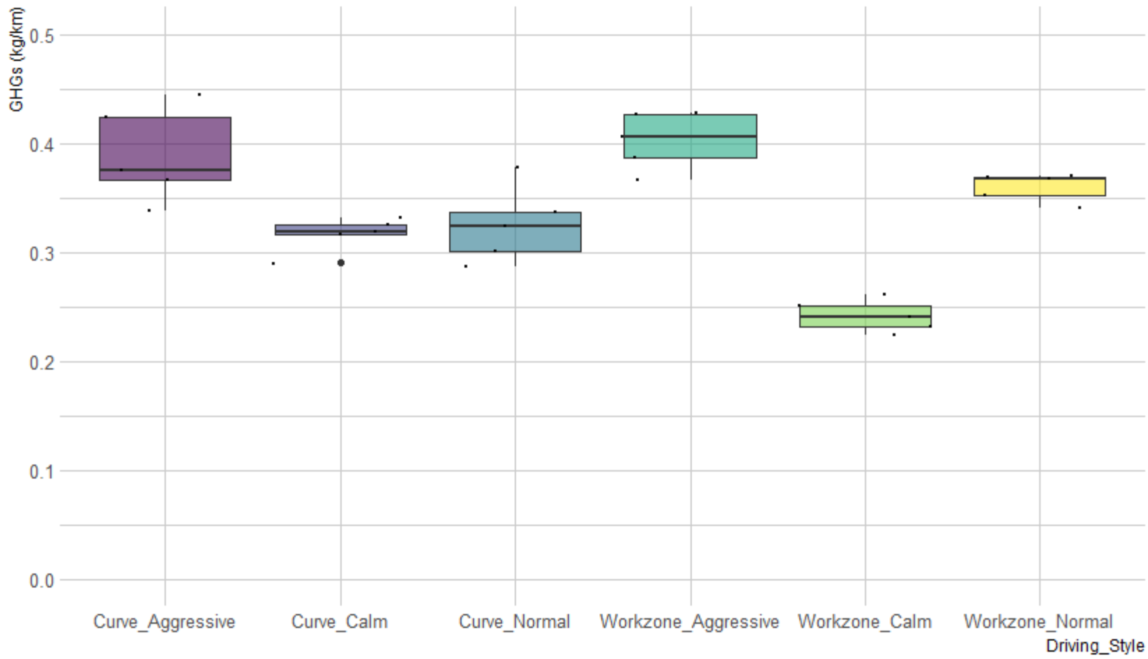

Figure 3-12 Emission estimates for different driving styles on curves and work zones

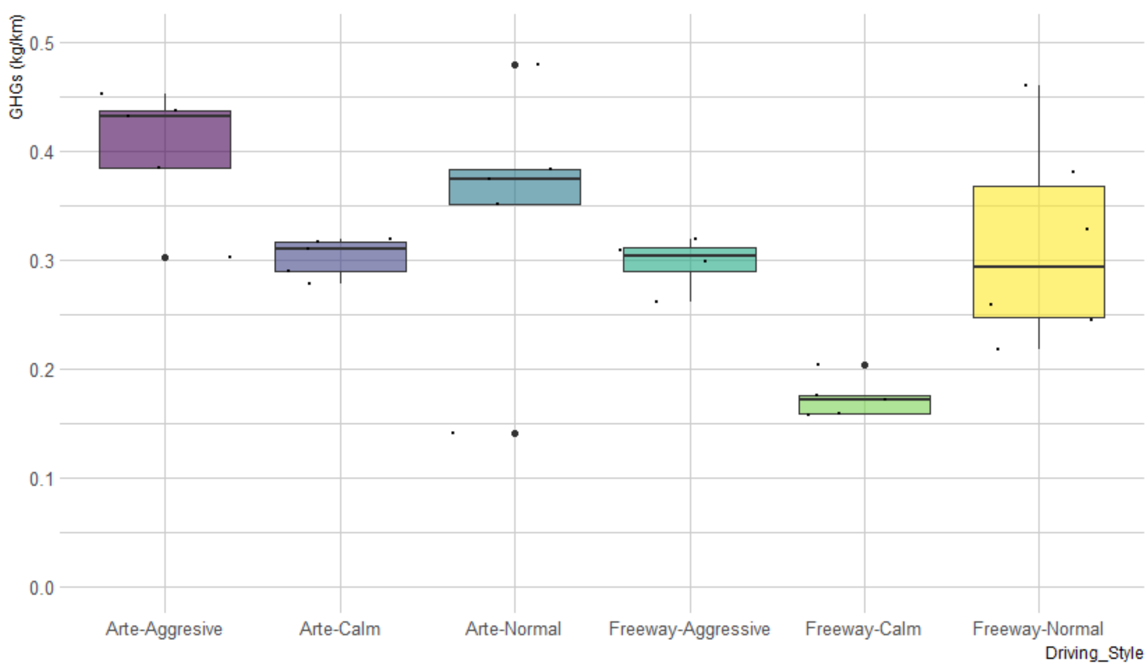

Figure 3-13 Emission estimates for different driving styles on freeways and arterials within curves and work zones

CONCLUSIONS

Global warming is one of the most serious challenges humans face in the 21st century, and many countries including the US are looking for new policies to reduce greenhouse gas emissions in the close future. Transportation is one of the largest sources of energy consumption and emissions in the United States. Thus, there is an immediate need for developing energy-efficient mobility systems with the aim of reducing energy, fuel consumption, and emissions. Work zones and curves are critical segments of the roads in a transportation road network since they can cause flow disruption and be a significant cause of variation in-vehicle operation. These could have a huge impact on fuel consumption and emissions and levels. However, there is limited literature dealing with the use of disaggregate second by second driving data to classify driving styles and investigate the impacts of driving variation in driving styles within work zones and curves on fuel economy and emissions. This study, therefore, focused on classifying driving styles using measures of driving volatility and analyzing how different driving styles and road types impact fuel economy and emissions within work zones and curves. To this aim, the paper benefits from the SHRP2 naturalistic driving data as one of the most comprehensive naturalistic driving studies ever conducted.

The clustering results show that the K-means algorithm yields better clustering results than the Hierarchical and K-medoids methods. The meaningful difference between the volatility measures for different groups of drivers helped the authors to classify driving events in different locations. Overall, results show that the proportions of aggressive driving in different locations and road classes are relatively low, indicating that aggressive driving is not a common behavior among drivers in these locations. It was found that aggressive driving events constitute 12.2% and 15.4% of events in work zones and curves respectively. Calm driving is still the major behavior in these areas which is consistent with the road conditions and traffic rules at these locations, which require slow and cautious driving. Regarding work zone and curve events that occurred in freeways and arterials, it was found that the percentage of aggressive driving is higher on arterials (25.80%) than on freeways (16.77%). It might be because of more complex and variant environment and traffic conditions, more complicated interactions with vulnerable road users, and higher density of access points along the roadway, which makes drivers have more volatile driving on these roads.

Driving style within both work zones and curves was observed to have a significant impact on fuel economy and emissions. Aggressive driving on curves revealed an average of 23% decrease in fuel economy and an 18.8% increase in emissions. Likewise, aggressive driving in work zones resulted in an average 59.1% decrease in fuel economy and a 39.9% increase in emissions. Driving styles on freeways and arterials were also observed to influence fuel economy and emissions significantly. On freeways, for instance, aggressive driving events were found to have on average 50.4% lower fuel economy and 41.6% higher emissions. Transitioning to different traffic flow conditions on freeways and arterial may be attributed to these findings. These results have implications for transportation agencies to improve work zone configurations and curves to reduce emissions. Future research could observe different types of curves for their impacts on emissions. Since vehicle connectivity and automation are expected to improve the behavior of human-driven vehicles, this research would help in identifying zones in which hard braking and cruising events are more likely to occur resulting in higher fuel consumption and emissions. Besides, these results can help to devise algorithms to improve Connected and Automated Vehicles (CAVs) operation and modify driving behavior based on observed regimes of driver styles. Future studies could be devoted to analyzing the impact of driving through different segments of a road considering different penetrations of electric vehicle powertrains.

CHAPTER 4 : INCORPORATING DRIVING VOLATILITY MEASURES IN THE DEVELOPMENT OF SAFETY PERFORMANCE FUNCTIONS FOR INTERSECTIONS

A version of this chapter is accepted for presentation at the 101th Transportation Research Board Annual Meeting.

ABSTRACT

Every year, about 40 percent of the crashes in the US are related to intersections. To deal with such crashes, Safety Performance Functions (SPFs) are vital elements of the predictive methods in the Highway Safety Manual. The predictions of crash frequencies and potential reductions due to countermeasures are based on exposure and geometric variables. However, the role of driving behavior factors, e.g., hard accelerations and declarations, which can lead to crashes, are not explicitly specified in SPFs. One way to capture driving behavior is to harness connected vehicle data and quantify performance at intersections in terms of driving volatility measures. Studies have found driving volatility to be associated with risk and safety-critical events. Therefore, volatility can serve as a surrogate for driving behavior. This study incorporates driving volatility measures in the development of SPFs for four-leg signalized intersections. The Safety Pilot Model Deployment (SPMD) data containing over 125 million Basic Safety Messages generated by over 2,800 connected vehicles are harnessed and linked with crash, traffic, and geometric data belonging to 102 signalized intersections in Ann Arbor, Michigan. The results show that including driving volatility measures in the intersection SPFs substantially improves the goodness-of-fit and predictive performance of the models. Also, the best results were obtained by applying Bayesian hierarchical Negative Binomial Models in which the spatial correlation between the signalized intersections are taken into

account. The results of this study can have implications for practitioners and transportation agencies.

INTRODUCTION

Due to conflicts and resulting crash risks at intersections, they are a front line in the battle for safety, with approximately 40% of crashes in the U.S. occurring at intersections. To deal with this, the Highway Safety Manual (HSM) provides Safety Performance Functions (SPFs) as tools for estimating crash counts for different facility types, including intersections. SPFs are used by agencies for network screening, selecting countermeasures for safety improvements, identifying crash patterns, and estimating the benefits and costs of projects (*92*). The HSM provides SPFs for two specific site types: 1. intersections and 2. roadway segments. Because of the high number of conflicting maneuvers such as turning left, turning right, and crossing, intersections are critical locations that often experience a high number of crashes. In this regard, the 2008 National Highway Traffic Safety Administration (NHTSA) comparison report shows that in 2008, about 40 percent of crashes in the US were related to intersections (*93*). Thus, a significant effort has been made by the agencies and practitioners to localize the intersection SPFs provided in the HSM for different jurisdictions and areas by either calibrating SPFs using calibration factors or developing jurisdiction-specific SPFs using local data. However, the missing part of these efforts is that they do not consider driving behavior in their SPF developments. The emergence of connected and automated vehicles (CAVs) equipped with advanced sensors for transmitting Basic Safety Messages (BSMs) provides a good opportunity for monitoring driving behavior at a microscopic scale. Such data contain valuable information regarding vehicles' movement information such as driver's kinematics, steering status, and heading in a naturalistic driving environment. Availability of these data provides a good opportunity for the practitioners to finally take into account driving behavior in evaluating the safety performance of different facilities.

Therefore, this study aims to incorporate driving behavior factors in the estimations of SPFs for four-leg signalized intersections using large-scale real-world connected and automated vehicle (CAV) data. To this aim, CAV data are linked with traditional data including crash and roadway inventory. To include driving behavior factors in the estimation of SPFs, the concept of intersection-based driving volatility was used which quantifies driving instability by capturing variations in vehicular movements in terms of speed, acceleration, and jerk (*43*). From the methodological perspective, this study applies rigorous statistical models including Negative binomial, Random effect negative binomial, and Bayesian hierarchical negative binomial to evaluate the performance of driving volatility measures in different models.

LITERATURE REVIEW

Many states in the US such as Kansas, California, Alabama, Michigan, Colorado, Florida, Illinois, Tennessee, and Maryland conducted studies to apply the SPFs in the HSM to their roadway segments or intersections (*94-106*). Generally, there are two common approaches in the implementation of SPFs for different jurisdictions: 1- Modifying base SPFs provided in the HSM using local conditions, 2- Developing local SPFs using jurisdiction-specific crash count and inventory data. In the former approach, celebration factors are calculated by the agencies to calibrate the base SPFs for states. A calibration factor higher than 1.0 indicates that crash frequency on a facility is higher than the crash frequency on facilities in the HSM's database and vice versa. In the latter approach, which is suggested by the HSM (*107*), agencies develop SPFs using the local crash and inventory data.

Although SPFs have been proposed by the HSM in 2010, the idea of estimating statistical models for predicting crash counts has been studied for decades. Due to the count nature of crash frequency, Poisson models were among the first models developed in crash frequency analyses (*108; 109*). However, the Poisson model is based on the assumption that the mean and variance of crash frequency are equal, which most of the time is not consistent with the characteristics of crash data which are either over-dispersed or under-dispersed (*110*). Therefore, Negative binomial models, as a generalization of Poisson models, were applied widely in studies to account for over-dispersion in crash count data (*111-114*). However, one of the shortcomings of Negative binomial models is that they are not able to handle under-dispersed crash data that can result in erroneous estimations (*115*). Some other studies suggested using Poisson lognormal models (*116; 117*) to add more flexibility to the model, and zero-inflated models (*118; 119*) to account for excessive zero crashes in data. These models, however, still are not able to deal with under-dispersed crash data (*110*). Therefore, Conway-Maxwell Poisson (*120*) and Gamma (*121*) models were applied to handle under-dispersion. Application of other forms of crash count models such as generalized additive models (*122*) and finite mixture and Markov switching models (*123*) have been limited mostly because of the complexity of estimation and interpretation.

One disadvantage of the models mentioned above is the assumption that the impact of independent variables on crash frequency is fixed, while these effects can vary across the observations due to the unobserved heterogeneity in the data. Therefore, many studies applied random parameter models to handle unobserved heterogeneity and improve the accuracy of estimations (*124-126*). Although random parameter models can address unobserved heterogeneity, they are not able to capture spatial dependency between groups of observations (e.g., a dense urban area with signalized interactions located close to each other have a potential for spatial correlation between adjacent intersections). Therefore, some researchers proposed the application of geographically weighted regression (GWR) models to incorporate the spatial correlation between the observation by allowing the association between dependent variable and parameter estimates to vary across space (*127*) However, one major shortcoming of GWR models is that they may not perform well with small sample sizes, and therefore, they might not be a good option for intersection SPFs. Generalized estimating equations (GEE) models are also applied to incorporate spatial correlation among observations (*128-130*). However, GEE models are limited in terms of considering the same correlation matrix for different groups of intersections (e.g., intersections in the same corridors), while different groups of intersections can have different correlation characteristics (*131*). Therefore, some recent studies applied Bayesian hierarchical models in transportation safety (*131-135*). Bayesian hierarchical models have more flexibility in terms of incorporating spatial correlation between intersections since they capture both within-group and between-group correlation. Furthermore, inference in a Bayesian framework can result in more accurate predictions by combining prior information with the observed data, especially for small sample sizes.

What is strangely missing in intersection SPFs is that they do not explicitly include driving behavior factors in their model estimation, while a study conducted on intersection-related crashes using the National Motor Vehicle Crash Causation Survey (NMVCCS) shows that driver-related factors contribute to about 96 percent of the intersection-related crashes (*136*). The main focus of the past research has been more on traffic and roadway factors. This is because usually, the conventional databases available to agencies and researchers do not cover elements related to driving behavior. Either the cost of the data collection for this information is high or they are not available. The results of the study conducted by Arvin et al. (*48*) show that there is a strong association between the frequency of different types of crashes and driving volatility measures. Building on this study, this paper contributes to potential improvements in intersection safety by explicitly incorporating driving behavior (volatility captured through Basic Safety Messages) in HSM's safety performance functions. This is important from two perspectives. First, incorporating driving behavior, as a missing link of crash frequency analysis, in the estimation of SPFs can increase the predictive power of predictive models. Second, it will build a basis for future studies to predict crash frequencies proactively in shorter time horizons by considering driving behavior factors as time-varying parameters. A further methodological advance is the application of spatially-oriented Bayesian techniques to more accurately predict future crashes and target relevant countermeasures.

DATA DESCRIPTION

Before starting the data collection, it is necessary to define an intersection accident. Although agencies have different definitions of an intersection accident, this study uses the HSM definition in which accidents that occurred within 250 feet from the center of an intersection are considered as intersection accidents (*107*). To develop SPFs for four-leg signalized intersections, this study integrates four different data sources: 1. BSM data generated by connected vehicles, 2. Traffic data, 3. Road inventory data, 4. Crash frequency data. This study benefits from high-resolution BSM data collected during the Safety Pilot Model Deployment (SPMD) program in Ann Arbor, Michigan which was carried out by the US Department of Transportation. Consisting of over 125 million BSMs generated by 2836 vehicles equipped with V2V and V2I communication technologies, the SPMD program is among the most comprehensive naturalistic driving data collection efforts in the US. This paper used a two-month subset of the data containing the information regarding vehicles' location (longitude, latitude, and elevation) and motion (speed and longitudinal and lateral acceleration) which is available publicly through the ITS data website (https://www.its.dot.gov/data/). A significant effort was made to prepare a unique database by assembling, pre-processing, and cleaning the raw SPMD data and preparing them for future analysis.

Using online maps, 105 four-leg signalized intersections were initially identified for the study. After excluding the intersections for which traffic data were not available, 102 intersections were chosen as the final sample. Figure 4-1 shows the location of these intersections on the Ann Arbor map. A significant effort was made to collect conventional data including historical crashes, traffic, and geometric data for the intersections from different data sources. Crash data between October 2012 and October 2013 (consistent with the data collection period in SPMD study), Speed limits, and AADT of minor and major approaches of the intersections were manually extracted from the Metropolitan Planning Organization Website (http://semcog.org/). Also, intersection inventory data such as the total number of lanes, presence of left-turn lane, and presence of right turn lane were collected from Google maps. Finally, to link the BSM data to the conventional data, circles with a radius of 250 feet were drawn and the coordinates of the circles were extracted from online maps. Next, the coordinates were used to filter vehicle trajectories for the selected intersections.

Table 4-1 represents the descriptive statistics of the variables. This table provides useful information about the distribution of volatility measures, geometric characteristics, and traffic features of the four-leg signalized intersections in the data. For instance, each year, an average of 17.68 crashes with a standard deviation of 10.78 happened at the intersections. Also, on average, at 41 percent of four-leg signalized intersections, at least one of the approaches provides either protected or protected/permissive left-turn signal phasing. Moreover, on average, left-turn lanes are present at 2.24 of the approaches in each intersection. Furthermore, a right turn on red is permitted in 81 percent of the intersections in the data. also, based on the data, 49 percent of the four-leg signalized intersections are located adjacent to the school area.

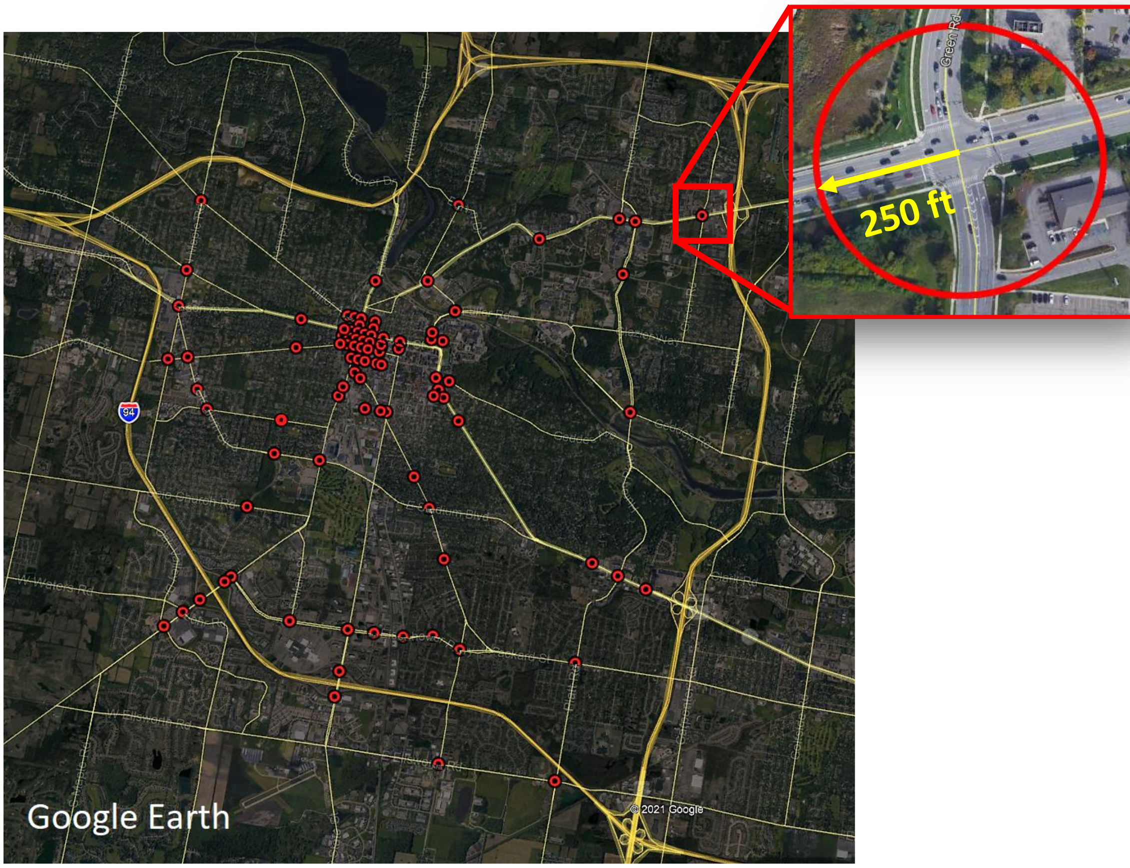

Figure 4-1. Location of studied four-leg signalized intersections in Ann Arbor, MI

Table 4-1 Descriptive statistics of the variables (N= 102 intersections)

Intercept	Description	Min	Max	Mean	S.D.
Dependent variable					
Total crashes per year	Total number of crashes within 250 ft of the center of the intersection	4.00	59.00	17.68	10.78
Intersection-related variables					
$\mathrm{AADT}_{\mathrm{maj}}$	Log form of annual average daily traffic of the major approach	8.52	10.77	9.72	0.57
$\mathrm{AADT}_{\mathrm{min}}$	Log form of annual average daily traffic of the minor approach	6.06	10.22	8.65	0.79
$\mathrm{Speed\ limit}_{\mathrm{maj}}$	Speed limit of the major approach	25.00	50.00	33.09	7.11
$\mathrm{Speed\ limit}_{\mathrm{min}}$	Speed limit of the minor approach	25.00	45.00	28.33	5.28
Left-turn lanes	Number of approaches with left-turn lane (0,1, 2, 3, 4)	0.00	4.00	2.24	1.47
Right-turn lanes	Number of approaches with right-turn lane (0,1, 2, 3, 4)	0.00	4.00	0.85	1.18
Left-turn signal phasing	Presence of protected or protected/permissive left-turn signal phasing (Yes = 1, No = 0)	0.00	1.00	0.41	0.50
Right turn on red	Whether right turn on red is permitted (Yes = 1, No = 0)	0.00	1.00	0.81	0.39
Red light cameras	Whether a red-light running camera is installed in the intersection (Yes = 1, No = 0)	0.00	1.00	0.16	0.37
Schools	Presence of schools within 1,000 ft of the center of the intersection (Yes = 1, No = 0)	0.00	1.00	0.39	0.49
Bus stop	Number of bus stops within 1,000 ft of the center of the intersection	1.00	17.00	7.53	4.39
Alcohol Sales Establishments	Number of alcohol sales establishments (liquor stores, bars, restaurants, or grocery stores) within 1,000 ft of the center of the intersection	0.00	51.00	8.00	10.26
Lighting	Presence of lighting in the intersection (Yes = 1, No = 0)	0.00	1.00	0.99	0.10

Table 4-2 Descriptive statistics of the variables (N= 102 intersections) (continued)

Intersection-based volatility measures					
Speed volatility measures					
$Speed - S_{dev}$	Standard deviation of speed (m/s)	6.34	14-60	10.06	1.84
$Speed - C_v$	Coefficient of variation of speed	0.28	0.73	0.55	0.09
$Speed - Q_{cv}$	Quartile of variation of speed	0.12	0.66	0.43	0.10
$Speed - D_{mean}$	Mean absolute deviation of speed (m/s)	5.11	11.68	8.41	1.62
$Speed - V_f$	Time-varying stochastic volatility of speed	4.97	19.37	11.19	2.10
Longitudinal acceleration volatility measures					
$AccDec_x - S_{dev}$ (m/s^2)	Standard deviation of both longitudinal acceleration and deceleration (m/s^2)	0.67	1.29	1.01	0.13
$AccDec_x - D_{mean}$ (m/s^2)	Mean absolute deviation of both longitudinal acceleration and deceleration (m/s^2)	0.43	1.07	0.78	0.13
$Acceleration_x - C_v$	Coefficient of variation of longitudinal acceleration	0.61	1.11	0.82	0.10
$Deceleration_x - C_v$	Coefficient of variation of longitudinal deceleration	0.66	1.23	0.85	0.11
$Acceleration_x - Q_{cv}$	Quartile of variation of longitudinal acceleration	0.45	0.73	0.60	0.06
$Deceleration_x - Q_{cv}$	Quartile of variation of longitudinal deceleration	0.52	0.79	0.64	0.05
Lateral acceleration volatility measures					
$AccDec_y - S_{dev}$ (m/s^2)	Standard deviation of both lateral acceleration and deceleration (m/s^2)	0.62	1.77	1.09	0.27
$AccDec_y - D_{mean}$ (m/s^2)	Mean absolute deviation of both lateral acceleration and deceleration (m/s^2)	0.17	0.73	0.37	0.14
$Acceleration_y - C_v$	Coefficient of variation of lateral acceleration	0.95	4.68	2.46	0.79
$Deceleration_y - C_v$	Coefficient of variation of lateral deceleration	1.72	4.98	3.46	0.76
$Acceleration_y - Q_{cv}$	Quartile of variation of lateral acceleration	0.63	0.97	0.80	0.10
$Deceleration_y - Q_{cv}$	Quartile of variation of lateral deceleration	0.57	0.98	0.81	0.09

METHODOLOGY

The main objective of this study is to incorporate driving behavior factors in the development SPFs for four-leg signalized undersections. The concept of driving volatility was used to quantify driving behavior in intersections. Driving volatility measures have been studied in various studies (*43; 45; 48*). Driving volatility measures indicate how much the individuals deviate from normal driving. Hence, larger values of driving volatilities are correlated with higher variations in speed, deceleration, and acceleration, and as a result, higher instability in driving. Past research found that driving volatility is positively correlated with the crash count (*43*) and severity (*46*). Thus, volatile driving might be considered as a sign of aggressive driving behavior which can meaningfully increase the risk of crashes. In this study, location-based driving volatility measures were calculated and used (*43; 137*). Location-based volatility measures quantify variability in instantaneous driving decisions at particular locations (e.g., intersections or segments). These volatility measures can be used to identify locations in which drivers often drive more volatile than other locations. Figure 4-2 presents the methodological approach of the study. To prepare the raw BSM data for driving volatility calculation, the following pre-processing steps were performed. First, the data were filtered to maintain only BSMs occurred in An Arbor, MI.

The data were cleaned from errors and outliers. Next, the coordinates of 102 selected four-leg signalized intersections were used to filter vehicle kinematic information on the intersections. After calculating the driving volatility measures, the conventional data including traffic counts, crash data, and inventory data were linked with these measures. Then, three groups of models including Negative Binomial, Random Effect

Negative Binomial, and Bayesian Hierarchical Negative Binomial models are applied for estimating SPFs for four-leg signalized intersections. Finally, to evaluate the performance of volatility measures in the SPFs a model comparison was made between the models using model assessment measures. The next sections first explain the calculations of driving volatility measures. Next, the modeling approach and model assessment measures used in this study are discussed in detail.

Driving volatility measures

Past research has developed and used several driving volatility measures for speed, lateral acceleration, longitudinal acceleration, and vehicular jerk (*43; 48; 117; 137; 138*) to assess variation in driving movement. Likewise, this study applies volatility functions to speed, longitudinal acceleration, and lateral acceleration. Table 4-2 shows the volatility functions used in this study. For more information, the readers are referred to (*43*).

Model specification

Negative binomial (NB) models (HSM SPFs)

Poisson and negative binomial regression models have been commonly used for crash frequency analyses because they are easy to estimate and interpret (*110*). The HSM, however, prefers negative binomial models over Poisson models as they better account for over-dispersed crash data (*107*).

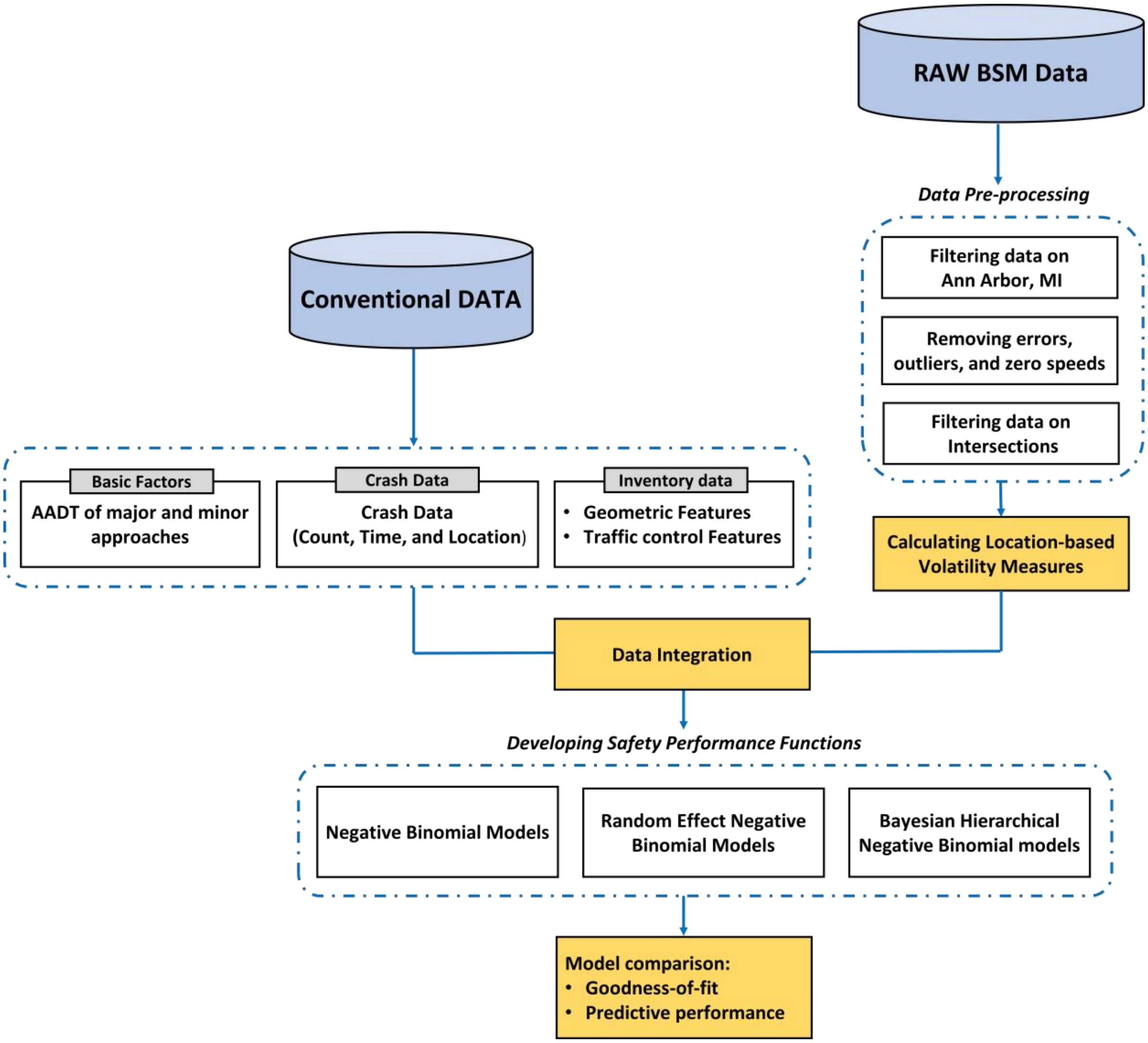

Figure 4-2. Methodological approach of the study

Table 4-3 Driving volatility measures used in the study

Measures of volatility	**Formulation**
Standard Deviation	$S_{dev} = \sqrt{\frac{1}{n-1}\sum_{i=1}^{n}(x_i - \bar{x})^2}$
Coefficient of variation	$C_v = \frac{S_{dev}}{\bar{x}} \times 100$
Mean Absolute Deviation	$D_{mean} = \frac{1}{n}\sum_{i=1}^{n}\lvert x_i - \bar{x}\rvert$
Quartile Coefficient of variation	$Q_{cv} = \frac{Q_3 - Q_1}{Q_3 + Q_1} \times 100$
Time-dependent dynamic volatility	$V_f = \sqrt{\frac{1}{n-1}\sum_{i=1}^{n}(r_i - \bar{r})^2}$ $r_i = \ln\left(\frac{x_i}{x_i - 1}\right) * 100$

Notes: $\bar{x}$ is the mean and Q_3 and Q_1 are the third and first quartiles

The HSM provides the following equation for estimating the average crash count for four-leg signalized intersections (*107*):

$$N_{SPF_{ij}} = \exp\left(a + b \times \ln\left(AADT_{(maj)_{ij}}\right) + \ c \times \ln\left(AADT_{(min)_{ij}}\right) + \varepsilon_{ij}\right) \tag{1}$$

where $N_{SPF_{ij}}$ is the predicted total crash frequency, $AADT_{maj}$ is the annual average daily traffic of the major road, $AADT_{min}$ is the annual average daily traffic of the minor road, ε_{ij} is the error term, and *a*, *b,* and *c* are the regression parameters to be estimated. Equation 1 presents the base SPF which only considers the key variables $AADT_{maj}$ and $AADT_{min}$. However, crash frequency of signalized intersections can be also explained by geometric design features, traffic control characteristics, and driving behavior factors which this study tries to incorporate in SPFs. Thus, intersection SPF can also be presented as follows:

$$N_{SPF_{ij}} = \exp(a + b \times \ln\left(AADT_{(maj)_{ij}}\right) + c \times \ln\left(AADT_{(min)_{ij}}\right) + \sum \beta_p X_{pij} + \varepsilon_{ij}\ ) \tag{2}$$

where X_p is a vector of additional independent variables and β_p is a vector of coefficients.

Random effects negative binomial (RENB) models

In random effect negative binomial models, a random effect is incorporated in the model to capture the unobserved heterogeneity between corridors:

$$N_{SPF} = \exp(a + b \times \ln\left(AADT_{(maj)_{ij}}\right) + c \times \ln\left(AADT_{(min)_{ij}}\right) + \sum \beta_p X_{pij} + \varepsilon_{ij} + \theta_j) \tag{3}$$

where $\theta_j \sim N(0,\ \sigma^2)$ are normally distributed independent random effects with zero mean and a constant variance.

Bayesian hierarchical negative binomial (BHNB) models

Bayesian hierarchical negative binomial models assume that not only intersections located on the same corridors are spatially correlated but this correlation is stronger when intersections are closer to each other. This spatial correlation can be structured using the adjacency matrix W (*135*):

$$\mathbf{w_{ij,i'j'}} = \begin{cases} \dfrac{\mathbf{1}}{\mathbf{d_{ij,i'j'}}}, & \textbf{if } \mathbf{j = j'} \\ \mathbf{0}, & \textbf{if } \mathbf{j \neq j'} \end{cases} \tag{4}$$

where ij represents intersection i on corridor j, $\mathrm{d_{ij,i'j'}}$ represents the distance between intersection ij and $\mathrm{i'j'}$ on the same corridor. Based on the adjacency matrix defined above, $\mathrm{w_{ij,i'j'}}$ is zero unless intersections are located on the same corridor. In this case, the $\mathrm{w_{ij,i'j'}}$ is inversely proportional to the spatial distance between the two intersections. BHNB models account for both unobserved heterogeneity among corridors and spatial correlation between intersections in a corridor by adding through the following equation:

$$N_{SPF} = \exp(a + b \times \ln\left(AADT_{(maj)_{ij}}\right) + c \times \ln\left(AADT_{(min)_{ij}}\right) + \sum \beta_p X_{pij} + \varepsilon_{ij} + \theta_j + \phi_{ij}) \tag{5}$$

where ϕ_{ij} are spatially autocorrelated random effects for capturing the spatial correlation between adjacent intersections which are typically represented by conditional autoregressive distributions. Several conditional distributions have been proposed in the literature for modeling these spatial random effects. This paper uses the following distribution proposed by (*139*) to model ϕ_{ij} in the Bayesian setting:

$$\phi_{ij}|\phi_{-ij} \sim N(\sum_{i \neq i'} \frac{w_{i'j,ij}\phi_{i'j}}{W_{j+}}, \frac{\tau^2}{W_{j+}}) \tag{6}$$

where ϕ_{-ij} is the vector of spatial random effects for any intersection on j_{th} corridor except for intersection ij, W_{j+} is the sum of weights on corridor j_{th}, and τ^2 is a scale parameter with an inverse-gamma prior distribution.

Bayesian procedure

In this study, models are estimated using the Bayesian inference method. Bayesian inference method applies Bayes' theorem to combine prior known distributions with the new evidence provided by the observed data to find updated (posterior) distributions. Incorporating prior knowledge in the model estimations can have several advantages such as they better account for uncertainty in the inference, require less data for the model estimation (*140*), offer more flexibility in terms of choosing different distributions (*140*), and address the regression-to-the-mean bias (*140*). Markov Chain Monte Carlo (MCMC) method is a common and powerful technique for a stochastic approximation of a posterior distribution by generating samples from the target posterior distribution in a sequential process in which the next sample is dependent on the existing sample (*141*). One of the most widely used MCMC algorithms is Gibbs sampling in which each variable is sampled conditioned on the values of other variables in the distribution (*142*).

Appropriate prior distributions were used to estimate the fixed and random-parameter models. Flat (uninformative) priors were used for estimating the fixed parameters in regression models in Eq. (1) and (2). An uninformative Normal distribution (0, 100^2) was used for regression coefficients in RENB and BHNB models. Also, it was assumed that the variance of the randomly distributed terms σ^2 in RENB and BHNB models and the variance of the spatially autocorrelated random effects τ^2 in BHNB model follow an Inverse-Gamma distribution $(10^{-3}, 10^{-3})$ which are in line with the previous studies in the field (*131; 135; 137; 143; 144*). Two Markov chains with 100,000 samples were run, the first 20,000 of which were discarded in the burn-in period. Also, the Potential Scale Reduction Factor (PSRF) was used as a convergence diagnostic (*145*). PSRF values less than 1.2 are suggestive of convergence (*146*). Furthermore, to test the significance of parameter estimates, the 95% Bayesian Credible Interval (BCI) was used. Following (*145*), if the 95% BCI of a parameter estimate does not contain zero, it can be considered significant at 95% level and vice versa.

Model selection measures

In this study, the Log Pseudo-Marginal Likelihood (LPML) and the Deviance Information Criterion (DIC) are used to compare the predictive performance and goodness-of-fit of the models. The DIC which is a generalization of the Akaike Information Criterion (AIC) (*147*) is commonly used in Bayesian analysis studies as a measure of model fit and complexity (*148*). The DIC can be calculated as follows:

$$DIC = \overline{D} + p_D \tag{7}$$

where $\overline{D}$, as a measure of goodness of fit, is the posterior mean of the deviance, and p_D, as a measure of complexity, is the effective number of parameters. Lower values of DIC indicate a better fit of models. In the case of comparison between two models, the difference in DIC can be a useful measure. Generally, the rules suggested by (*149*) for the model comparison using AIC can be applied for DIC (*148*). As a rule of thumb, a DIC difference between 3 and 7 indicates a significant difference, and a DIC difference greater than 10 completely excludes the model with higher DIC from the candidates (*148; 149*). The LPML, which is based on the leave-one-out-cross validation technique, measures the predictive performance of the models. To calculate LPML, first, the conditional predictive ordinate (CPO) should be calculated for each observation. The CPO of the *i*th observation is the predictive density of the *i*th observation (y_i), given the rest of the observations excluding *i*th observation (y_{-i}) (*150*):

$$CPO_i = p(y_i|y_{-i}) = \int p(y_i|\theta)\, p(\theta|y_{-i})\, d\theta \tag{8}$$

where θ is the vector of parameters in the model. Therefore, the LPML can be calculated using the equation below (*150*):

$$LPML = \sum_{i=1}^{n} \log(\mathrm{CPO}_i) \tag{9}$$

Generally, greater values of LPML show a better predictive performance. The difference in LPML can be exponentiated to use the similar criteria suggested for Bayes factors in (*151*). Following (*151*) an exponentiated difference between 3 and 20 indicates positive evidence, between 20 and 150 shows strong evidence, and greater than 150 shows very strong evidence for favoring a model with a higher LPML over a model with a lower LPML.

RESULTS AND DISCUSSION

The main objective of this study is to incorporate driving volatility measures in four-leg signalized intersection SPFs and evaluate the impact of these variables on the performance of the SPFs. Two this aim, three groups of models were developed: base SPFs, SPFs with volatility measures, and full SPFs with volatility measures and additional variables. Each group of models includes a fixed parameter negative binomial model as the conventional form of SPFs provided in the HSM, and two random parameter models including a random effect negative binomial and a Bayesian hierarchical model. The following sections first discuss model estimation results and interpretation of variables in the models. Then, estimated models are compared based on the goodness-of-fit and performance measures.

Model estimation results

Table 4-3 shows the model estimation results for base SPFs considering only $AADT_{maj}$ and $AADT_{min}$ in the models. Expectably, variables $AADT_{maj}$ and $AADT_{min}$ have positive correlations with the crash frequency of intersections in all models. The larger coefficient of $AADT_{maj}$ in the models shows that traffic volume of the major approach has a stronger impact on the number of crashes at the intersections. Table 4-4 shows the model estimation results of SPFs taking into account volatility measures. Three driving volatility measures of $Speed - C_v$, $Deceleration_x - C_v$, and $Acceleration_y - C_v$ had a significant and positive correlation with crash frequency at four-leg signalized intersections. Among the driving volatility measures, $Speed - C_v$ which represent the variation of vehicles' speed at intersections has the strongest effect on the number of crashes at intersections, followed by the coefficient of variation in longitudinal deceleration ($Deceleration_x - C_v$) and lateral acceleration ($Acceleration_y - C_v$). The positive association of $Speed - C_v$ with crash frequency indicates that four-leg signalized intersections with a higher variation in speed are likely to have a higher number of crashes. This is in line with the results reported in (*48; 137*). $Deceleration_x - C_v$ represents higher rates of sudden and abrupt breaking at intersections and strong and positive association of this variable with crash frequency of signalized intersections can be because hard braking can specifically increase the probability of rear-end crashes (*152; 153*). This is also consistent with the findings in (*48*). Furthermore, $Acceleration_y - C_v$ is positively correlated with the number of crashes at intersections. Also, the positive correlation of $Acceleration_y - C_v$ with crash frequency reveals that an increase in the variation of lateral acceleration can decrease the number of crashes at four-leg signalized intersections.

Table 4-4 Estimation results of models without volatility measures

Variables	NB		RENB		BHNB	
	Mean (S.D.)	**95% BCI**	**Mean (S.D.)**	**95% BCI**	**Mean (S.D.)**	**95% BCI**
Intercept	-0.32 (0.37)	(-0.98, 0.42)	-0.89 (0.93)	(-2.19, 1.09)	-0.31 (0.9)	(-1.87, 1.32)
$\mathbf{AADT_{maj}}$	0.21 (0.33)	(0.15, 0.27)	0.20 (0.09)	(0.03, 0.37)	0.15 (0.07)	(0.03, 0.30)
$\mathbf{AADT_{min}}$	0.12 (0.24)	(0.08, 0.17)	0.19 (0.05)	(0.09, 0.27)	0.18 (0.06)	(0.09, 0.30)
Summary of Statistics						
No. of observations	102					
Dispersion parameter	3.88 (0.38)	(3.11, 4.66)	3.49 (0.43)	(2.76, 4.31)	2.80 (0.34)	(2.15, 3.49)
Note: NB=Negative Binomial, **RENB**= Random Effect Negative Binomial, **BHNB**= Bayesian Hierarchical Negative Binomial						

Table 4-5 Estimation results of models with volatility measures

Variables	NB		RENB		BHNB	
	Mean (S.D.)	**95% BCI**	**Mean (S.D.)**	**95% BCI**	**Mean (S.D.)**	**95% BCI**
Intercept	-2.19 (0.66)	(-3.51, -1.06)	-3.43 (1.30)	(-5.38, -0.40)	-2.66 (1.31)	(-5.08, -0.57)
$\mathbf{AADT_{maj}}$	0.19 (0.04)	(0.12, 0.29)	0.15 (0.07)	(0.02, 0.27)	0.09 (0.05)	(0.00, 0.20)
$\mathbf{AADT_{min}}$	0.09 (0.03)	(0.04, 0.16)	0.15 (0.06)	(0.03, 0.28)	0.06 (0.04)	(-0.01, 0.15)
$\mathbf{Speed - C_v}$	3.14 (0.30)	(2.59, 4-68)	4.02 (0.71)	(2.51, 5.06)	4.43 (1.04)	(3.09, 6.23)
$\mathbf{Deceleration}_x - \mathbf{C_v}$	0.51 (0.29)	(0.01, 1.08)	1.09 (0.42)	(0.38, 1.86)	1.31 (0.78)	(0.22, 2.61)
$\mathbf{Acceleration}_y - \mathbf{C_v}$	0.06 (0.03)	(0.01, 0.12)	0.09 (0.05)	(-0.01, 0.18)	0.17 (0.07)	(0.04, 0.30)
Summary of Statistics						
No. of observations	102					
Dispersion parameter	4.22 (0.42)	(3.45, 5.08)	3.84 (0.48)	(3.06, 4.69)	3.08 (0.38)	(2.38, 3.80)

Note: NB=Negative Binomial, **RENB**= Random Effect Negative Binomial,
BHNB= Bayesian Hierarchical Negative Binomial

Traditionally, geometric design and traffic control features have been included in the SPFs developed for signalized intersections. Table 4-5 presents the model estimation results of SPFs including these variables besides the driving volatility measures. Note that only significant variables were kept in the final models. Based on the results, besides the volatility measures, variables $AADT_{maj}$, $AADT_{min}$, *right turn lanes*, *left-turn signal phase*, *right turn on red*, *Red-light camera,* and *school* could meaningfully explain the dependent variable in the models. Overall, the signs and magnitudes of the explanatory variables are logical. For instance, variable *right turn lanes* is negatively correlated with the number of crashes, indicating that a higher number of approaches with a right turn lane decreases the number of crashes at four-leg signalized intersections. It can be because right-turn lanes can decrease the number of conflicts between the right-turning vehicles and the through traffic (*154; 155*). Interestingly, variable *left-turn signal phase* has a positive association with crash frequency in four-leg signalized intersections. It is probably because although the presence of a protected or a permissive-protected left-turn signal phase can decrease the left-turn and pedestrian crashes, it possibly increases the rear-end (*156*) and overtaking crashes (*157*), which can ultimately increase the total crash count at intersections. Moreover, the positive correlation between variable *right turn on red* and crash frequency shows that allowing the drivers to turn right on red increases the number of crashes at four-leg signalized intersections. It might be because the adoption of right-turn-on-red laws in intersections can increase right-turning, pedestrian, and bicyclist crashes (*158; 159*). Also, variable *red-light camera* is positively correlated with the crash count at intersections. It is in contrast with the findings in (*160; 161*). However, this positive association does not necessarily mean that the presence of red-light cameras increases crash frequency at intersections, but these cameras probably are installed at intersections in which the rate of red-light running violations and crashes are high. Moreover, the presence of schools near the intersection is found to have a negative correlation with the number of crashes at intersections. It is probably because drivers usually drive with caution in these areas.

Model comparison

Table 4-6 shows the comparison of the estimated models using goodness-of-fit and predictive performance measures. Two approaches can be used for the model comparison: within-group comparison and between-group comparison. In the first approach, the performance of different types of models (NB, RENB, and BHNB) will be compared with each other. In the second approach, however, three groups of models (e.g., base SPFs, SPFs with volatility measures, and full SPFs) can be compared in order to evaluate the effect of incorporating different variables on the performance of the models. The results show the performance of models is directly associated with the complexity of the models, i.e., BHNB performs better than the RENB model, and RENB model performs better than the NB model. For example, the difference in DIC ($\Delta\mathrm{DIC}$) between the BHNB and RENB models in base SPFs is 2.73, indicating that the BHNB has a better fit compared to the RENB model. A similar trend exists for other predictive performance measures (LPML, MAD, and MSE), showing that more complex models have lower error and higher predictive performance. These results are expected because more complex models better capture unobserved heterogeneity in crash data.

Table 4-6 Estimation results of models with volatility measures

Variables	NB		RENB		BHNB	
	Mean (SD)	**95% BCI**	**Mean (SD)**	**95% BCI**	**Mean (SD)**	**95% BCI**
Intercept	-2.15 (0.70)	(-3.52, -0.78)	-3.59 (0.73)	(-5.11, -2.15)	-2.33 (0.87)	(-4.15, -0.98)
$\mathbf{AADT_{maj}}$	0.14 (0.05)	(0.03, 0.24)	0.10 (0.08)	(-0.04, 0.25)	0.08 (0.06)	(-0.03, 0.25)
$\mathbf{AADT_{min}}$	0.10 (0.03)	(0.04, 0.17)	0.16 (0.06)	(0.06, 0.26)	0.10 (0.05)	(0.01, 0.22)
$\mathbf{Speed - C_v}$	3.33 (0.47)	(2.43, 4.25)	4.34 (0.78)	(3.02, 5.67)	3.54 (0.44)	(2.65, 4.22)
$\mathbf{Deceleration}_x - \mathbf{C_v}$	0.72 (0.35)	(0.04, 1.40)	1.06 (0.55)	(0.00, 2.10)	1.12 (0.43)	(0.29, 1.89)
$\mathbf{Acceleration}_y - \mathbf{C_v}$	0.08 (0.03)	(0.01, 0.14)	0.12 (0.05)	(0.06, 0.23)	0.12 (0.06)	(-0.01, 0.23)
Right turn lanes	-0.09 (0.02)	(-0.14, -0.04)	-0.07 (0.03)	(-0.13, -0.02)	-0.05 (0.05)	(-0.13, 0.02)
Left-turn signal phase	0.22 (0.06)	(0.10, 0.34)	0.25 (0.13)	(0.05, 0.44)	0.19 (0.04)	(0.10, 0.26)
Right turn on red	0.13 (0.06)	(0.00, 0.25)	0.39 (0.04)	(0.32, 0.47)	0.15 (0.05)	(0.05, 0.23)
Red-light camera	0.14 (0.07)	(0.01, 0.27)	0.12 (0.1)	(-0.09, 0.26)	0.10 (0.10)	(-0.03, 0.30)
School	-0.03 (0.01)	(-0.06, -0.01)	-0.03 (0.02)	(-0.05, -0.01)	-0.03 (0.01)	(-0.03, -0.05)
Summary of Statistics						
No. of observation	102					
Dispersion parameter	4.73 (0.47)	(3.78, 5.81)	4.39 (0.55)	(3.46, 5.41)	3.49 (0.43)	(2.66, 4.38)

Note: NB=Negative Binomial, **RENB**= Random Effect Negative Binomial,
BHNB= Bayesian Hierarchical Negative Binomial

Table 4-7 Performance comparison of base SPFs, SPFs with volatility measures, and full SPFs

Measure	Base SPFs			SPFs with volatility measures			Full SPFs		
	NB	**RENB**	**BHNB**	**NB**	**RENB**	**BHNB**	**NB**	**RENB**	**BHNB**
$\bar{\mathbf{D}}$	1027.97	570.59	569.71	957.23	565.40	563.93	913.21	564.94	563.11
$\mathbf{p_D}$	1.76	80.60	78.75	5.38	79.06	78.09	10.84	74.94	74-62
DIC	1029.73	651.19	648.46	962.61	644.46	642.02	924.05	639.88	636.73
LPML	-518.78	-336.4	-336.8	-492.3	-332.2	-330.7	-486.0	-329.2	-325.9
MAD	8.01	1.62	1.54	7.55	1.49	1.41	7.14	1.39	1.33
MSE	106.20	3.95	4-66	94.34	3.29	3.09	86.62	2.95	2.74

These findings are consistent with the results reported in (*131; 143*). To evaluate how effective driving volatility measures are in the models, a comparison can be made between base SPFs and SPFs with volatility measures. For example, the difference in DIC ($\Delta\mathrm{DIC}$) between the base NB model and NB model with volatility measure is 67.12. Similarly, $\Delta\mathrm{DIC}$ between RENB and BHNB models are 6.73, and 6.44, respectively. These results indicate that incorporating the driving volatility measures in SPFs improves the goodness of fit of the models substantially. Also, higher LMPL and lower MAD and MSE of SPFs with volatility measures show that these models have a better predictive performance compared to the base SPFs. Furthermore, the $\Delta\mathrm{DIC}$ between the SPFs with volatility measures and full SPFs are 38.56, 4.58, and 5.29 showing that taking into account the geometric design and traffic control features in the full SPFs improves the performance of the models significantly. Also, the full SPFs have the highest LMPL and the lowest MAD and MSE indicating that these models have the highest forecast accuracy among the models.

CONCLUSION

Intersections are among critical spots in transportation networks because of the high number of conflicting maneuvers and variation in speed at these locations. Safety performance functions (SPFs) in the HSM are widely applied by practitioners as an effective tool for network screening, selecting countermeasures for safety improvements, identifying crash patterns, and estimating benefits and costs of projects. Significant efforts have been made in the literature for developing SPFs for intersections. However, the missing part of these efforts is that they do not take into account driving behavior features in their SPF developments. The development of connected and automated vehicles (CAVs) capable of sending and receiving Basic Safety Messages (BSMs) provides a good opportunity for monitoring drivers' behavior at a microscopic scale. Therefore, the main objective of this study is to incorporate driving behavior factors in the development of SPFs for four-leg signalized intersections using large-scale real-world CAV data. To this aim, CAV data are linked with traditional data including crash and roadway geometry, and the concept of intersection-based driving volatility was used to quantify driving instability by capturing variations in vehicular movements in terms of speed, acceleration, and deceleration. To examine the performance of driving volatility measures in SPFs different groups of models including conventional negative binomial (NB), random effect negative binomial (RENB), and Bayesian hierarchical negative binomial (BHNB) models were estimated and goodness-of-fit and predictive performance of them were compared with each other.

Results show that three driving volatility measures of coefficient of variation in speed ($Speed - C_v$), coefficient of variation in longitudinal deceleration ($Deceleration_x - C_v$), and coefficient of variation in lateral acceleration ($Acceleration_y - C_v$) were significant in the models and had a strong positive association with crash frequency at four-leg signalized intersections. Also, AADT of major and minor approaches, presence of dedicated left-turn signal phase, number of approaches with a right-turn lane, right turn on the red, presence of a red-light camera, and presence of school(s) near the intersections are among the geometric design and traffic control features that could meaningfully explain the dependent variable in the models. Furthermore, the log pseudo-marginal likelihood (LPML), the deviance information criterion (DIC), the mean squared error (MSE), and the mean absolute deviation (MAD) were used for comparing the goodness-of-fit and predictive performance of the models. Overall, it was found that incorporating the driving volatility measures in the estimation of SPFs improves the goodness of fit and predictive performance of the models substantially. Furthermore, the results revealed that more complex models outperform the conventional NB models in terms of predictive performance and goodness of fit. Especially, BHNB models were found to have the best performance among the models, indicating that accounting for spatial correlation between the intersections can improve the performance of intersection SPFs.

The results of this study have implications for planners, practitioners, and transportation agencies. Besides the Safety Pilot Model Deployment (SPMD) data used in this study, CAV data are available in Tampa (*162*) and New York CAV pilot (*163*) tests. Therefore, with the advance of CAVs, BSM data become available to researchers unprecedentedly.

This study demonstrated the concept of applying driving volatility measures as effective measures of driving instability at intersections. Similar frameworks can be developed to calculate these measures in real-time for proactive monitoring of intersection networks and detect intersections where there is a high probability of a crash. Future research also can include volatility measures in the development of SPFs for different crash types such as single-vehicle crashes, multiple-vehicle crashes, and pedestrian crashes.

The methodology of this study can be utilized by the agencies and practitioners to incorporate driving behavior factors in the development of jurisdiction-specific SPFs. This study showed that adding behavioral data to the predictive methods in HSM can improve the performance of prediction models substantially. However, to make this idea more convincing to the practitioners, more analysis is required to show the improvements in the out-of-sample forecast performance of SPFs using new data. Also, another convincing part of the new approach is its focus on volatile and aggressive drivers. Therefore, the methodology of this study can help the practitioners to adopt effective strategies to reduce aggressive driving to decrease crashes at intersections.

ACKNOWLEDGMENT

This study was partially supported by the Collaborative Sciences Center for Road Safety, CSCRS, a U.S. DOT funded National Transportation Center, under the Grant No. 69A3551747113.

CHAPTER 5 : UNDERSTANDING HOW RELATIONSHIPS BETWEEN CRASH FREQUENCY AND CORRELATES VARY FOR MULTILANE RURAL HIGHWAYS

A version of this chapter is published in the journal of *Accident Analysis & Prevention.*

Mohammadnazar, A., Mahdinia, I., Ahmad, N., Khattak, A. J., & Liu, J. (2021). Understanding how relationships between crash frequency and correlates vary for multilane rural highways: Estimating geographically and temporally weighted regression models. Accident Analysis & Prevention, 157, 106146.

ABSTRACT

Safety Performance Functions (SPFs) are critical tools in the management of highway safety projects. SPFs are used to predict the average crash count per year at a location, such as a road segment or an intersection. The Highway Safety Manual (HSM) provides default safety performance functions (SPFs), but it is recommended that states in the U.S. develop jurisdiction-specific SPFs using local crash data. To do this for the state of Tennessee, crash, and road inventory data were integrated for multi-lane rural highway segments for the years 2013-2017. In addition to developing SPFs similar to those contained in the HSM, this study applied a new methodology to capture variation in crashes in both space and time. Specifically, Geographically and Temporally Weighted Regression (GTWR) models for the localization of SPFs were developed. The new methodology incorporates temporal aspects of crashes in the models because the impact of a specific variable on crash frequency may vary over time due to several reasons. Results indicate that GTWR models remarkably outperform the traditional regression models by capturing spatio-temporal heterogeneity. Most *parameter* estimates were found to vary substantially across space and time. In other words, the association of contributing variables with the number of crashes can vary from one region or period of

time to another. This finding weakens the idea of transferring default SPFs to other states and applying a single localized SPF to all regions of a state. Enabled by growing computational power, these results emphasize the importance of accounting for spatial and temporal heterogeneity and developing highly localized SPFs. The methodology of this study can be used by researchers to follow the temporal trend and location of critical factors to identify sites for safety improvements.

LITERATURE REVIEW

Several studies have been conducted on large truck safety. The dependent variables in these studies are usually severity (*164-169*), propensity (*170; 171*), and/or frequency of large-truck-involved crashes (*168*). The effects of driver condition (e.g., impaired and distracted), driver characteristics (e.g., age and gender), driver behavior (e.g., speeding and lane change), road characteristics (e.g., curves and median width), weather conditions (e.g., inclement weather), and traffic conditions (e.g., speed limit and AADT) have been investigated in previous studies on large-truck-involved crashes. Binary probit, ordered probit, multinomial logit, and negative binomial are among the most used models. Data used in these studies are mostly based on police reports (*164-169; 172-174*), although some studies have integrated additional data from interviews and medical records (*165*).

Large-truck-involved crashes can be categorized by single- (*166; 170; 175; 176*) and multiple-vehicle crashes (*164-169; 172; 173*). Regarding single-vehicle crashes, large truck rollovers have been a matter of concern in previous studies (*170; 175-178*) because they can cause traffic congestion, transport disruption, and danger not only to occupants but also to others (*170*). In the 2017 study by (*179*), the authors also evaluated effective factors on injury severity in run-off-road crashes involving large trucks. Several studies have explored contributing factors to occupant injury severity in multiple-vehicle crashes (*180-182*). These studies consider different types of collisions such as angle, sideswipe, head-on (*181*), and rear-end crashes (*180; 181*), etc. In (*181*) for instance, it was found that head-on and sideswipe crashes are more severe than other crash types. Additionally, several studies have focused on crash location. A crash can occur at a work zone (*172; 183*), an intersection (*184*), an interstate highway (*174*), or an urban area (*164; 171; 173*). Therefore, contributing factors and their effects on crash severity and propensity can be different. For example, it was revealed in 2004 by (*172*) that large-truck-involved crashes that occur in work zones are usually more severe than other crashes, especially if they occur on two-way undivided roadways with higher speed limits.

The literature shows that numerous studies have been done on large-truck-involved crashes to evaluate the effect of different contributing factors on crash severity. However, few studies have specifically looked at single-vehicle large truck crashes. These studies mostly evaluated rollover crashes (*170; 175-177*). A recent study evaluated run-off-road crashes involving large trucks (*179*). However, a run-off-road crash can include different types of collisions such as crashing into a fixed object, moving object, pedestrian, or bicyclist, or it can be considered a non-collision crash (e.g., off-road rollover and overturn on terrain). Consequently, the characteristics and countermeasures for these crashes will be different. Because fixed-object crashes are the most frequent single-vehicle crash type among large trucks, it is worth studying them separately. Furthermore, although the effects of drivers' physical conditions and driving errors on crash injury severity have been explored in the literature, studies focusing on large-truck drivers are rare. Especially, one limitation of the studies conducted on truck-involved crashes is that large-truck drivers might not be at fault in the crashes involving more than one vehicle. Therefore, the pure effect of large-truck drivers' behavior on the severity of the crashes cannot be specified accurately. Therefore, this limitation can be overcome by investigating large-truck drivers' behavior in fixed-object crashes since the only driver involved in the crash is the large-truck driver. Furthermore, one of the missing aspects in current large-truck crash studies is the issue of unobserved heterogeneity. Conventional databases used in the crash severity studies are limited in the sense that they only contain a small fraction of the factors contributing to the severity of collisions, and therefore, many other factors are unobserved to the researchers. This can result in so-called unobserved heterogeneity in the model, which, if not addressed, can lead to biased parameter estimates, poor goodness of fit, and incorrect inferences (*185*). Therefore, this study accounts for unobserved heterogeneity by using a random parameter ordered probit model which allows the parameters to vary across the observations.

In summary, this study contributes to the field from three aspects:

1. It explores the physical conditions and driving errors of large-truck drivers that correlate with the most severe injuries in fixed-object crashes.
2. It investigates the pure effect of large-truck drivers' behavior on the severity of the crashes.
3. It applies a random parameter model to account for unobserved heterogeneity in the analysis of large-truck-fixed-object crashes.

INTRODUCTION

The Highway Safety Manual (HSM) provides researchers and practitioners with analytical tools and models for predicting the safety performance of various highway facilities (*107*). Safety Performance Functions (SPFs) are one of the fundamental tools used in the HSM for estimating the average number of crashes for a specific type of facility. SPFs assist agencies in network screening, such as identifying locations with the highest potential for improvement, and decision-making processes, such as choosing among alternatives at a project level (*92*). However, one of the weaknesses of SPFs is that these functions do not account for the differences between jurisdictions while the roadside composition, traffic condition, geometric features, and the way agencies report crashes can vary for each state or jurisdiction (*107*). To overcome this problem, the HSM suggests two solutions: 1. Calibration of SPFs using Calibration Factors and 2. Development of jurisdiction-specific SPFs using the states' own data. Many agencies have already developed SPFs using crash predictive models. These models follow a "one-size fits all" approach while quantifying the effects of a specific variable on crash frequency through the use of a "global" parameter. The use of a "global" parameter estimate suggests that the effect of a specific variable remains constant throughout diverse locations and over different periods. However, the effect of a specific variable on crash frequency may be different in different locations (e.g., the effect of lane width on crash frequency in Knoxville may be different than that in Memphis) due to diverse socio-economic, traffic, and roadway conditions. Similarly, the impact of specific variables on crash frequency may vary with time which may be due to roadway maintenance, rehabilitation, culture, and environmental change, etc. Hence, this study is designed to answer the question "Do

SPFs parameters vary significantly across space and time?" To answer this question, this study used Geographically and Temporally Weighted Negative Binomial Regression (GTWNBR) models to explore the variation of SPFs parameters in a spatio-temporal domain. Using space- and time-referenced crash data, GTWNBR models can estimate parameters for a specific location and period. Therefore, the transferability of global SPFs to a state can be examined. Part C of the HSM provides SPFs for several roadway types and classes including rural two-lane, two-way roads, rural four-lane divided and undivided multilane highways, and urban and suburban arterials (*107*). This study, however, only focuses on rural four-lane divided highways in order to explore how relationships between crash frequency and correlates vary across space and time on this type of roadway.

METHODOLOGY

Figure 5-1 shows the conceptual framework of this study. Conventional SPFs provided by the HSM are a function segment length and Annual Average Daily Traffic (AADT) that operate on the assumption that the correlation between crash frequencies and influential factors are independent of space and time. Although HSM proposes the idea of using calibration factors to make SPFs transferable to other states, such an adjustment is at a coarse level that cannot properly address the spatio-temporal heterogeneity of crash frequencies across the states. Therefore, this study aims to use geographic spatio-temporal techniques to explore the variability of SPFs as road crash frequency predictors across divided multilane rural highway segments in the state of Tennessee. GTWNBR models enable us to predict crash frequencies for specific locations and time intervals and provide us with the opportunity to evaluate the local effect of associated factors on crash frequencies. In this study, in addition to the GTWNBR models, global SPFs are estimated to draw a comparison between these models from the perspective of the goodness of fit and the stationarity of contributing variables across space and time. Whether it is a GTWNBR model or a global model, two groups of the variable have been used for model estimation. The first group contains AADT and segment length, which are currently used in the HSM as SPF estimators, while the second group contains traffic and geometric features in addition to these two variables. In this study, the models using the first group of variables are called “standard models”, and the models using additional variables are called “models with additional factors”.

Data description

The accuracy and performance of GTWNBR models to a large extent depend on the resolution of the space- and time-referenced data. This is because high-resolution data better explains the heterogeneity of associated variables across different locations and over time. Therefore, considerable effort was put into collecting and combining the data for all divided multilane rural highways across Tennessee from different data sources. A total of 943 segments were identified from the Enhanced Tennessee Roadway Information Management System (E-TRIMS) developed by the Tennessee Department of Transportation (TDOT).

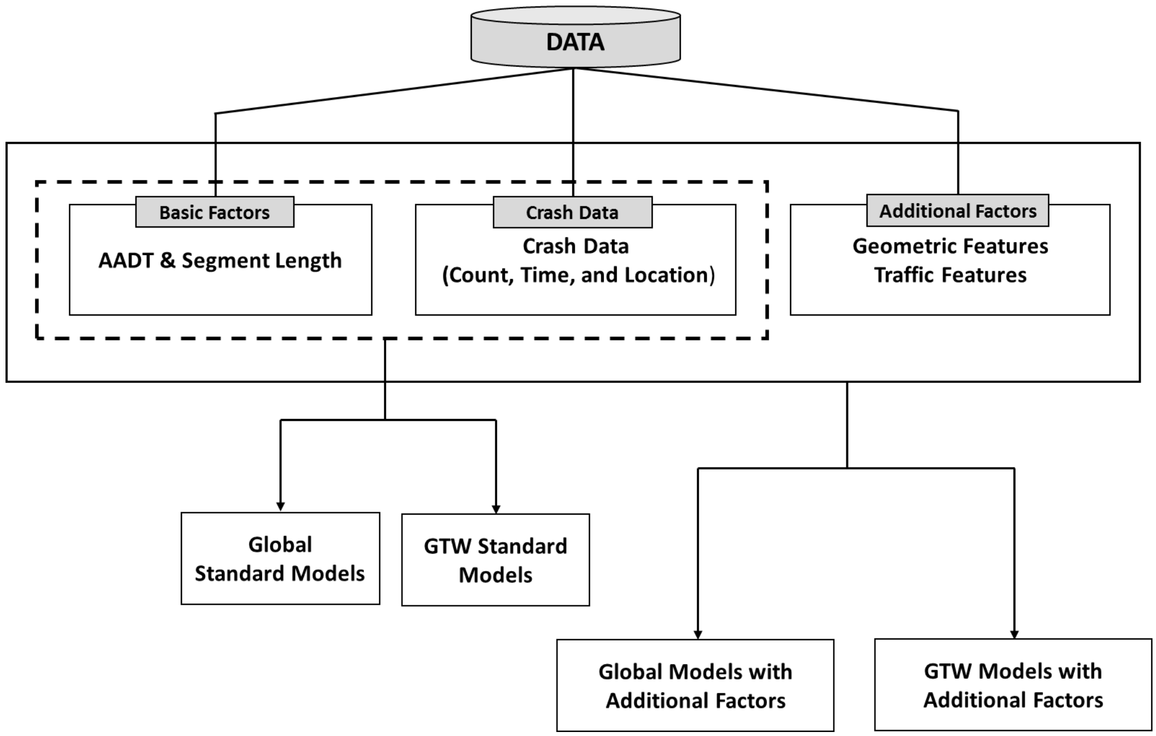

Figure 5-1. Conceptual framework of the study

Figure 5-2 shows locations of these segments in Tennessee along with the state's four regions. Next, crash data of the segments between 2013 and 2017 was manually extracted through the E-TRIMS crash summary reports. Then, geometric and traffic data (e.g. speed limit and AADT) were collected from TDOT's Image Viewer as depicted in Figure 5-3. To check the accuracy of the extracted data, crash frequency of the segments between 2013 and 2017 was compared with the sum of the number of crashes for each year. Results showed an accurate matching for all 943 segments. After omitting the segments shorter than 0.10 miles and segments with no AADT records, 4715 crash observations belonging to 943 segments remained as the final dataset. Figure 5-4 and 5.5 show the distributions, averages, and their regression to the five-year average between 2013 and 2017 for crash frequency and AADT respectively. Based on Figure 5-4, the highest and lowest average crash frequency occurred in 2017 and 2015 respectively, while in other years, the average crash frequency was quite close to the 5-year average crash frequency. Average AADT, however, had a rising trend between 2013 and 2017 that showed a monotonical increase in traffic volume during that period (Figure 5-5). Tables 5-1 and 5-2 also show the descriptive statistics and frequencies of the explanatory variables collected for model estimation, respectively. These tables provide useful information regarding the segments; for example, on average 1.76 crashes with a standard deviation of 3.39 occurred on the segments. Moreover, 10.5 percent of the studied segments have full access control, and 8.27 percent are located in commercial areas. Also, the speed limit for a few segments in the data was 70 mph, which is not a typical speed limit for multilane highways.

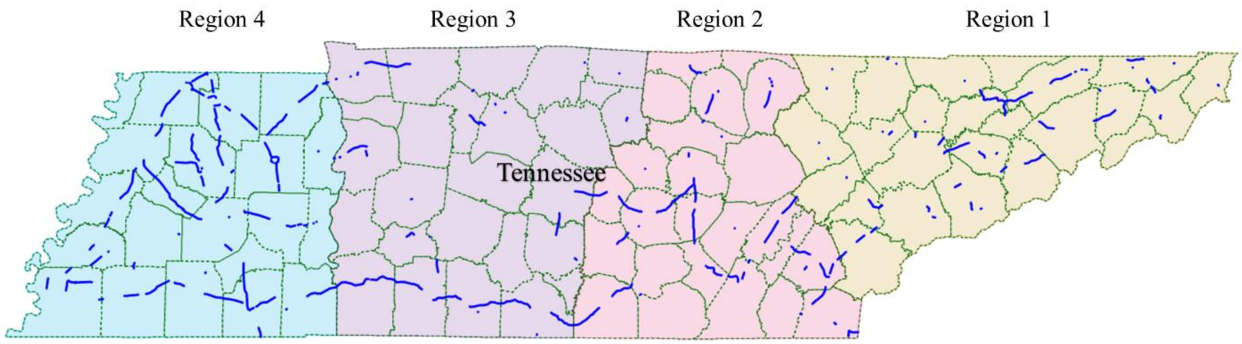

Figure 5-2 Locations of divided multilane rural highways across Tennessee

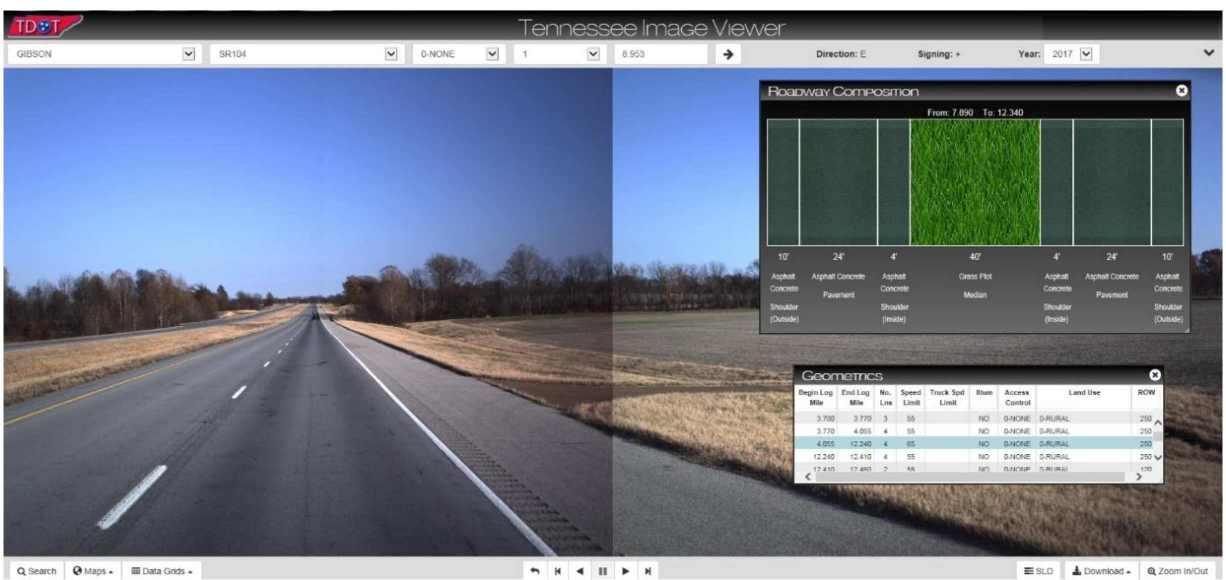

Figure 5-3 A picture in E-TRIMS software and the Tennessee image viewer web application for extracting geometric features of the segments

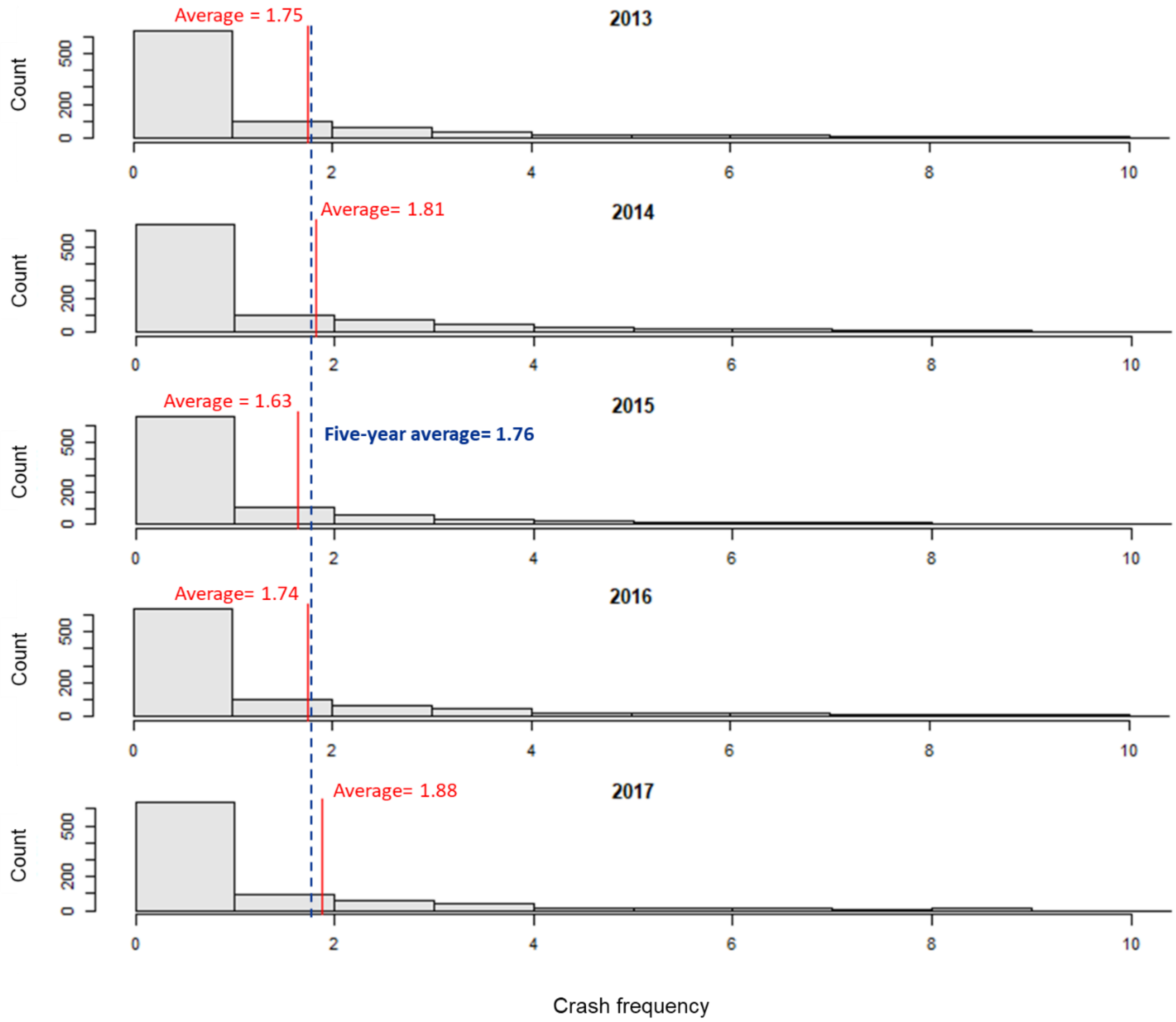

Figure 5-4 Distributions and temporal trend of average crash frequency between 2013-2017

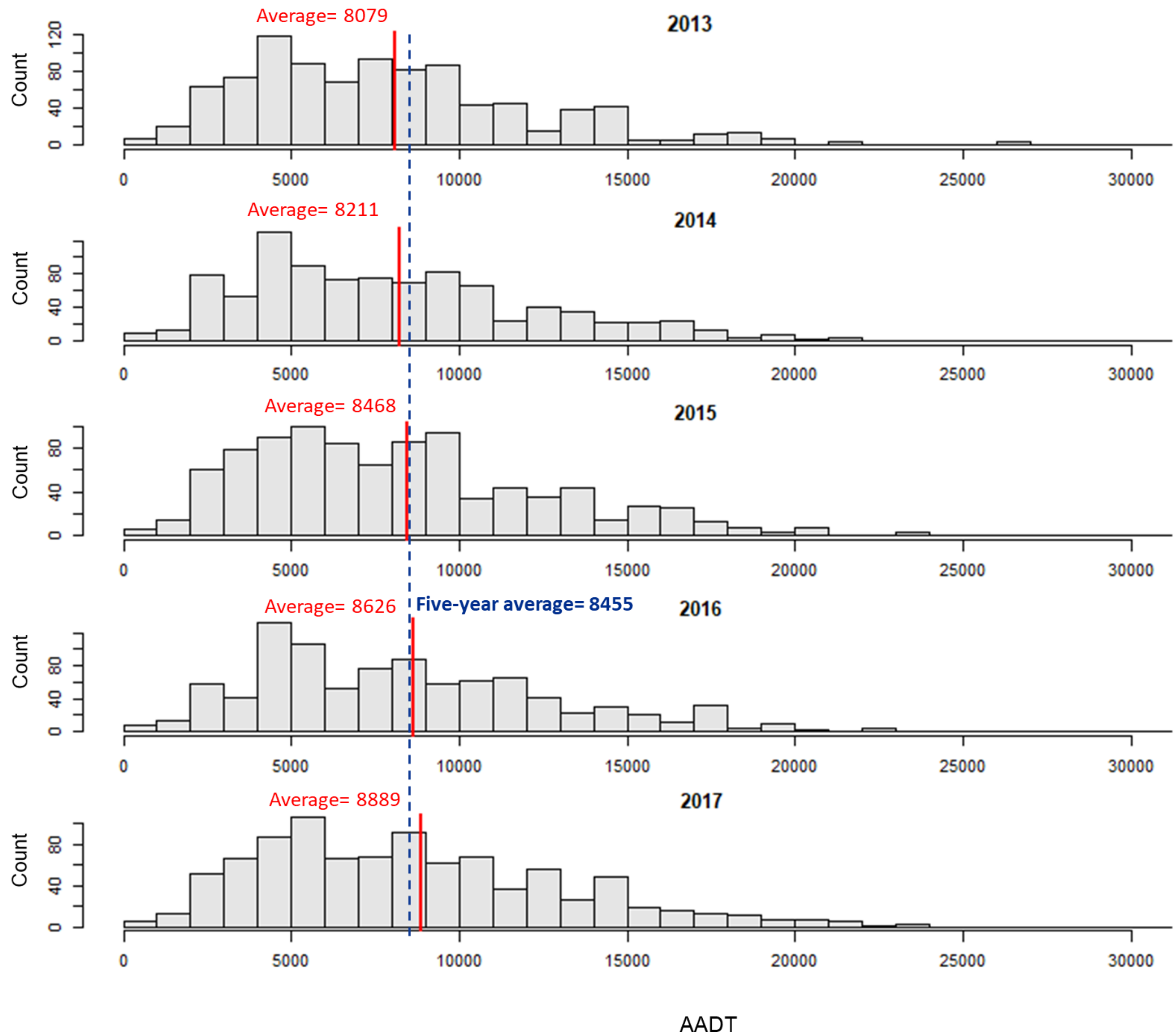

Figure 5-5 Distributions and temporal trend of average AADT between 2013-2017

Table 5-1 Descriptive statistics of continuous variables

Variable	N	min	max	mean	std.dev
Total crash	4715	0.00	55.00	1.76	3.39
AADT	4715	433.00	49016.00	8455.00	5321.36
Segment Length (mile)	4715	0.1	5.87	0.70	0.87
Speed limit (mile/h)	4715	30.00	70.00	57.16	8.05
Shoulder width* (ft)	4715	1.00	11.00	6.90	1.32
Median width (ft)	4715	2.00	360.00	36.61	24.37
Lane width (ft)	4715	10.00	12.00	11.99	0.10
Truck percentage (%)	4715	0.00	90.00	12.97	7.99

* Total of left and right shoulders

Table 5-2 Frequencies of categorical variables

Variables	Frequency	%	Variables	Frequency	%
Terrain types			**Shoulder type inside**		
Flat	310	6.58	Asphalt concrete	4195	88.97
Rolling	4195	88.97	Gravel	520	11.03
Mountainous	210	4.45	**Shoulder type outside**		
Land use			Asphalt concrete	4610	97.77
Rural	4250	90.13	Portland cement concrete	60	0.13
Commercial	390	8.27	Gravel	45	0.95
Residential	75	1.59	**Median type**		
Roadway Lighting			Barrier	245	5.19
No	4065	86.21	Grass	4055	86.00
Yes	235	4.98	Painted	265	5.62
Unknown	415	8.81	Other	150	3.18
Access-control			**Presence of Rumble strips**		
No	4195	88.97	No	1185	25.13
Partial	25	0.53	Yes	3530	74.86
Full	495	10.50			

Number of observations = 4715

Global SPFs- Negative Binomial models

The HSM provides the equation below as a function for predicting the average crash frequency for divided multilane highways (*107*):

$$N_{SPF} = \exp(a + b \times \ln(AADT) + \ln(L)) \quad (1)$$

$$or$$

$$N_{SPF} = L \times \exp(a + b \times \ln(AADT))$$

where N_{SPF} is the total number of crashes per year, *L* is the segment length (miles), *AADT* is the annual average daily traffic (*vehicles/day*) on the segment, and *a* and *b* are the regression parameters to be estimated. As it is presented in equation (1), the coefficient of the variable *Segment Length* equals one, meaning that the segment length functions as a multiplier in which its weight on the number of crashes is always constant. However, the effect of the segment length on the crash frequency might be different in different locations and jurisdictions. In other words, a lower number of road crashes can occur in long segments with uniform environments than in short segments with more complex and variable environments. Therefore, transportation experts usually consider a more general version of the above equation:

$$N_{SPF} = \exp(a + b \times \ln(AADT) + \mathrm{c} \times \ln(L)) \quad (2)$$

where parameter *c* is the coefficient of logarithmic form of the segment length *L*. If the estimated *c* equals one, equation (2) would be the same as equation (1). Among various regression models used for coefficient estimation, Poisson regression and negative binomial regression are the most widely used models which have shown the most compatibility with the count nature of crash frequencies (*110*). In the Poisson regression model, mean and variance are considered to be equal. However, the negative binomial model allows the variance and mean to be different, depending on the value of the overdispersion parameter *a:*

$$VAR[Y_i] = E[Y_i] \times [1 + aE[Y_i]] \tag{3}$$

where $E[Y_i]$ is mean or fitted value, $VAR[Y_i]$ is variance, and *a* is the dispersion parameter. If $a = 0$, the negative binomial distribution would be equivalent to the Poisson model. In other words, the Poisson model is a specific form of the negative binomial that restricts the dispersion parameter to 1. The HSM considers a negative binomial distribution for SPF estimation because it is very well suited to crash data with overdispersion (*107*).

As mentioned, the standard SPF provided by HSM only takes the key variables *AADT* and *Segment Length* into account. However, the crash frequency can depend on some other factors such as traffic and geometric features of the segment. Therefore, another form of SPF can be defined as below:

$$N_{SPF} = \exp(a + b \times \ln(AADT) + c \times \ln(L) + \sum \beta_k X_k) \tag{4}$$

where X_k is a vector of additional explanatory factors and β_k is a vector of the corresponding coefficient to be estimated along with the logarithmic form of the key variables *AADT* and Segment length *L*. In this study, SPFs defined in equations 2 and 4 with negative binomial distribution were estimated as global models.

Local SPFs- Geographically and Temporally Weighted Negative Binomial Regression models

Global regression models rest on the assumption that a single model can represent all parts of a region for different time intervals. However, in large regions and periods, heterogeneity in the data may result in a different relationship between explanatory variables in the model (*186; 187*). In other words, the effect of an independent variable on a response variable can be significant in an area and interval while it is insignificant in another or it could even have a reverse impact. Therefore, GTWNBR models can efficiently address the heterogeneity of spatio-temporal data and estimate parameters for a specific location and period. In GTWNBR models, every observation is considered as a centroid, and instead of taking all the observations into account for the model estimation, a sample of observations that geographically and temporally have the most proximity to the target observation is used for the model estimation. The neighboring observations of each sample are weighted in accordance with their spatio-temporal distance from the central observation such that the closer an observation is to the centroid, the more weight it receives. Having data with *n* observations, *n* separate regression models are performed to estimate the final GTWNBR. This results in a much longer processing time and requires a powerful system; however, the final output represents a much finer model with localized model estimates. In this study, Geographically and Temporally Weighted Negative Binomial (GTWNBR) models were created using a modeling tool developed in the environment of R. The next sections discuss the process of model estimation used in this study.

Determining weights using Adaptive bi-square kernel function

To determine geographical weights for the neighboring observations in a sample, the adaptive bi-square kernel function can be used (*187; 188*):

$$w_j^s(u_i, v_i) = \left[1 - \left(\frac{d_{ij}}{b}\right)^2\right]^2 \tag{5}$$

where u_i and v_i are the longitude and latitude coordinates of centroid *i*, $w_j^s(u_i, v_i)$ is a geographical weight assigned to the observation j with centroid *i*, d_{ij} is the special distance between observation *j* and the centroid *i*, and *b* is the kernel bandwidth which is the distance between centroid *i* and the farthest observation in the local sample. Likewise, temporal weights can be calculated as follows:

$$w_j^t(t_i) = \left[1 - \left(\frac{t_{ij}}{b}\right)^2\right]^2 \tag{6}$$

where $w_j(t_i)$ is the temporal weight assigned to the observation j occurring at t_j, t_{ij} is the temporal distance between observation *j* and the centroid *i* occurring at t_i, and *b* is the kernel bandwidth which is the distance between the centroid *j* and the farthest observation in the local sample. Assuming that time and location have the same effect on the model, the spatio-temporal weights will be calculated using the equation below:

$$w_j^{st}(u_i, v_i, t_i) = w_j^s(u_i, v_i) \times w_j^t(t_i) \tag{7}$$

where w_j^{st} is the spatio-temporal weight of the observation located in coordination (u_j, v_j) and occurred at t_i.

Selecting the optimal bandwidth for neighboring observations

After calculating weights, observations will be sampled based on their spatio-temporal distance from the centroids such that adjacent observations are more likely to be sampled together. The key parameter is the local sample size, which is often called optimal bandwidth. After running the model several times for different bandwidths, the bandwidth should be optimized to determine which bandwidth will result in a model that is a better fit with the current data. In this study, the Akaike Information Criterion (AIC) was used to find the optimum bandwidth (*147; 188*):

$$AIC = -2L + 2k + \frac{2k(k+1)}{n-k-1} \tag{8}$$

Where *k* is the number of explanatory parameters, *L* is the log-likelihood of the estimated model, and *n* is the number of observations. The lower AIC values indicate a better model fit with the data, and as a result, a better bandwidth. The optimum bandwidth depends on various factors including the number of observations, explanatory parameters, and model type. In this study, the optimal bandwidth for the estimation of the GTWR model is 850 observations. This means that for each centroid with a specific location and crash year, a negative binomial model with a local sample size of 850 observations is estimated. This sample size meets the recommended sample size mentioned in other studies (*115*).

Performing weighted negative binomial regression

After calculating spatio-temporal weights for observations in a local sample, GTWNBR can be estimated as follows (*186*):

$$N_{SPF} = \exp\left(a(u_i, v_i, t_i) + b(u_i, v_i, t_i) \times \ln(AADT) + c(u_i, v_i, t_i) \times \ln(L) + \sum_k \beta_k(u_i, v_i, t_i) \times X_{ik}\right) \tag{9}$$

where $a(u_i, v_i, t_i)$, $b(u_i, v_i, t_i)$, and $c(u_i, v_i, t_i)$ are local intercepts, and parameters are included for *AADT* and segment length *L*. Also, considering additional variables for model estimation $\sum_k \beta_k(u_i, v_i, t_i)$ are the local parameters for variables $X_1, X_2, \ldots, X_k$. In the case of considering only key variables (AADT and segment length), $\sum_k \beta_k(u_i, v_i, t_i)$ equals zero.

Model selection approach

In order to draw a comparison between models, the log-likelihood for models should be calculated. The log-likelihood of the global negative binomial can be calculated using the equation below:

$$L = \sum_{i=1}^{N} \{y_i \ln(a\mu_i) - (y_i + \frac{1}{a}) \ln(1 + a\mu_i) + \ln\left(\Gamma\left(y_i + \frac{1}{a}\right) - \ln\left(\Gamma\left(\frac{1}{a}\right)\right) - \ln(\Gamma(y_i + 1)\}\right\} \tag{10}$$

where *a* is the dispersion parameter of the estimated model. The same functions can be used for GTWNBR models. Note that in this study, it is assumed that the spatial and temporal variation is only allowed for parameters, and therefore, the dispersion parameter *a,* which is estimated for the global negative binomial regression, will be used for the GTWNBR model. For model selection, AIC values explained in equation (8) and the

McFadden Pseudo R^2 are used. The McFadden Pseudo R^2 can be calculated as below (*189*):

$$McFadden\ Pseudo\ R^2 = 1 - \frac{ln\, L}{ln\, L_{intercept}} \tag{11}$$

where $\ln L$ is the loglikelihood value of the full model and $\ln L_{intercept}$ is the likelihood value of the model without predictors. Higher values of McFadden $Pseudo\ R^2$ and lower values of AIC (*147*) show a better fit of the model with the data. As a rule of thumb, a ten-point difference in AIC shows a significant improvement in the model's goodness-of-fit (*190*).

Non-stationary Test

Local parameters estimated by GTWNBR models are time- and space-dependent. However, the variation of these parameters across space and time is not always significant, meaning that the parameters estimated by the local model are very close to the global ones. As a result, the non-stationary test is performed to compare the model estimates of global and local models (*187; 188*). The Non-stationary Test for each variable can be done as follows:

$$\mathrm{IQR} = \beta^{upper} - \beta^{lower} \begin{cases} > 1.96(S.E.)\ and\ \ \max|z| > 1.96, & Non-staionary\ Test\ is\ passed \\ otherwise, & Non-stationary\ Test\ is\ failed \end{cases} \tag{12}$$

where *IQR* is an interquartile range (the difference between the 75^{th} and 25^{th} percentile) of coefficient β, *S.E.* is the standard error vlaue from the global model, and $|z|$ is the z-value of the parameters in the local model. If a coefficient in a local model passes the non-stationary test, it means that the coefficient significantly varies across space and time, and it is worth evaluating in a spatio-temporal domain.

RESULTS AND DISCUSSION

Standard Global and Local SPFs with Key Variables

Table 5-3 shows the model estimation results of global standard SPFs based on the negative binomial distribution considering the logarithmic forms of the key variables *AADT* and *Segment Length*. As expected, variables *AADT* and *Segment Length* in both models could meaningfully address the response variable ($|z| > 1.96$). The positive coefficient of these variables indicates that they are positively associated with road crash frequencies. In other words, a higher volume and a longer segment indicate a higher number of expected crashes on the segment. Also, the marginal effects of the variables show that an increase in $ln(AADT)$ increases the average crash frequency by 0.872. Whereas, for $ln(Segment\ length)$ this value is 0.776.

Table 5-4 shows the estimation results of the local GTWNBR model. This table provides the distribution parameters (min, max, mean, standard deviation values, and lower/upper quartiles) for the estimates. Based on the results, parameters of variables *ln (AADT)* and *ln (segment length)* respectively vary in the range of 0.589 to 1.548 and 0.514 to 1.113 with mean values of 0.676 and 0.602, which is rather close to their global values in the global model. Moreover, comparing local models with global ones, AIC and McFadden $\text{Pseudo}\ R^2$ values show that local models have a better fit with the data and capture unobserved heterogeneity better than the global model.

Table 5-3 Estimation results of the global standard negative binomial model with key variables

Variable Estimate	Standard Negative Binomial			
	β	$\frac{dy}{dx}$ *	**S.E.**	**p-value**
Intercept	-5.23		0.32	0.00
ln (AADT)	0.681	0.87	0.04	0.00
ln (Segment length)	0.606	0.78	0.02	0.00
Number of observations			4715	
Log-likelihood at Convergence LL(β)			-7601.84	
Log-likelihood at Intercept LL(0)			-8427.76	
McFadden's R2			0.09	
AIC			15209.67	
Dispersion parameter			0.85	
Chi-squared test for overdispersion			11307.86	

* Marginal effect

Table 5-4 Estimation results of the local standard GTWNBR model with key variables

Variable Estimate	GTWNBR								
	Mean β	**std.dev β**	**Min β**	**Lower β**	**Median**	**Upper β**	**Max β**	**Max $\|z\|$**	**Min $\|p\|$**
Intercept	-5.20	0.53	-12.95	-5.56	-5.06	-4.93	-4.45	-6.47	0.00
ln (AADT)	0.68	0.06	0.59	0.64	0.66	0.72	1.55	7.46	0.00
ln (Segment Length)	0.60	0.05	0.51	0.58	0.59	0.64	1.11	13.26	0.00
Number of observations						4715			
Log-likelihood at Convergence LL(β)						-7584.22			
Log-likelihood at Intercept LL(0)						-8427.76			
McFadden Pseudo-R^2						0.10			
AIC						15174.45			

Global and local model estimations with additional variables

Table 5-5 shows the model estimation results of the negative binomial model considering additional explanatory variables besides *AADT* and *segment length*. This model shows the global correlation between contributing parameters and roadside crash frequency. Note that only significant variables ($p - value < 0.05$) are reported in the table. Similar to standard models explained in the last part, *AADT* and *segment length* have direct associations with the roadside crash frequencies. Also, generally, the sign and magnitude of the additional variables are logical. For example, the variable *speed limit* has a negative sign, indicating that on highways with higher speed limits, a lower number of crashes has occurred, which is consistent with the results of previous studies (*191; 192*). It is probably because high-speed limits are usually selected on safer segments. *Access control* is another traffic variable that is negatively associated with crash frequency. In other words, highways with full access-control are expected to have a lower number of crashes. This is because of lower merging and diverging traffic which can have a negative impact on a highway's mainstream traffic. Moreover, different categories of the variable *land use* indicate that roadside crashes are more likely in commercial areas compared to the areas with rural land use. The higher number of crashes in commercial areas can be because of higher variation in the environment, more complex relationships between road users, and a higher number of access points in commercial areas, which can result in a higher number of aggressive driving events on these roads (*63*). This result is in line with the findings of Kim et al. (*193*). Regarding the geometric features of the segments, results indicate that on segments with a wider median and lane, a lower number of crashes is expected. This is in agreement with the literature (*194-196*). Also, a lower number of crashes are expected on the segments with grass and painted medians compared to segments with median barriers. The presence of rumble strips in segments has been shown to decrease crash frequency. This is because the presence of rumble strips can reduce the number of run-off-road crashes (*197*). Furthermore, truck percentage was found to be negatively associated with the frequency of crashes on multilane highways. This result is in line with the findings in previous studies (*192; 198*).

Table 5-6 shows the estimation results of local models considering additional variables as well as non-stationary test results of independent variables. Similar to the standard local models, the min, max, mean, standard deviation, and lower and upper quartile values for each coefficient were found. These variables show the distribution and variation range of parameters across space and time. For instance, based on the model results, the estimate of variable *ln (segment length)* has a mean value of 0.718, ranging from 0.597 to 0.865, with a standard deviation of 0.050. The non-stationary test can also help us compare the estimation results of the GTWNBR model with the global NB model. Based on the results, variables *median type, land use (category of residential),* and *access control* did not pass the non-stationary test. The rest of the variables, however, passed the non-stationary test indicating that they vary significantly across space and time, and they have a non-stationary correlation with crash frequency.

Table 5-7 presents a comparison of the goodness-of-fit of global and local models based on AIC and $\text{Pseudo}\,\mathrm{R}^2$ statistics. Based on the results, compared to the conventional global models, using the local model with key variables and the local model with additional variables increased the McFadden R^2 by 11.1% and 16.7 % respectively.

Table 5-5 Estimation results of the global negative binomial model with additional variables

Variable Estimate		Negative Binomial with Additional Variables			
		β	$\frac{dy}{dx}$ *	S.E.	p-value
Intercept		2.98	-	2.12	0.16
ln (AADT)		0.65	0.77	0.04	0.00
ln (Segment Length)		0.71	0.85	0.02	0.00
Speed limit		-0.01	-0.02	0.00	0.00
Lane Width		-0.65	-0.78	0.18	0.00
Median Width		-0.01	-0.01	0.00	0.00
Median type (Base: Barrier)	Grass	1.27	1.02	0.12	0.00
	Painted	1.33	3.06	0.15	0.00
	Other	1.68	4.91	0.18	0.00
Land Use Base: Rural	Commercial	0.43	0.61	0.07	0.00
	Residential	-0.20	-0.21	0.16	0.22
Access control (Base: No Access control)	Partial	-0.27	-0.28	0.33	0.42
	Full	-0.23	-0.25	0.08	0.00
Rumble strips present		-0.11	-0.14	0.05	0.02
Truck percentage		-0.01	-0.01	0.00	0.01
Number of observations		4715			
Log-likelihood at Convergence LL(β)		-7426.01			
Log-likelihood at intercept LL(0)		-8525.84			
McFadden's R^2		0.12			
AIC		14882.02			
Dispersion parameter		1.00			
Chi-squared test for overdispersion		8180.87			

* Marginal effect

Table 5-6 Estimation results of GTWNBR with additional variables

Variable Estimate		**GTWNBR**									**Non-stationarity**	
		Mean β	**std.dev β**	**Min β**	**Lower β**	**Median**	**Upper β**	**Max β**	**Max $\lvert z \rvert$**	**Min $\lvert p \rvert$**	**Delta**	**Test**
Intercept		2.88	3.92	-5.80	0.23	3.54	5.49	22.70	1.48	0.14	5.27	No
ln (AADT)		0.65	0.08	0.53	0.60	0.62	0.69	1.05	7.71	0.00	0.09	Yes
ln (Segment length)		0.72	0.05	0.60	0.69	0.71	0.76	0.87	14.46	0.00	0.07	Yes
Speed limit		-0.02	0.01	-0.03	-0.02	-0.02	-0.01	0.00	3.57	0.00	0.02	Yes
Lane Width		-0.64	0.36	-2.29	-0.90	-0.66	-0.38	0.07	2.73	0.01	0.52	Yes
Median Width		-0.01	0.00	-0.02	-0.01	-0.01	-0.01	0.00	4.13	0.00	0.00	Yes
Median type (Base: Barrier)	Grass	1.29	0.22	0.55	1.16	1.24	1.40	1.87	5.14	0.00	0.23	No
	Painted	1.30	0.29	-2.51	1.18	1.34	1.45	1.78	3.57	0.00	0.27	No
	Other	1.39	0.64	-3.07	0.86	1.69	1.89	2.17	3.96	0.00	1.03	Yes
Land Use Base: Rural	Commercial	0.42	0.14	0.12	0.28	0.48	0.54	0.77	3.10	0.00	0.26	Yes
	Residential	-0.76	0.46	-1.68	-1.04	-0.76	-0.45	0.82	1.89	0.06	0.60	No
Access control (Base: No Access control)	Partial	-0.48	0.99	-2.39	-1.31	-0.37	0.09	1.35	1.67	0.09	1.40	No
	Full	-0.25	0.16	-0.59	-0.32	-0.24	-0.14	0.36	1.78	0.07	0.18	No
Rumble strips		-0.10	0.16	-0.47	-0.18	-0.10	-0.02	0.26	2.87	0.00	0.16	Yes
Truck percentage Presence		-0.01	0.01	-0.04	-0.01	-0.01	0.00	0.00	2.29	0.02	0.01	Yes
Number of observations		4715										
Log-likelihood at Convergence LL(β)		-7310.288										
Log-likelihood at Convergence LL(0)		-8525.84										
McFadden Pseudo-R^2		0.14										
AIC		14650.576										

Table 5-7 Comparison of goodness-of-fit of models

Model	McFadden R^2	Δ R^2 (%)	AIC	Δ(AIC)
Global model with key variables	0.09	11.1	15209.67	35.22
Local GTWNBR model with key variables	0.10		15174.45	
Global model with additional variables	0.12	16.7	14882.02	231.44
Local GTWNBR model with additional variables	0.14		14650.576	

Also, the difference between AIC values for global and local models with key variables and additional variables are 35.22 and 231.44, respectively.These results show that local SPFs estimated using the GTWNBR models have a significantly better fit with the data compared to the global models. It could be because local models better capture the spatio-temporal heterogeneity in crash counts by allowing the explanatory variables to vary across space and time. The higher values of McFadden $\mathrm{Pseudo}\ \mathrm{R}^2$ in these models also indicate that these models explain more of the variation in crash counts. Furthermore, results indicate that full SPFs with additional variables outperform the base SPFs with key variables, showing that adding meaningful explanatory variables related to geometric design, traffic characteristics, and land use improves the goodness-of-fit of SPFs. Overall, the local GTWNBR model with additional variables has the best fit with the data, because it has the lowest AIC (14650.57) and the highest McFadden $\mathrm{Pseudo}\ \mathrm{R}^2$ value (0.14). Therefore, this model was selected for the non-stationary test and further evaluation of SPF parameters.

Spatial variation of local parameter estimates in Tennessee

Figure 5-6 illustrates the spatial variation of local coefficients at a county level in Tennessee considering only variables that passed the non-stationary test. Color was used to indicate the average value of a coefficient for all the multilane highways located in each county. An increased number of crashes was represented by red, whereas green was used to indicate a decrease in crashes associated with eight key variables. Note that for some counties, there was no data, and therefore, they are in white. Generally, Figure 5-6 shows that parameter estimates can be partially stationary in some regions but variable across jurisdictions. For example, Figure 5-6(a) shows that *AADT* has relatively stable parameters in west Tennessee. This shows that the impact of *AADT*, as a positively correlated variable for crash frequency, is lower in western counties. Going from the west of Tennessee to the east, the effect of the variable *AADT* increases significantly. Especially in eastern counties, *AADT* has the highest impact on the number of crashes. It might be because of a specific condition of highways or the driving habits of the people in this region. Also, as it is depicted in Figure 5-6(b), greater values for the estimates of variable *Segment length* are concentrated in the northeast of Tennessee, while in central and eastern areas, segment length has a smaller impact on crash frequencies. Also, less variation across western counties indicates that the impact of segment length on crash frequency is stationary in this region. Figure 5-6(c) also shows the variation of estimates for the variable *commercial land use*. The association of whether a highway segment has commercial land use is stronger in southern and south-central Tennessee. The lowest associations of commercial land use with crash frequency were found in east Tennessee, which might be because of lower access point densities that result in a lower number of conflicts on the segments. Regarding the variable *speed limit* (Figure 5-6(d)), the positive association of speed limit with crash frequency is stronger in northeastern and western regions compared to the central areas. Importantly, in some parts of south-central regions, speed limit is negatively associated with the number of crashes. *Lane width* and *median width,* as two geometric characteristics of segments, also have non-stationary relationships with crash frequency. Based on Figure 5-6(e) and Figure 5-6(f), the spatial pattern of these two variables is different as the association of lane width with crash frequency is stronger in southern and south-central Tennessee, while the association between median width and crash frequency is stronger in eastern Tennessee.

Furthermore, as depicted in Figure 5-6(g), *truck percentage* has a higher correlation with the number of crashes in western regions. Also, while there is a negative association between crash frequency and truck percentage in western and central areas, the signs of parameters change in eastern Tennessee. Regarding the spatial variation of the variable *rumble strips presence*, Figure 5-6(h) shows that there is a significant variation in the sign and magnitude of parameters. While there is a negative association between rumble strip presence and crash frequency in east Tennessee, the sign of the correlation changes to positive in western regions. However, this positive association could be because a higher number of crashes occurs on segments with rumble strips in these areas, and that does not indicate that the presence of rumble strips on the segments increases crash frequency.

Temporal variation of local parameter estimates in Tennessee

In addition to the spatial variation, the temporal variation of parameter estimates can be evaluated. For instance, Figure 5-7 illustrates the spatial variation of variables *ln (AADT)* and *ln (segment length)* between 2013 and 2017 across the state of Tennessee. As it is depicted in the figure, although there was a positive association between these two variables and the number of crashes between 2013 and 2017, the spatial pattern of parameters varied over time. For instance, in 2013, the association between AADT and crash frequency is the strongest in East Tennessee, while in 2014 and 2016, higher values of parameters shifted toward the west and mid-west Tennessee. However, in 2015 and 2017, the strongest correlations were concentrated in central Tennessee. Furthermore, the magnitude of parameters varied between 2013 and 2017.

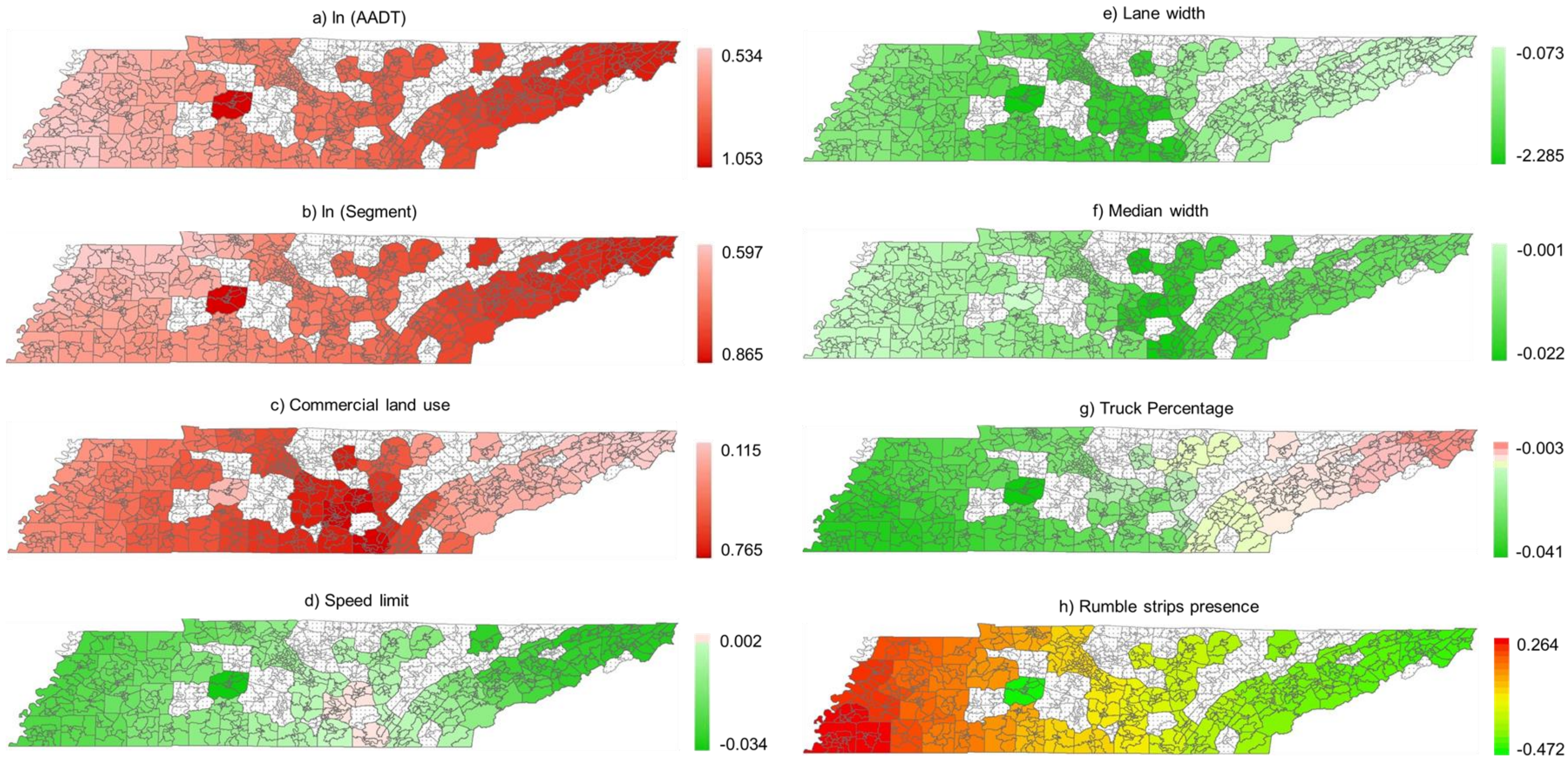

Figure 5-6 Illustration of the spatial variation of local parameter estimates in Tennessee at county level

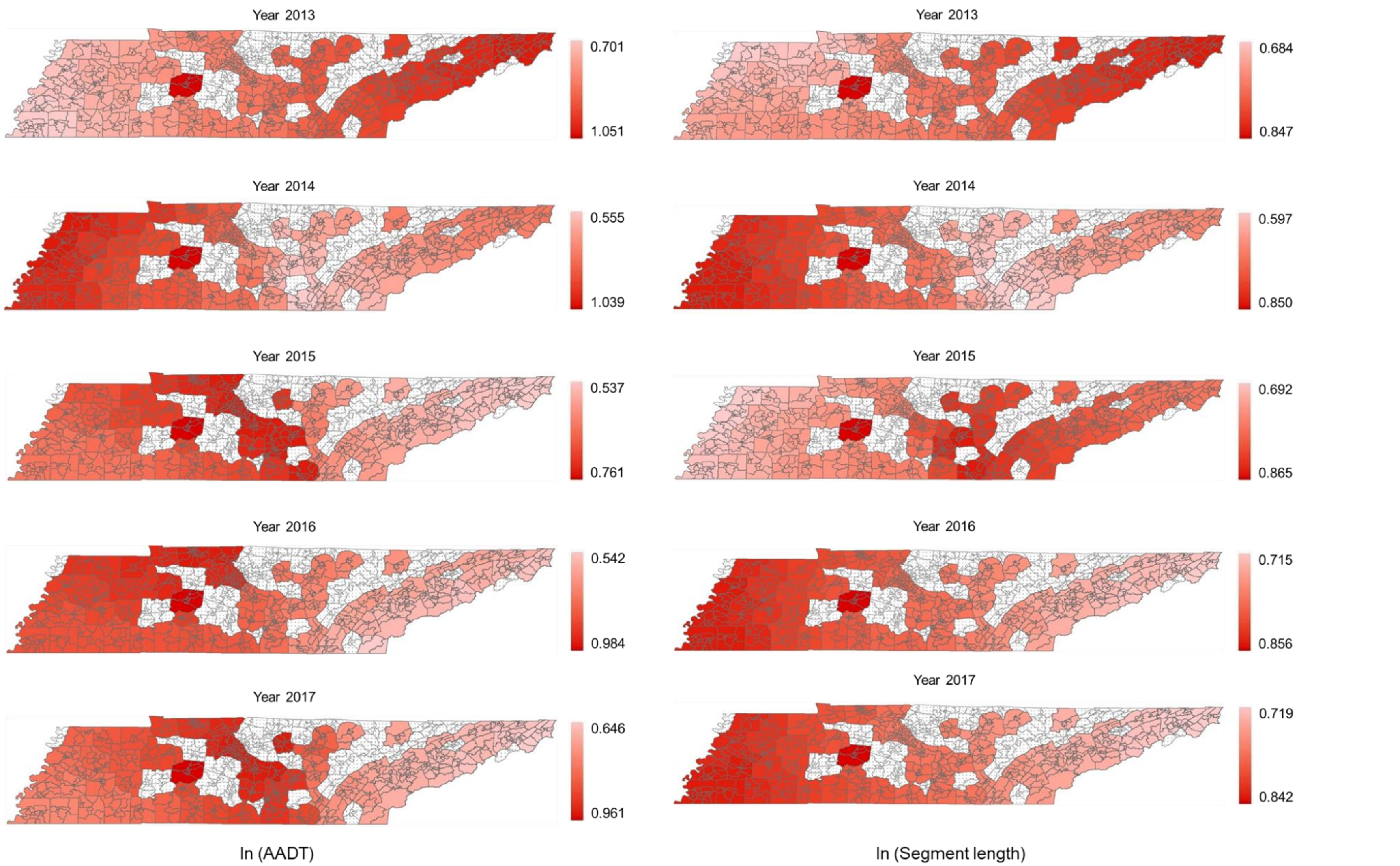

Figure 5-7 Spatial variation of parameters of variables AADT and segment length between 2013-2017 across the state of Tennessee

For example, ranging from 700 to 1.051, the effect of *AADT* on crash frequency is the highest in 2013. For the variable *ln (segment length)*, higher values of parameters are concentrated in the west and mid-west Tennessee in 2014, 2016, and 2017. However, in 2013 and 2015, the association between segment length and crash frequency is the strongest in eastern regions.

Figure 5-8 also gives a general view of the temporal variation of parameter estimates between 2013 and 2017 based on the average of estimates over space. As depicted in the figure, some variables such as *median width* and *truck percentage* are roughly stationary over time with a minor variation, while some other variables such as *rumble strip presence*, *speed limit,* and *ln (AADT)* show considerable fluctuations over time. For instance, parameters of the variable *rumble strip presence* decrease significantly between 2013 and 2014, then they rise between 2014 and 2016, and then they fall again after 2016. Importantly, although the variable has a positive association with the number of crashes in 2013, the sign of the association changed after 2014. Also, regarding the variable *ln (AADT),* the association of AADT with crash frequency has decreased between 2013 and 2016 and then increased after 2016. Furthermore, some variables such as *lane width, commercial land use,* and *ln (Segment length)* have a rising trend over time. While an increase in positive parameters results in a greater effect of variables on the number of crashes (e.g., parameters of variable *commercial land use*), an increase in negative parameters reduces the effect of variables on the number of crashes (e.g., parameters of variable *lane width*). The increase in the effect of the variable *commercial land use* can be because of the establishment of new big businesses along the highways, which attract more traffic.

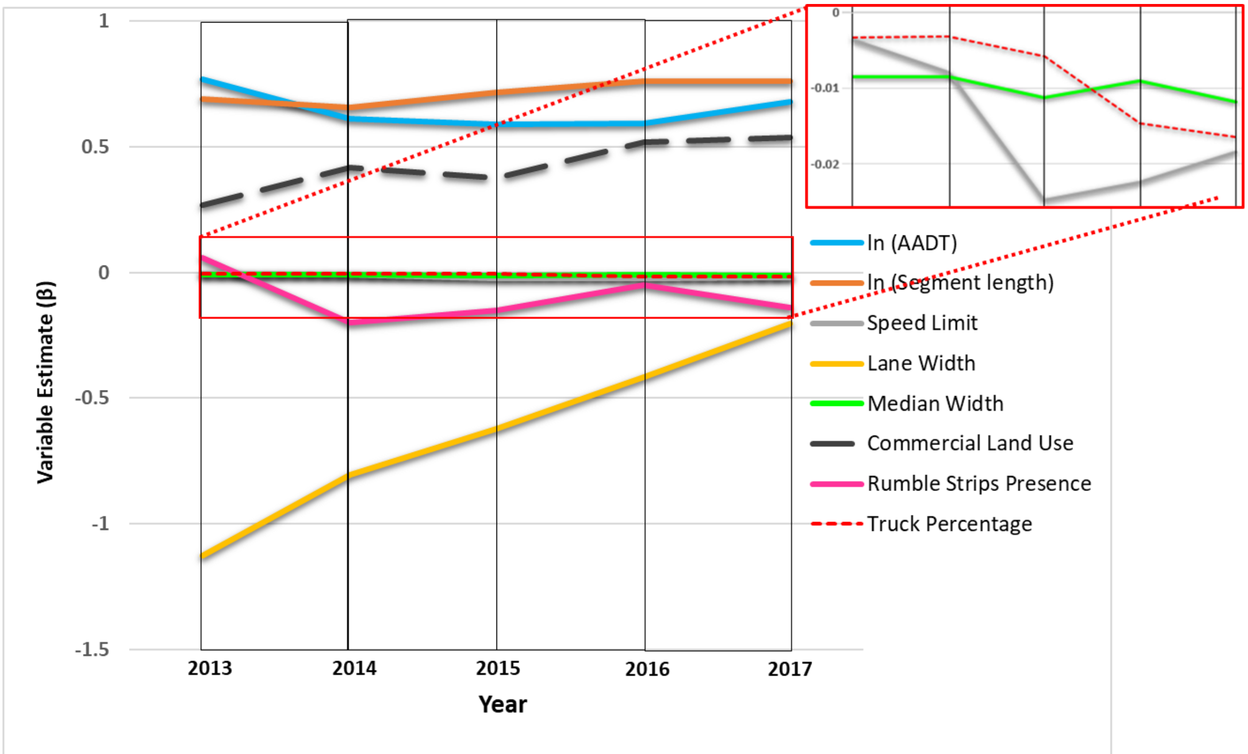

Figure 5-8 Temporal variation of variable estimates (averaged over space)

In other words, assuming that the land use and the number of access points have been constant between 2013 and 2017, business expansions along the highways might have increased the number of conflicts between the main traffic and the traffic to and from access points, which could lead to a higher number of crashes on these roads. These trends give foresight to researchers and planners on research-worthy topics and projects for safety improvement in the future.

Comments on safety performance predictions using GTWNBR models

While a key purpose of this study is to incorporate the temporal element explicitly in crash models and understand how crashes vary in space and time, GTWNBR models can be used as a safety predictive tool for different roadway facilities, such as highways, freeways, and intersections.

Theoretically speaking, GTWNBR models could yield more accurate predictions than the conventional SPFs in the HSM mainly because they address spatio-temporal heterogeneity in crash data. However, there are two important points regarding the application of GTWNBR models for safety predictions.

Firstly, GTWNBR models are not transferable to other areas and jurisdictions. This is because in the development of GTWNR models, space-and-time-referenced crash data are used, and as a result, parameters vary across space and time. Therefore, when it comes to a local crash frequency prediction for a selected site, GTWNBR models refer to the location of the site to provide parameters that have been estimated specifically for that location. As a result, GTWNBR models can only be used for the jurisdiction for which they have been developed. If GTWNBR models are to be used for safety performance predictions, then agencies would be expected to develop jurisdiction-specific SPFs using the local data.

Secondly, the application of the GTWNBR models should account for regression to the mean bias, as this is one of the most common challenges in crash frequency predictions. Regression to the mean is the natural tendency of crash frequency to fluctuate around the true mean as a non-systematic variation in observed crash data (*107; 199*). As a result of regression to the mean phenomenon, a site with a high number of crashes (in a particular year) might be selected for treatment while the high crash frequency can be due to random variation in the crash frequency (*107*). Although GTWNBR models allow the mean to vary across space and time, which can mitigate the regression to the mean bias to some extent, regression to the mean bias is not fully accounted for by these models. If GTWNBR models are used for crash frequency estimation in before-after studies, further research is needed to achieve better results by applying methods that are similar to the empirical Bayes method (*200*).

LIMITATIONS

The accuracy of the results reported in this study largely depends on the accuracy of the data used in the model estimation. For example, it is possible that some crashes were not reported because they did not involve injury or significant property damages. Other factors such as traffic and geometric factors also can be reported with an error. Moreover, the models presented in this paper are limited to the variables available in the database. The effect of unobserved factors such as climate, population density, crash reporting policies, and driving behavior on the crash frequency of divided multilane highways was not explored in this study. Also, in this study, the crash data between 2013 and 2017 was used for the analysis. Since in the estimation of GTWR Models, it is crucial to have AADT and crash data of a segment for each year in the study period, the authors were limited to consider study period of 2013-2017 for which valid traffic data were available although more recent crash data could be obtained. When available, more recent data can be used in future studies to explore the current variation of parameters across space and time. Furthermore, geographically-weighted models heavily depend on the coordinates of the data points. In this study, the middle point of each segment was considered representative of the whole segment. This can result in errors on long segments, although geometric and traffic features of a segment are supposed to be uniform along the segment length. While this study proposes a practical framework for SPF estimation in the spatio-temporal domain, the results of this study are not transferable to other states and jurisdictions because of the unique characteristics of each region. Especially, GTWNBR models require space- and time-referenced data, and therefore, parameters estimated by these models vary spatio-temporally for Tennessee. As a result, the models' results cannot be directly used for other areas with different geographically distributed networks of highways. The GTWNBR method can be used to get local estimates of parameters in other states or countries.

CONCLUSION

Safety performance functions (SPFs) have been widely used to help identify contributing factors in traffic crashes, prioritize sites for improvements, and assess the effectiveness of safety treatments. However, the spatio-temporal instability of SPFs is of substantial concern to practitioners. Therefore, the main contribution of this study comes from the localization of SPFs used in the HSM by accommodating spatio-temporal instability in road crashes. Localization over space and time can impact how SPFs are applied in future HSM practice. While the estimates of SPFs provided in the HSM may provide satisfactory results, the results of this study indicate that more reliable results can be obtained by developing localized SPFs that account for unobserved heterogeneity. In this regard, this paper demonstrates the application of Geographically and Temporally Negative Binomial Regressions (GTWNBR) as rigorous local models and draws a comparison between these models and conventional models used for SPF localization. Compared with existing literature, the scope was expanded to explore the variation of variables over both space and time simultaneously. As expected, the GTWNBR models showed a better fit to the data compared with conventional global models. Also, it was found that including additional information related to geometric design, traffic characteristics, and land use in the models improves the goodness-of-fit of SPFs.

Previous studies have used global models that assumed that the effect of explanatory variables was spatio-temporally stationary. However, the results of the non-stationary test in this study show that this assumption is not always correct within the state of Tennessee, as the majority of the contributing factors varied significantly across space and time. Illustration of variable estimates on maps in this study also revealed that variable estimates are stationary within specific regions but vary from East to West in Tennessee. Therefore, the association of a variable with the number of crashes is not constant for all parts of Tennessee. The spatial analysis of parameters in this study shows that variables *AADT*, *segment length*, and *median width* have the highest impact on crash frequency in eastern regions, while variables *commercial land use* and *lane width* have the strongest association with crash frequency in southern and south-central Tennessee. Also, the associations of variables *speed limit* and *Truck percentage* with crash frequency are the highest in northeastern and western regions respectively. These spatial variations can be due to changes in socio-economic conditions, traffic characteristics, roadway conditions, and some other unobserved factors such as cultural diversities that can relate to spatial contexts.

Importantly, the temporal variation of parameter estimates was evaluated between 2013 and 2017. It was found that some variables were stable over this period (e.g., shoulder width and segment length), but other variables varied considerably from one year to another. Also, it was found that the spatial pattern of parameters varied over time. For instance, in 2013, the association between AADT and crash frequency was the strongest in east Tennessee, while in 2015, the strongest correlations were concentrated in central Tennessee. These variations could stem from socio-economic development, cultural, and environmental changes in a specific region that make that area vulnerable or resistant to a specific factor.

Overall, the spatio-temporal variation of contributing factors in this study implies that ignoring temporal and spatial instability and considering variable estimates to be constant over time and for an entire jurisdiction is simplistic, given the new developments in analysis methods. The GTWNBR models demonstrate an advanced set of tools that provide planners and practitioners with a better understanding of critical parameters associated with crash frequency for different regions. These will result in more accurate predictions of future crashes and the impacts associated with roadway (geometric) factors. The methodology presented in this study also provides the opportunity to follow the trend of contributing factors over a period to identify potential areas of future focus for safety improvements. As previously mentioned, the methodology of this study can be used for the localization of SPFs for other jurisdictions, but the results of this study cannot be generalized to other locations because of the distinctive characteristics of each state and jurisdiction. The best results are likely obtained by examining data specifically collected for a state. For future studies, GTWNBR can be used for SPF calibration in other states and draw a comparison between the results. Also, while the GTWNBR models in this study are developed based on the total number of crashes, insights from previous studies on frequency-severity modeling (*201-203*) can be combined with GTWNBR models to explore the spatio-temporal variation of the explanatory variables at different severity levels. Furthermore, although this study evaluated the temporal variation of contributing factors, further research is needed to understand and project future trends and relationships between contributing factors and crash frequency.

ACKNOWLEDGMENTS

This study was funded by the Tennessee Department of Transportation and the U.S. DOT through the Collaborative Sciences Center for Road Safety (Grant No. 69A3551747113). The authors thank the Tennessee Department of Transportation for their guidance during the data collection process. The views in this paper are solely those of the authors who are responsible for the content of this publication.

CHAPTER 6 : HOW ARE PHYSICAL CONDITIONS AND DRIVING ERRORS OF LARGE-TRUCK DRIVERS ASSOCIATED WITH INJURY SEVERITY IN FIXED-OBJECT COLLISIONS?

A version of this chapter is under review in the *Journal of Transportation Safety & Security.* Also, a version of this paper was presented in the 100th Transportation Research Board Annual Meeting 2021, Washington DC.

ABSTRACT

According to the U.S. Department of Labor, the trucking industry experienced the highest number of fatalities among all occupations in 2017. Over 75 percent of these fatalities were related to roadway accidents. Police-reported crashes show that fixed-object crashes are one of the most fatal and frequent crash types among large trucks, which raises occupant safety concerns. Strangely, these crashes are lightly researched in the literature. Especially, our knowledge of driver behavior factors contributing to injury is limited. While large-truck drivers' physical conditions and driving errors have been recognized as major factors in large-truck-involved crashes, their association has not been viewed from the heterogeneity perspective. Also, the pure effect of large-truck drivers' behavior on the severity of large-truck crashes cannot be estimated in multiple-vehicle crashes because large-truck drivers might not be at fault for the accident. Therefore, this study focuses on the effect of large-truck drivers' physical conditions and driving errors on the severity of large-truck-fixed-object crashes while controlling for crash characteristics and roadway features. To address unobserved heterogeneity in these crashes, a random parameter ordered probit model was estimated using North Carolina crash and inventory data between 2013-2017. The results show that having a medical condition, having illnesses, falling asleep while driving, impaired driving, and fatigued

driving have strong positive associations with large-truck-fixed-object crash severity. It was also found that driving errors such as speeding, oversteering, and aggressive driving increase the probability of experiencing fatal and injury crashes. This can help technology developers in the trucking industry and planners and engineers in the transportation field make informed decisions about safety countermeasures.

LITERATURE REVIEW

Significant efforts have been made by several states in the US including Alabama, California, Colorado, Florida, Illinois, Kansas, Maryland, Michigan, and Tennessee to adopt the SPFs provided in the HSM for their states. The focus of these SPFs adoptions is on roadway segments (*94-98*), intersections (*99; 204; 205*), or both (*95; 100; 102; 103; 105; 106; 206-208*). Generally, these agencies have taken three approaches to implementing SPFs for their states: 1. Calibrating HSM-provided SPFs (*94; 98; 102; 105; 207-210*), 2. Developing jurisdiction-specific SPFs (*96; 99; 100; 103; 204; 211*), and 3. Utilizing a hybrid approach, which is a combination of the first two approaches (*95; 97; 106; 205; 206*). In the first approach, agencies only report calibration factors for calibrating SPFs for their states. Calibration factors can have values greater than 1.0 for roadways with a higher number of crashes or less than 1.0 for roadways with a lower number of crashes than the roadways used by the HSM for developing SPFs. In this regard, the transferability of SPFs has been the focus of some recent studies. Farid et al., for example, estimated a transfer index to evaluate the transferability of SPFs across different states. They also proposed a Modified Empirical Bayes measure which provides calibration factors for each segment (*212*). Other studies explored the transferability of

HSM-developed SPFs outside the US using the data of other countries (*213-215*). In approaches 2 and 3, which is the focus of this study, agencies develop their own predictive models using local crash data. This approach is encouraged by the HSM because it might result in more reliable estimates (*107*).

A wide variety of predictive crash models has been used to explore the association of contributing factors with crash occurrence. It has been found that traditional linear regression models are inappropriate approaches for modeling crash count data due to the skewed distribution (*216*). Poisson regression models were then proposed to account for the non-normal and skewed distribution of crash data (*217*). The key issue with the Poisson regression model was that it assumes that the mean is equal to the variance. However, this is not usually the case in crash data. Negative binomial (Poisson-Gamma) regression models were then proposed to relax the constraint of the mean being equal to variance accommodating over-dispersion (i.e., mean is lower than variance) in the data (*110; 214*). However, one key weakness of negative binomial models is that these models cannot account for under-dispersion (i.e., mean is higher than variance), which can lead to flawed estimates in cases of small data (*115*). Poisson lognormal (*133*) and Conway-Maxwell Poisson Models (*120*) were then proposed to account for under-dispersion in crash data. Similarly, zero-inflated Poisson and zero-inflated negative binomial models were proposed to account for over-dispersion issues due to excessive zeros (*218-220*). The zero-inflated Poisson and negative binomial models provide more flexibility; however, a key weakness of these approaches is the long-term mean equals zero in a safe situation which could lead to biased estimates (*110; 221*). Similarly, generalized additive models provide smoothing functions for independent variables. However, the application of such models to crash data has been limited due to the inclusion of more parameters (*222; 223*). Some studies applied the finite mixture and Markov switching models for modeling crash frequency, however, the complex processing framework limits their application (*224; 225*).

In most of the aforementioned models, the effects of explanatory variables are considered fixed, which in fact can vary due to unobserved factors. Numerous studies proposed random parameter or mixed count data models to account for unobserved heterogeneity (i.e., allowing one variable with different parameters across observations), enhancing the model prediction capabilities (*124-126; 196; 226; 227*). While random parameter or mixed logit models are very helpful in capturing unobserved heterogeneity, they do not capture potential variation in parameter estimates across space. Thus, the geographically weighted regression (GWR) models were applied to capture spatial variation in the effects of specific attributes of on-road crashes across diverse locations (*192; 228-230*). GWR models assume that points physically closer to each other, situated on the same roadway type, and having similar physical attributes (e.g., lane width, median type, and the number of lanes, etc.) resemble each other more closely than points that are relatively far apart. In GWR models, weights are assigned to variables based on nearest neighbor philosophy giving localized parameter estimates (*230*). However, one drawback of GWR models is that these models do not account for temporal variation in the effects of a specific attribute on crash frequency. Besides the spatial variability of crashes, road crashes also exhibit temporal variability. For instance, the effects of driving behavior, vehicle design, and roadway conditions on crash frequency may change over time because of the decay of information. Therefore, there is a need to apply models that can account for temporal variability in the effects of time-related attributes, which if ignored can lead to unobserved heterogeneity. The temporal aspect related to road crashes has been accommodated in some of the previous studies (*231-234*). The temporal instability in crash data is largely ignored in these studies. A recent study (*235*) discusses the temporal instability of statistical models commonly estimated in crash analysis, which can be due to the change in driver decision-making and safety attitudes over time, cognitive biases, and the effect of macroeconomics on risk-taking behavior. Overlooking the temporal and spatial instability in crash frequency models can result in erroneous conclusions and misleading inferences (*235*). However, most of the previous studies either did not address spatio-temporal heterogeneity or if they did, they only accommodate the unobserved heterogeneity in the error terms and assume that the parameters of explanatory variables are fixed across space and/or time. This study contributes to the field by applying a rigorous methodological framework to incorporate spatio-temporal instability of road crashes by allowing the effects of explanatory variables to vary across space and time. The Geographically and Temporally Weighted Negative Binomial Regression (GTWNBR) model is applied to investigate the variation of SPF parameters on divided multilane rural highways across space and time simultaneously. The results of this study will develop localized safety improvement programs while considering the spatio-temporal nature of crashes across Tennessee.

INTRODUCTION

Large-truck crashes have disastrous impacts on the country's economy considering the costs of property and cargo damage, and the medical, social, and delivery delay costs (*236*). Based on a technical report by the Federal Motor Carrier Safety Administration

(FMCSA), the cost of large-truck-involved crashes was on average $289,549 per crash between 2001 and 2003. The total annual cost of large-truck-involved crashes was estimated to be $39.5 billion, including emergency services, medical care, property damage, reduced productivity, and lost quality of life (*237*). In 2016, large trucks made up only 4 percent of all registered vehicles, but 9 percent of the total vehicle-miles traveled (VMT) in the U.S. Such high VMT might put truck drivers at higher risk for accidents. According to the U.S. Department of Labor, the trucking industry experienced the highest number of fatalities among all occupations in the U.S. in 2017. Over 75 percent of these fatalities were related to roadway accidents (*238*). In 2015, the ratio of fatalities to injuries for large-truck-involved crashes was 0.035, while this value for non-truck-involved crashes was 0.013 (*239*). This shows that higher crash severity is expected in large-truck-involved-crashes, which could be due to large trucks' higher gross weight, longer vehicle length, and longer braking distance (*169*). Police reports of motor vehicle crashes from 2018 show that 10.8 percent of fatalities in large-truck-involved crashes (including large-truck occupants, occupants of other vehicles, and nonoccupants) were from single-vehicle crashes (*240*). However, when it comes to only large truck occupants, approximately 60 percent of these fatalities were from single-vehicle crashes (*240*), indicating that large-truck occupants experience more single-vehicle severe crashes than multiple-vehicle severe crashes. The 2008 National Highway Traffic Safety Administration (NHTSA) comparison report based on the Fatality Analysis Reporting System (FARS) crash data also shows similar proportions of large-truck single-vehicle crashes. Based on this report, 65 percent of the fatalities in large-truck crashes between 1988 and 2008 were from single-vehicle crashes (*93*). Among different types of single-vehicle large-truck crashes, fixed object crashes are the most frequent ones. Based on the Federal Motor Carrier Safety Administration (FMCSA) report, between 2015 and 2017, fixed object crashes made up roughly 50 percent of all single-vehicle crashes involving large-trucks (*241*). Furthermore, according to the Large Truck Crash Causation Study (LTCCS), driver-related factors contribute to 87 percent of large-truck crashes across the U.S. (*242*). Truck-involved crashes of North Carolina between 2013 and 2017 also show that in at least 36 percent of the large-truck-involved crashes, physical conditions of the driver (e.g., fatigue, illness, and impaired driving) have been one of the critical reasons for the crash. This percentage is even higher for driving errors (e.g., speeding, illegal maneuver, and inattention), playing a key role in 60 percent of the large-truck-involved crashes (*242*). Therefore, the focus of this study is to investigate the effect of large-truck drivers' physical conditions and driving errors on the severity of fixed-object crashes involving large trucks.

DATA DESCRIPTION

In this study, five years (2013-2017) of crash data from North Carolina (NC) provided by the Highway Safety Information System (HSIS) was used for crash analysis. HSIS data are of good quality, and they represent a spectrum of crash injury types that range from no injury to fatal injury. This study aims to evaluate crash severity. Therefore, three separate datasets were merged. The first dataset, the "accident file," provides accident characteristics such as time and location of the crash, crash type, and weather conditions. The "vehicle file" contains characteristics of the vehicles involved in the crash such as type of vehicle, driver sex, driver age, driver's physical conditions, and driver performance. Finally, the information related to road features was obtained from the third dataset, the “road file.” This dataset contains information regarding the roadway inventory such as median width, shoulder width, and Annual Average Daily Traffic (AADT). Overall, information from 931,609 crashes was obtained from the data set, of which 42,648 crashes were found to be large-truck-involved crashes. In the last step, a subset of large-truck-involved crashes containing 3,037 fixed-object crashes was selected for the model estimation. To ensure that each collision happened between a large truck and a fixed object, only single-vehicle crashes were considered for this study.

Tables 6-1 and 6-2 present the descriptive statistics and frequency analysis of the explanatory variables used for model estimation. Variables *driver age* and *speed limit* were categorized to examine their non-linear associations with the dependent variable. Also, this provides us with the opportunity to evaluate individuals among different age groups. The tables also provide useful information about the road segments on which the crashes occurred; for example, the average median width was 11.011 with a standard deviation of 28.429. On average, 8,498 vehicles passed these segments per day. Regarding the severity of the crashes, 0.6 percent of the crashes were fatal while 1.1 percent of them were severe-injury crashes. However, based on this table, the majority of crashes (80.1 percent) were property-damage crashes. Furthermore, 10.6 percent of the crashes occurred at intersections, showing that fixed-object crashes are quite frequent in these areas. Approximately 23.5 percent of the crashes were located on curves, but the majority of the crashes (76.4 percent) occurred on straight sections. For age ranges, large-truck drivers between 46 and 60 years of age were more frequently involved in fixed-object large-truck-involved crashes than other age groups. Male drivers constituted around 97.2 percent of involved drivers.

Table 6-1 Descriptive statistics of the continuous variables

Variable	min	max	mean	std.dev
$\log AADT$	4.1	12.1	9.0	1.5
Median Width (ft)	0.0	950.0	11.0	28.4
Left shoulder width (ft)	0.0	20.0	6.3	4.1
Right shoulder width (ft)	0.0	20.0	6.6	4.2

Table 6-2 Frequency analysis of the categorical variables

Variable	Count	percent	Variable	Count	percent
Crash Features					
Injury severity			**Location Type**		
Killed	20	0.7	No feature	2246	74.0
Severe Injury	33	1.1	Bridge	133	4.4
Other Visible Injury	209	6.9	Underpass	96	3.2
Complaint of Pain	342	11.3	Intersection	324	10.7
Non-Injury	2433	80.1	Ramp	48	1.6
Road Features					
Roadway Class			**Roadway Lighting**		
Two-way	1712	56.4	Daylight	2147	70.7
Freeway	623	20.5	Dusk	32	1.1
Divided Highway	210	6.9	Dawn	64	2.1
Undivided Highway	215	7.1	Dark with light	108	4-6
Others	277	9.1	Dark without Light	686	22.6
Roadway Alignment			**Weather conditions**		
Straight	2321	76.4	Clear	2542	83.7
Curve	716	24-6	Rainy	433	14.3
Roadway surface			Snowy	35	1.2
Dry	2258	74.3	Fog	27	0.9
Wet	679	22.4	**Terrain**		
Snow	100	32.9	Flat	760	25.0
Road Access			Rolling	1957	64.4
No access	1727	56.9	Mountainous	320	10.5
Full access	828	27.3	**Speed Limit**		
Partial access	141	4.6	<45	538	17.7
Unknown	341	11.2	>45	2499	82.3
Driver Features					
Driver Gender			**Driver Age**		
Male	2954	97.3	<=20	19	0.6
Female	83	2.7	21-30	510	16.8
Driver Restraint Usage			31-45	910	30.0
Wearing Seatbelt	2920	96.1	46-60	1073	35.3
Not Wearing Seatbelt	54	1.8	> 60	525	17.3
Unknown	63	2.1	**Contributing Factor**		
Driver's Physical Condition			No factor	1722	56.7
Normal	2809	92.5	Disregard signs & signals	129	4.2
Having Illness	7	0.2	Speeding	26	0.9
Fatigue	31	1.0	Failure to reduce speed	69	2.3
Falling asleep	119	3.9	Improper lane change	26	0.9
Impairment (Alcohol & Drug)	35	1.2	Wrong-way driving	66	2.2
Medical Condition	36	1.2	Oversteered	291	9.6
			Aggressive driving	193	6.4
			Defective equipment	139	4.6

Regarding the drivers' physical conditions, drivers who were impaired by alcohol, drugs, or medications made up 1.1 percent of the large-truck drivers. Medical conditions (e.g., having a heart attack, poor eyesight, or seizure) contributed to 1.1 percent of the crashes, and 3.9 percent of the drivers fell asleep, fainted, or lost their consciousness before crashing into a fixed object. For driver errors, 12.3 percent of the drivers exceeded a safe speed before the crash, 6.3 percent exhibited aggressive driving, 4.5 percent operated with defective equipment, and 0.8 percent executed an improper lane change which contributed to the crash. The rest of the variables can be interpreted similarly.

METHODOLOGY

Figure 6-1 shows the conceptual framework of the study. In the past, various modeling methods have been employed to estimate crash severity, the most common being binary/multinomial logit models (*167; 168; 243; 244*), ordered logit/probit models (*172; 245-247*), random parameter multinomial logit models (*47; 248; 249*), and random parameter ordered probit/logit models (*164; 183; 250; 251*). Generally, there are two common approaches to crash severity analysis: ordered or unordered discrete response. The major difference between these two approaches is that ordered discrete response models account for the ordinal nature of crash severity (*252*). Previous studies have demonstrated that each model has its strength and weaknesses, and there is no general rule for choosing one particular model over another (*253*). However, unobserved factors , which are mostly not possible to collect, arise in crash severity analyses, and their correlations with observed factors can result in biased and misleading outcomes.

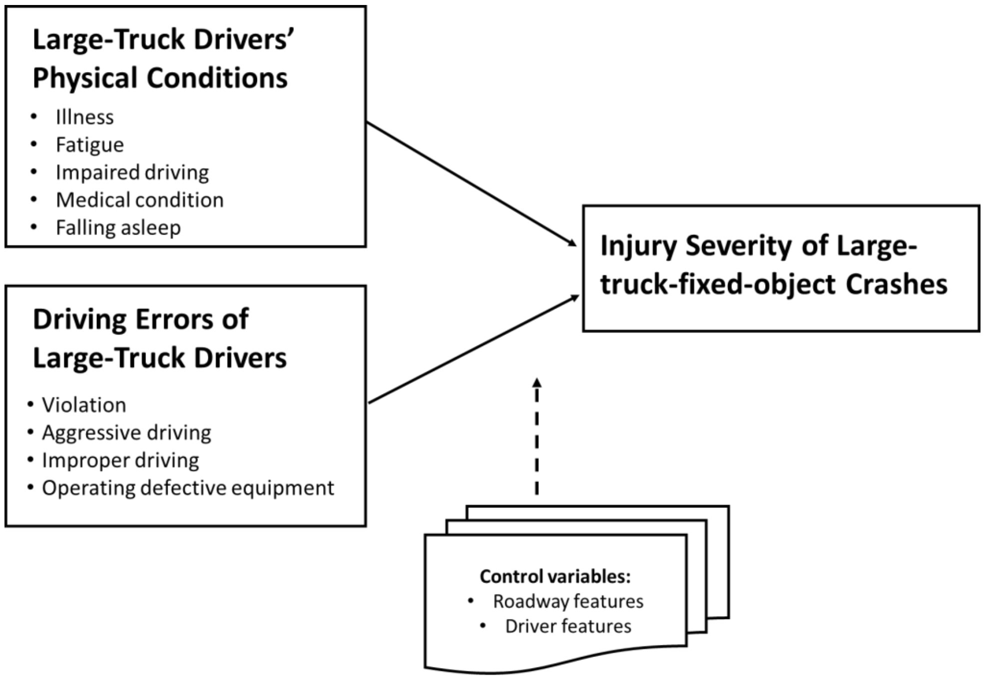

Figure 6-1 Conceptual framework of the study

This issue, often referred to as unobserved heterogeneity, should be addressed in the modeling process (*253*). Therefore, this study utilizes a random parameter ordered probit model to evaluate the effects of contributing factors on injury severity in fixed-object large-truck-involved crashes. The random parameter ordered probit model not only considers the ordinal nature of crash severity but also addresses unobserved heterogeneity by allowing the estimated parameters to vary across observations. Furthermore, to mitigate the bias and variability in the model resulting from under-reporting of less severe crashes, crash severity in descending order (level 0 for fatal crashes and level 5 for property damage-only (PDO) crashes) was used for the dependent variable (*254*).

Random Parameter Ordered Probit Model

The basis for the random parameter ordered probit model is the same as the ordered probit model. Consider the following linear equation:

$$z_i^* = \beta\, x_i + \varepsilon_i \tag{1}$$

where z_i^* is a latent continues function for observation i, x_i is the vector of explanatory variables considered for crash severity prediction, β is the vector of estimable coefficients, and ε_i is the stochastic error term assumed to follow a logistic distribution. y_i^* is an unobserved variable that can be used to determine the observed crash severity category as follows:

$$\begin{aligned} &y = 0 \;\; if\; z \le \mu_1 \\ &y = 1 \;\; if\; \mu_1 \le z \le \mu_2 \\ &y = 2 \;\; if\; \mu_2 \le z \le \mu_3 \\ &y = \cdots \end{aligned} \tag{2}$$

$$y = j \;\; if \; z \geq \mu_j$$

where μ_j are the cut points of the crash severity levels which are estimated along with the coefficients. Then, the crash severity level probabilities of j are calculated:

$$\begin{aligned} &P(y = 0|X_i) = F(\mu_1 - \beta\, x_i) \\ &P(y = 1|X_i) = F(\mu_2 - \beta\, x_i) - F(\mu_1 - \beta\, x_i) \\ &P(y = 2|X_i) = F(\mu_3 - \beta\, x_i) - F(\mu_2 - \beta\, x_i) \\ &P\,(y = \cdots|X_i) \\ &P(y = j|X_i) = 1 - F\left(\mu_j - \beta\, x_i\right) \end{aligned} \tag{3}$$

where F is the cumulative distribution function for the normal distribution. Next, to extend the standard ordered probit model to a random parameter ordered probit model, an error term is introduced to the model to incorporate the correlations between observed and unobserved factors (*255*):

$$\beta_i = \beta + \varphi_i \tag{4}$$

where φ_i is a normally distributed term. Therefore, the latent function in equation (2) can be rewritten as follows (*255*):

$$z_i^* = \beta\, x_i + \varepsilon_i' \tag{5}$$

where ε_i' is the new stochastic error term (*255*):

$$\varepsilon_i' = \varphi_i\, x_i + \varepsilon_i \tag{6}$$

In this study, the Akaike Information Criterion (AIC) was used to assess the model's goodness of fit (*147; 188*):

$$AIC = -2L + 2k + \frac{2k(k+1)}{n-k-1} \tag{7}$$

where *n* is the number of observations, *k* is the number of explanatory parameters, and *L* is the log-likelihood of the estimated model. Lower AIC values indicate a better model fit with the data.

RESULTS AND DISCUSSION

A stepwise approach was used to select the final set of variables for the model. Table 6-3 presents the estimated results for the ordered probit model with random and fixed parameters. Note that only variables with significant associations with the response variable (z-value > 1.96) were kept in the final model. Several distributions such as the lognormal, triangular, uniform, and normal were considered for the random parameters, of which the normal distribution resulted in the lowest AIC value and a higher number of meaningful random parameters. The estimated results show that three variables, *Road alignment*, *Ln (AADT)*, and *Speed Limit,* were random parameters in the model, meaning that they significantly varied across the observations. The rest of the independent variables along with the constant were found to be fixed parameters. Regarding the models' goodness of fit, lower AIC values in the ordered probit model with random parameters indicate a better fit with the data than the ordered probit with fixed parameters.

Table 6-3 Model results for the ordered probit Model with random and fixed Parameters

Variable		Random Parameters Model		Fixed Parameters Model	
		Exp (β)	z-value	Exp (β)	z-value
Constant		0.27	15.52	0.44	16.11
Physical Conditions of the Driver (Base: Normal)	Illness	0.40	-2.44	0.57	-1.95
	Fatigue	0.35	-3.72	0.52	-2.52
	Falling Asleep or Loss of Consciousness	0.41	-7.58	0.55	-5.28
	Impaired driving (Medications, Drugs, Alcohol)	0.13	-4-68	0.27	-2.90
	Medical Condition	0.78	-9.59	0.85	-6.96
Driving Errors	Disregarding signs and signals	0.49	-1.51	0.63	-1.16
	Speeding	0.35	-2.43	0.50	-1.85
	Failure to reduce speed	0.70	-0.89	0.82	-0.61
	Improper lane change	0.52	-1.07	0.64	-0.70
	Wrong-way driving	0.47	-3.71	0.62	-2.78
	Oversteering	0.43	-7.87	0.58	-5.59
	Aggressive driving	0.75	-7.40	0.83	-5.24
	Operating defective equipment	1.34	-1.92	1.23	-1.44
Road Lighting (Base: Daylight)	Dusk	0.58	0.74	0.70	0.67
	Dawn	1.10	-3.08	1.05	-2.27
	Dark with Lighting	0.92	0.41	0.94	0.24
	Dark Without Lighting	1.29	-1.15	1.19	-0.99
Road Surface (Base: Dry)	Wet	4.09	3.44	2.51	2.66
	Snow	0.27	5.36	0.81	-4.66
Road Alignment (Base: Straight)	Curve		---	1.06	-3.33
Ln (AADT)			---	0.81	2.92
Speed Limit (Base: < 45)			---	-0.44	7.35
Random Parameters					
Road Alignment (Base: Straight)	Curve	1.13	5.71		---
Ln (AADT)		0.74	-4.18		---
Speed Limit (Base: < 45)		0.53	-5.39		---
Goodness of fit		N= 3037 AIC = 3866.30 LL = -1903.14		N= 3037 AIC = 3873.80 LL = -1909.91	

Marginal effects interpret the effect of a specific variable on crash severity probabilities. Generally, marginal effects reflect the changes in the likelihood of experiencing a specific level of injury severity with a one-unit change in the independent variable compared to the base level while holding the other variables constant (*252*). Table 6-4 shows the marginal effects of the ordered probit model with random parameters for the five levels of injury severity.

Control Variables

To explore the pure effect of large-truck drivers' physical conditions and driving errors on the severity of fixed object large-truck-involved crashes, this study controls for other contributing factors related to road, crash, and human characteristics. Based on the results, control variables *Ln (AADT)*, *speed limit, surface condition,* and *road lighting* could meaningfully influence the response variable (z-value > 1.96). Variable *Ln (AADT)* was found to be random and normally distributed with a mean of 0.126 and a standard error of 0.022. The variable *Ln (AADT)* is negatively associated with crash severity, probably because large-truck drivers in higher volumes are more likely to decrease their speed to avoid crashes, which can decrease fixed-object crash severity. The variable *speed limit* was also found to be random with a mean of -0.628 and a standard error of 0.116. This variable's negative sign indicates that roadways with speed limits of 45 mph or higher experience higher injury severities. Large-truck drivers often drive faster on roadways with higher speed limits. Therefore, they hit fixed objects at a higher speed, which can result in higher injury severities. *Road alignment* is another random variable in the model with a mean of -0.206 and a standard error of 0.072.

Table 6-4 Marginal effects for significant variables of the ordered probit model with random

Variable		Marginal Effects (%)				
		Fatal	Severe injury	Moderate injury	Minor injury	No injury
Physical Conditions of the Driver (Base: Normal)	Illness	2.32%	2.90%	12.14%	10.33%	-27.69%
	Fatigue	1.09%	1.55%	7.48%	7.55%	-17.66%
	Falling Asleep or Loss of Consciousness	1.34%	1.86%	8.75%	8.56%	-20.51%
	Impaired driving (Medications, Drugs, Alcohol)	1.21%	1.70%	8.08%	7.98%	-18.98%
	Medical Condition	6.60%	6.37%	20.59%	12.49%	-46.04%
Driving Errors	Disregarding signs and signals	0.18%	0.30%	1.76%	2.22%	-4.46%
	Speeding	0.79%	1.18%	5.95%	6.34%	-14.25%
	Failure to reduce speed	0.12%	0.20%	1.19%	1.54%	-3.05%
	Improper lane change	0.23%	0.38%	2.18%	2.68%	-5.47%
	Wrong-way Driving	0.70%	1.07%	5.48%	5.97%	-13.22%
	Oversteering	0.75%	1.14%	5.91%	6.52%	-14.31%
	Aggressive driving	0.96%	1.40%	6.99%	7.35%	-16.70%
	Operating defective equipment	0.20%	0.34%	1.98%	2.47%	-4.99%
Road Lighting (Base: Daylight)	Dusk	-0.14%	-0.26%	-1.73%	-2.56%	4.69%
	Dawn	0.50%	0.78%	4.20%	4.80%	-10.28%
	Dark with Lighting	-0.04%	-0.07%	-0.42%	-0.58%	1.10%
	Dark Without Lighting	0.06%	0.10%	0.62%	0.83%	-1.61%
Road Surface (Base: Dry)	Wet	-0.14%	-0.25%	-1.60%	-2.26%	4.24%
	Snow	-0.30%	-0.62%	-4.83%	-8.68%	14.43%
Road Alignment (Base: Straight)	Curve	0.21%	0.36%	2.15%	2.75%	-5.47%
Ln (AADT)		-0.05%	-0.09%	-0.53%	-0.71%	1.37%
Speed Limit (Base: < 45)		0.39%	0.74%	5.18%	8.22%	-14.52%

Estimate results show that, relative to crashes on straight road sections, those on horizontal curves are more likely to have severe injury outcomes. This might be because it is usually more difficult for large-truck drivers to control their vehicles on curves. *Road Surface* and *Road Lighting* were found to be fixed in the model. There was a negative correlation between wet and snowy surfaces and crash severity. For example, crashes occurring on wet road surfaces are 4.24 percent more likely to result in property damage (no injury). This finding could be due to higher awareness and lower speeds in these conditions. For *Road Lighting,* results indicate that crashes occurring at *dawn* are 1.28 percent more likely to result in fatalities and severe injuries. This could be because drowsy driving and poor vision are more likely during this time of the day.

Physical conditions of large-truck drivers

The focus of this study is to explore the effect of large-truck drivers' physical conditions and driving errors on the severity of fixed-object crashes. As presented in Table 6-3, large coefficients of variables related to physical conditions of large-truck drivers indicate that they have strong correlations with fixed-object crash severity. Results show that a large truck driver having a *medical condition*, e.g. heart disease, poor eyesight, seizure disorders, or diabetes (*256*), is one of the most important physical conditions positively correlated with crash severity. Marginal effects also show that large-truck drivers with a *medical condition* are 12.97 percent more likely to be involved in a fatal or severe injury crash. The association of large-truck drivers' medical conditions with severity and crash risk has been found in several previous studies. In (*181; 257*), for example, higher injury severity was found to be associated with vision problems. Drivers with diabetes (*257; 258*) and heart disease (*257; 259*) were also found to be more involved in severe crashes than healthy drivers. Higher injury severity among large-truck drivers with a medical condition could be the result of a higher potential of experiencing sudden impairment in awareness and judgment when driving among these drivers (*260*).

Having an *acute illness* is also strongly correlated with large-truck crash severity. Modeling results show that large-truck drivers who have an illness are 5.22 percent more likely to be involved in fatal or severe injury crashes compared to normal drivers. Unlike medical conditions, which are chronic illnesses with enduring and stable effects, acute illnesses, e.g., flu and vomiting, develop suddenly and last for a shorter period. Therefore, the effect of these illnesses on large-truck drivers is mostly unpredictable (*261*).

A strong association between *impaired driving* and large-truck-involved crash injury severity has been found in several studies (*170; 180; 262; 263*). The results of this study also show that *impaired driving* is positively and strongly associated with the severity of fixed-object crashes involving large trucks. Marginal effects reveal those large-truck drivers who are intoxicated with alcohol, drugs, or medication are 2.91 percent more likely to be involved in a fatal or severe injury fixed-object crash. The higher risk for impaired large-truck drivers can be explained by the influence of alcohol and drugs on driving performance. It has been found that alcohol and drug abuse have a negative influence on drivers' vision, perception, reaction time, driving skills, and vigilance. It was also found that impaired drivers are more likely to exhibit risky driving behaviors (*264; 265*), which can increase the chances of being involved in a fatal crash.

Large-truck driver fatigue is one of the primary causes of large-truck accidents, stemming from long working hours. Based on the Large Truck Crash Causation Study (LTCCS), driver fatigue has been reported as a contributing factor in 13 percent of the large truck-involved crashes (*242*). Modeling results indicate that large truck driver *fatigue* has a positive association with injury severity in fixed-object crashes. This follows the findings of previous studies (*266; 267*). Referring to Table 6-4, fatigue driving increases the chances of a large-truck driver being involved in a fatal or severe injury crash by 2.64 percent. This is because fatigue can result in poor driving performance, slow reaction time, and decreased vigilance, which can increase the risk of a fatal crash for large-truck drivers (*268*).

Falling asleep while driving is one of the common causes of single-vehicle crashes. In a survey of 593 large-truck drivers in the U.S., 25 percent reported that at least once, they had fallen asleep while driving in the past year (*269*). The results of this study also show that large-truck drivers who fall asleep or lose consciousness have a higher chance of being severely injured in fixed-object crashes. The marginal effects of this variable indicate that drowsy driving increases the likelihood of involvement in severe injury crashes by up to 3.2 percent, a finding in line with (*266; 270*).

Driving Errors of Large-Truck Drivers

Model results indicate that speeding, wrong-way driving, oversteering, and aggressive driving behavior are the driving error-related variables that meaningfully address the response variable and have a positive association with crash severity. Speeding has been recognized as one of the major contributing factors in fatal crashes. Based on an NHTS report, speeding was involved in approximately one-fourth of traffic fatalities in the U.S. in 2017 (*271*). The model results in this study also show that speeding is positively associated with injury severity in large-truck-fixed-object crashes. Based on the marginal effects, speeding increases the likelihood of a fatal or severe injury crash by 1.97 percent.

This increase could be because geometric features of roadways are usually determined based on speed limits and driving at a higher speed than the speed limit can result in the loss of control of the large truck. This finding is in line with findings in past research (*169; 272; 273*).

Wrong-way driving occurs when a vehicle moves against the legal direction of traffic (*274*). Wrong-way driving often results in severe crashes because they lead to head-on crashes. Based on the results, wrong-way driving of large-truck drivers is associated with a 1.77 percent higher risk of fatal or severe fixed-object crashes. This finding follows the results of previous studies (*275; 276*).

Aggressive driving is another driving error that increases the risk of fatal fixed-object crashes involving large trucks. Based on NHTSA, aggressive driving occurs when "an individual commits a combination of moving traffic offenses so as to endanger other persons or property" (*277*). Results of this study show that large-truck drivers who exhibit aggressive driving are 2.36 percent more likely to be involved in a fatal or severe injury crash. This result is consistent with the finding in (*178; 278*).

Oversteering occurs when the large-truck driver applies too much power to the rear wheels which can cause them to skid so that the back of the large truck starts awing out. This can result in loss of control by the large-truck driver which can lead to a fixed-object crash. Oversteering is more common in large trucks because they are mostly rear-wheel drive vehicles. The results indicate that oversteering increases the likelihood of a fatal or severe injury crash by 1.89 percent.

Implications of The Results

This study shows how large-truck drivers' physical conditions and driving errors can increase the risk of severe and fatal fixed-object crashes. One of the implications of the findings is to underscore the importance of periodic medical monitoring of large-truck drivers. Currently, large-truck drivers in the U.S. are required to take the Department of Transportation's medical exam every 24 months (*279*). Since the mental and physical health conditions of drivers might change in this period, shorter intervals for reevaluation can be considered to better monitor the physical conditions of large-truck drivers. Impaired driving is an important factor that is difficult to monitor. Strict law enforcement and periodic drug testing can act as deterrents to impaired driving. Also, based on the Federal Motor Carrier Safety Administration (FMCSA), large-truck drivers in the U.S. are allowed to drive up to 11 hours, 8 hours of which can be consecutive without any break (*280*). This long driving time can increase crash risk significantly (*281*). Shorter hours of service with sufficient breaks may prevent fatigued driving and falling asleep at the wheel (*282*). In this regard, strict hours of service regulations in the European Union (EU) can be a good example. Large-truck drivers in the EU are required to take at least a 45-minutes break after every 4.5 hours of driving (*283*). Using biometric driver monitoring systems can also be an effective tool for monitoring large-truck drivers to detect the signs of drowsy driving (*284*). Furthermore, it was found that speeding, aggressive driving, oversteering, and wrong-way driving increase the risk of severe and fatal large-truck-involved fixed-object crashes. Although oversteering and wrong-way driving might happen due to unintended human errors which makes them hard to control, speeding and aggressive driving can be trackable and controllable using advanced technologies.

Connected trucks and truck platooning are two of the latest technologies that can help fleet managers to track and control speeding and aggressive driving in their fleet.

LIMITATIONS

The accuracy of the findings presented in this study highly depends on the crash data used for the model estimation. The crash data provided by the HSIS are based on police-reported data in North Carolina. Some of the police reports may not be accurate, but the extent of inaccuracy is unknown to the authors. Also, some crashes with no injury outcome were possibly not included in the data because they were not reported to the police. Consequently, the crash data used in this data might not represent the entire population of large-truck-fixed-object crashes in North Carolina.

CONCLUSION

The intellectual merit of this research comes from focusing on the safety of large-truck drivers whose often hazardous occupation is linked to the transportation of goods. This study investigates the large-truck fixed-object crashes to find out how the physical conditions of large-truck drivers and the driving errors they make correlate with more severe injuries in crashes. Investigating fixed object crashes as frequent single-vehicle crashes helps us examine the pure effect of large-truck drivers' behavior on the severity of large truck crashes. To explore these associations, this study controls for other contributing factors related to road, crash, and human characteristics. Notably, this study estimates a random parameter ordered probit model to capture unobserved heterogeneity in the crash data. The model results show that the driver's physical conditions, driving errors, road lighting, road surface conditions, road alignment, AADT, and the speed limit have meaningful associations with the severity of large-truck fixed-object crashes. Also, road alignment, AADT, and speed limit were found to be random parameters, indicating that the effect of these variables on crash severity varies across observations. Based on the findings, having a medical condition, having an illness, falling asleep while driving, being impaired, and experiencing fatigue significantly increase the probability of large-truck drivers being involved in a fatal or severe injury crash. These relationships might be because of the higher potential of sudden impairment in awareness and judgment and the negative impact on drivers' vision, perception and reaction time, vigilance, and driving performance. Driving errors are other human-related factors that were found to be strongly associated with injury severity in large-truck-fixed-object crashes. The results indicate that speeding, going the wrong way, oversteering, and aggressive driving are among the driving errors which are directly correlated with crash severity. Driving errors might result from having a physical condition. For example, a large truck driver impaired by alcohol or drugs might drive aggressively or commit a traffic violation (e.g., speeding and wrong-way driving).

Furthermore, some control variables were found to be significant. Large-truck drivers on roadways with higher speed limits are more likely to be involved in severe fixed-object crashes. Regarding roadway lighting conditions, it was found that a crash occurring at dawn increases the likelihood of a severe crash compared to crashes occurring in daylight. Additionally, AADT was found to be negatively associated with crash severity. Finally, the results show that compared to crashes on straight road sections, those on horizontal curves are more likely to have a fatal or severe crash outcome.

This study uses 5-year crash data between 2013 and 2017 from North Carolina, but the study's methodology can be used for future studies on other areas. The results of this study cannot be generalized to other states because of the distinctive characteristics of other states and jurisdictions. The best results will likely be obtained by examining data specifically collected from the state of interest.

The results of this study provide planners and practitioners with a better understanding of critical parameters associated with crash severity in large-truck-fixed-object crashes, which are the most common single-vehicle crash type in North Carolina. The findings of this study can be used by researchers to identify areas of future focus for safety improvements. Similar studies can be conducted in the future for other states and jurisdictions for comparison. Geographically weighted models could be applied to evaluate the variations among the contributing factors. Furthermore, these studies could examine other types of large-truck-involved crashes such as rear-end, head-on, and angle crashes.

ACKNOWLEDGMENT

The authors would like to thank the following financial support for the research, authorship, and/or publication of this article: This project was supported by the Tennessee Department of Transportation, TDOT, and the Collaborative Sciences Center for Road Safety, a U.S. Department of Transportation National University Transportation Center promoting safety.

CHAPTER 7 : CONCLUSION

CONCLUSION

The performance of a transportation system highly depends on the drivers' behavior because driving behavior is one of the main causes of traffic accidents and one of the key factors in fuel consumption and vehicle emissions studies. However, driving behavior has not been thoroughly studied in previous studies probably because collecting data related to driving behavior and human factors are so complex and costly. Therefore, mostly in transportation studies, the effect of driving behavior is ignored, and instead, the main focus is on infrastructure and vehicle factors which might not fully explain dependent variables. However, recently, the development of advanced sensors, connected vehicles (CVs), location-based services (LBS), video and radar surveillance has provided unprecedented access to new high-resolution microscopic-level data on driver's location, maneuver, speed, travel time, and crash/near-crash events in real-world driving conditions. Such rich data enable transportation engineers to evaluate and monitor instantaneous driving behavior and safety performance of different road types and facilities in a spatio-temporal domain. Therefore, the main objective of this study is to develop a framework to harness the new large-scale data to comprehensively study driving behavior under a naturalistic driving condition in different road types and facilities. Specifically, this dissertation creates a unique database by assembling and combining big data generated by connected and automated vehicles (CAVs), Naturalistic Driving Study (NDS) data, and conventional traffic and crash data. To this aim, rigorous statistical techniques such as Geographically and Temporally weighted regressions (GTWR), Bayesian Conditional Autoregressive (CAR) models, and machine learning methods are applied to extract useful information from the data to better understand the driving behavior in naturalistic and connected vehicles environments. In this study, the concept of “driving volatility” which is a surrogate safety measure of unsafe and aggressive driving behavior is used. As a rigorous measure of micro driving behavior, driving volatility shows the degree of deviation from the norm which can help us to predict driving behavior in the short term.

This dissertation explores driving behavior and transportation system performance at different levels. Specifically, the main focus of this dissertation is on aggressive drivers who not only put their selves and others at risk but also contribute more to greenhouse gas emissions. At the driver level, this study tracks individual drivers to evaluate differences in their driving styles on different roadways. One advantage of this approach is detecting risky drivers who continuously drive aggressively during the observation period or drivers who always drive calmly. Also, a driving score is proposed to assess drivers’ performance on different roadways. Furthermore, as another example of a driver-level study of driving behavior, the study evaluates the effects of truck drivers’ physical condition and driving errors on the injury severity of fixed-object large truck crashes. At the location level, emissions and fuel consumption of vehicles within work zones and curves are analyzed which are critical scenarios in transportation systems. Using the naturalistic driving data, the Vehicle Specific Power (VSP) model and Autonomie model are used to compare emissions and fuel consumption of drivers with different driving styles at these locations. At the roadway level, the study uses the CAV data to investigate how the perception of an aggressive, normal, and calm driving style varies across different road types. Also, the proportion and distribution of different driving styles on different roadways are investigated in order to see how frequent risky driving behaviors are on different roadways. Crash frequency of rural multilane highways is another topic investigated at the roadway level. The Geographically and Temporally Weighted Negative Binomial Regression (GTWNBR) model is used to investigate the variation of Safety performance functions (SPF) parameters on divided multilane rural highways across space and time simultaneously. At the network level, the dissertation incorporates driving behavior factors in the estimation of SPFs using temporal volatility measures. To this aim, the CAV data from the Safety Pilot Model Deployment study are combined with traditional safety data to predict crash frequency in a network of four-leg signalized intersections in Ann Arbor, MI.

In summary, the main contribution of this dissertation is to evaluate transportation system performance in correlation with driving behavior at different levels (i.e., driver level, location level, location level, network level) by harnessing big data from real-world driving conditions and integrating them with conventional data. Also, this study introduces new applications of driving volatility measures as well-known surrogate measures of unsafe driving in transportation safety studies. Although previous studies mostly used driving volatility measures in supervised learning studies using observed crash data, this study applied these measures for unsupervised classification of driving styles and detection of aggressive drivers in different neighborhoods. Secondly, the study used driving volatility measures in the analysis of fuel consumption and emissions to evaluate the impact of aggressive driving on fuel economy and emissions in real-world driving condition. Third, although previous studies revealed the association of driving volatility measures with crash frequency for different facilities, this study explored the feasibility of incorporating these measures in the development of Safety Performance Functions

(SPFs) in a systematic way consistent with the procedure in the Highway Safety Manual (HSM). Notably, it can address one of the most important limitations of HSM predictive methods which is the lack of taking into account driving behavior factors in the prediction of crash frequency on different facilities. From the methodological aspect, this study applied rigorous statistical models such as Geographically and Temporally weighted regression (GTWR) models to investigate the variation SPFs parameters across space and time simultaneously. To this end, a unique code was developed in R programming software to incorporate spatio-temporal instability of road crashes by allowing the effects of explanatory variables to vary across space and time. Also, the dissertation demonstrates the application of Bayesian hierarchical modeling for integrating the special correlation between adjacent signalized intersections in a network of intersections. This dissertation includes a variety of topics such as crash frequency/severity analysis, driving style classification, fuel consumption, and emission. The findings of this study provide new insight into the field of transportation at different levels. This study helps the researchers and practitioners follow the spatio-temporal trend of critical safety factors, locations, and facilities with high risky driving behaviors, fuel consumption, and emission to identify sites and roadways for safety and fuel efficiency improvements. Also, the methodology of this study can be used for monitoring driving behavior and detecting risky drivers on different roadways.

REFERENCES

[1] Elander, J., R. West, and D. French. Behavioral correlates of individual differences in road-traffic crash risk: An examination of methods and findings. *Psychological bulletin,* Vol. 113, No. 2, 1993, p. 279.
[2] Kalsoom, R., and Z. Halim. Clustering the driving features based on data streams.In *INMIC*, IEEE, 2013. pp. 89-94.
[3] Brombacher, P., J. Masino, M. Frey, and F. Gauterin. Driving event detection and driving style classification using artificial neural networks.In *2017 IEEE International Conference on Industrial Technology (ICIT)*, IEEE, 2017. pp. 997-1002.
[4] Feng, Y., S. Pickering, E. Chappell, P. Iravani, and C. Brace. Driving style analysis by classifying real-world data with support vector clustering.In *2018 3rd IEEE International Conference on Intelligent Transportation Engineering (ICITE)*, IEEE, 2018. pp. 264-268.
[5] Aljaafreh, A., N. Alshabatat, and M. S. N. Al-Din. Driving style recognition using fuzzy logic.In *2012 IEEE International Conference on Vehicular Electronics and Safety (ICVES 2012)*, IEEE, 2012. pp. 460-463.
[6] Dörr, D., D. Grabengiesser, and F. Gauterin. Online driving style recognition using fuzzy logic.In *17th International IEEE Conference on Intelligent Transportation Systems (ITSC)*, IEEE, 2014. pp. 1021-1026.
[7] Taubman-Ben-Ari, O., M. Mikulincer, O. Gillath, and Prevention. The multidimensional driving style inventory—scale construct and validation. *Accident Analysis and Prevention,* Vol. 36, No. 3, 2004, pp. 323-332.
[8] Farah, H., A. Polus, S. Bekhor, and T. Toledo. Study of passing gap acceptance behavior using a driving simulator. *Advances in Transportation Studies an International Journal*, 2007, pp. 9-16.
[9] Useche, S. A., B. Cendales, F. Alonso, J. C. Pastor, L. Montoro, and behaviour. Validation of the Multidimensional Driving Style Inventory (MDSI) in professional drivers: how does it work in transportation workers? *Transportation research part F: traffic psychology,* Vol. 67, 2019, pp. 155-163.
[10] van Huysduynen, H. H., J. Terken, J.-B. Martens, and B. Eggen. Measuring driving styles: a validation of the multidimensional driving style inventory.In *Proceedings of the 7th International Conference on Automotive User Interfaces and Interactive Vehicular Applications*, 2015. pp. 257-264.
[11] Deng, C., C. Wu, N. Lyu, and Z. Huang. Driving style recognition method using braking characteristics based on hidden Markov model. *PloS one,* Vol. 12, No. 8, 2017, p. e0182419.
[12] Meiring, G., and H. Myburgh. A review of intelligent driving style analysis systems and related artificial intelligence algorithms. *Sensors,* Vol. 15, No. 12, 2015, pp. 30653-30682.
[13] Alessandrini, A., A. Cattivera, F. Filippi, and F. Ortenzi. Driving style influence on car CO2 emissions.In *2012 international emission inventory conference*, 2012.
[14] Ranacher, P., R. Brunauer, S. C. Van der Spek, and S. Reich. A model to estimate and interpret the energy-efficiency of movement patterns in urban road traffic. *Computers, environment and urban systems,* Vol. 59, 2016, pp. 152-163.
[15] Mensing, F., E. Bideaux, R. Trigui, J. Ribet, and B. Jeanneret. Eco-driving: An economic or ecologic driving style? *Transportation Research Part C: Emerging Technologies,* Vol. 38, 2014, pp. 110-121.
[16] Van Mierlo, J., G. Maggetto, E. Van de Burgwal, and R. Gense. Driving style and traffic measures-influence on vehicle emissions and fuel consumption. *Proceedings of the Institution*

of Mechanical Engineers, Part D: Journal of Automobile Engineering, Vol. 218, No. 1, 2004, pp. 43-50.
[17] Xu, T., X. Zhang, C. Claramunt, and X. Li. TripCube: A Trip-oriented vehicle trajectory data indexing structure. *Computers, Environment and Urban Systems,* Vol. 67, 2018, pp. 21-28.
[18] Zhou, X., W. Yu, and W. C. Sullivan. Making pervasive sensing possible: Effective travel mode sensing based on smartphones. *Computers, environment and urban systems,* Vol. 58, 2016, pp. 52-59.
[19] Lu, Y., and Y. Liu. Pervasive location acquisition technologies: Opportunities and challenges for geospatial studies. *Computers, environment and urban systems,* Vol. 36, No. 2, 2012, pp. 105-108.
[20] Ishibashi, M., M. Okuwa, S. i. Doi, and M. Akamatsu. Indices for characterizing driving style and their relevance to car following behavior.In *SICE Annual Conference 2007*, IEEE, 2007. pp. 1132-1137.
[21] Canale, M., and S. Malan. Analysis and classification of human driving behaviour in an urban environment. *Cognition, Technology & Work,* Vol. 4, No. 3, 2002, pp. 197-206.
[22] Murphey, Y. L., R. Milton, and L. Kiliaris. Driver's style classification using jerk analysis.In *2009 IEEE Workshop on Computational Intelligence in Vehicles and Vehicular Systems*, IEEE, 2009. pp. 23-28.
[23] Qi, G., Y. Du, J. Wu, and M. Xu. Leveraging longitudinal driving behaviour data with data mining techniques for driving style analysis. *IET intelligent transport systems,* Vol. 9, No. 8, 2015, pp. 792-801.
[24] Wang, R., and S. M. Lukic. Review of driving conditions prediction and driving style recognition based control algorithms for hybrid electric vehicles.In *2011 IEEE Vehicle Power and Propulsion Conference*, IEEE, 2011. pp. 1-7.
[25] Aggressive driving: Research update. *American Automobile Association Foundation for Traffic Safety*, 2009, pp. 5-6.
[26] Castignani, G., T. Derrmann, R. Frank, and T. Engel. Driver behavior profiling using smartphones: A low-cost platform for driver monitoring. *IEEE Intelligent Transportation Systems Magazine,* Vol. 7, No. 1, 2015, pp. 91-102.
[27] Wang, W., J. Xi, A. Chong, and L. Li. Driving style classification using a semisupervised support vector machine. *IEEE Transactions on Human-Machine Systems,* Vol. 47, No. 5, 2017, pp. 650-660.
[28] Choudhary, A. K., and P. K. Ingole. Smart phone based approach to monitor driving behavior and sharing of statistic.In *2014 Fourth International Conference on Communication Systems and Network Technologies*, IEEE, 2014. pp. 279-282.
[29] Alpar, O., and R. Stojic. Intelligent collision warning using license plate segmentation. *Journal of Intelligent Transportation Systems,* Vol. 20, No. 6, 2016, pp. 487-499.
[30] Sun, R., W. Y. Ochieng, and S. Feng. An integrated solution for lane level irregular driving detection on highways. *Transportation Research Part C: Emerging Technologies,* Vol. 56, 2015, pp. 61-79.
[31] MacAdam, C., Z. Bareket, P. Fancher, and R. Ervin. Using neural networks to identify driving style and headway control behavior of drivers. *Vehicle System Dynamics,* Vol. 29, No. S1, 1998, pp. 143-160.
[32] Li, G., S. E. Li, B. Cheng, and P. Green. Estimation of driving style in naturalistic highway traffic using maneuver transition probabilities. *Transportation Research Part C: Emerging Technologies,* Vol. 74, 2017, pp. 113-125.
[33] Bejani, M. M., and M. Ghatee. A context aware system for driving style evaluation by an ensemble learning on smartphone sensors data. *Transportation Research Part C: Emerging Technologies,* Vol. 89, 2018, pp. 303-320.

[34] Mantouka, E. G., E. N. Barmpounakis, and E. I. Vlahogianni. Identifying driving safety profiles from smartphone data using unsupervised learning. *Safety Science,* Vol. 119, 2019, pp. 84-90.
[35] Higgs, B., and M. Abbas. A two-step segmentation algorithm for behavioral clustering of naturalistic driving styles.In *16th International IEEE Conference on Intelligent Transportation Systems (ITSC 2013)*, IEEE, 2013. pp. 857-862.
[36] Yao, Y., X. Zhao, Y. Wu, Y. Zhang, and J. Rong. Clustering driver behavior using dynamic time warping and hidden Markov model. *Journal of Intelligent Transportation Systems*, 2020, pp. 1-14.
[37] Suzdaleva, E., and I. Nagy. An online estimation of driving style using data-dependent pointer model. *Transportation Research Part C: Emerging Technologies,* Vol. 86, 2018, pp. 23-36.
[38] Blana, E., and J. J. H. f. Golias. Differences between vehicle lateral displacement on the road and in a fixed-base simulator. Vol. 44, No. 2, 2002, pp. 303-313.
[39] Godley, S. T., T. J. Triggs, B. N. J. A. a. Fildes, and prevention. Driving simulator validation for speed research. Vol. 34, No. 5, 2002, pp. 589-600.
[40] Groeger, J. A., G. J. A. A. Murphy, and Prevention. Driver performance under simulated and actual driving conditions: validity and orthogonality. Vol. 143, 2020, p. 105593.
[41] GPS.gov. *Official U.S. government information about the Global Positioning System (GPS) and related topics, GPS Accuracy*. https://www.gps.gov/systems/gps/performance/accuracy/#speed.
[42] *Urban Street Design Guide*. National Association of City Transportation Officials, Washington, DC, 2013.
[43] Kamrani, M., R. Arvin, and A. J. Khattak. Extracting useful information from Basic Safety Message Data: an empirical study of driving volatility measures and crash frequency at intersections. *Transportation Research Record,* Vol. 2672, No. 38, 2018, pp. 290-301.
[44] Arvin, R., M. Kamrani, and A. J. Khattak. How instantaneous driving behavior contributes to crashes at intersections: extracting useful information from connected vehicle message data. *Accident Analysis and Prevention,* Vol. 127, 2019, pp. 118-133.
[45] Wang, X., A. J. Khattak, J. Liu, G. Masghati-Amoli, and S. Son. What is the level of volatility in instantaneous driving decisions? *Transportation research part C: emerging technologies,* Vol. 58, 2015, pp. 413-427.
[46] Arvin, R., M. Kamrani, and A. J. Khattak. The role of pre-crash driving instability in contributing to crash intensity using naturalistic driving data. *Journal of Accident Analysis and Prevention,* Vol. 132, 2019, p. 105226.
[47] Cerwick, D. M., K. Gkritza, M. S. Shaheed, and Z. Hans. A comparison of the mixed logit and latent class methods for crash severity analysis. *Analytic methods in accident research,* Vol. 3, 2014, pp. 11-27.
[48] Arvin, R., M. Kamrani, and A. J. Khattak. How instantaneous driving behavior contributes to crashes at intersections: extracting useful information from connected vehicle message data. *Accident Analysis & Prevention,* Vol. 127, 2019, pp. 118-133.
[49] Kamrani, M., R. Arvin, and A. J. Khattak. The role of aggressive driving and speeding in road safety: Insights from SHRP2 naturalistic driving study data.In *Transportation Research Board 98th Annual Meeting, Washington DC*, 2019.
[50] Arvin, R., and A. Khattak. Harnessing big data generated by connected vehicles to monitor safety performance: Application of Geographically Weighted Negative Binomial Regression. Presented at Transportation Research Board, Washington DC, 2020.
[51] Arvin, R., and A. J. Khattak. Harnessing big data generated by connected vehicles to monitor safety performance: Application of geographically weighted negative binomial regression. Presented at Transportation Research Board 99th Annual Meeting, Washington DC, 2020.

[52] Jain, A. K. Data clustering: 50 years beyond K-means. *Pattern Recognition Letters,* Vol. 31, No. 8, 2010, pp. 651-666.
[53] Gan, G., C. Ma, and J. Wu. *Data clustering: theory, algorithms, and applications*. Siam, 2007.
[54] Park, H.-S., and C.-H. Jun. A simple and fast algorithm for K-medoids clustering. *Expert systems with applications,* Vol. 36, No. 2, 2009, pp. 3336-3341.
[55] Kaufman, L., and P. J. Rousseeuw. *Finding groups in data: an introduction to cluster analysis*. John Wiley & Sons, 2009.
[56] Kassambara, A., and F. Mundt. Package 'factoextra'. *Extract and Visualize the Results of Multivariate Data Analyses*, 2016.
[57] Maechler, M., P. Rousseeuw, A. Struyf, M. Hubert, and K. Hornik. Package 'cluster'. *Dosegljivo na*, 2013.
[58] Hong, J.-H., B. Margines, and A. K. Dey. A smartphone-based sensing platform to model aggressive driving behaviors.In *Proceedings of the SIGCHI Conference on Human Factors in Computing Systems*, ACM, 2014. pp. 4047-4056.
[59] Milton, J. C., V. N. Shankar, and F. L. Mannering. Highway accident severities and the mixed logit model: an exploratory empirical analysis. *Accident Analysis & Prevention,* Vol. 40, No. 1, 2008, pp. 260-266.
[60] Horowitz, C. A. Paris agreement. *International Legal Materials,* Vol. 55, No. 4, 2016, pp. 740-755.
[61] The White House. *President Biden Sets 2030 Greenhouse Gas Pollution Reduction Target Aimed at Creating Good-Paying Union Jobs and Securing U.S. Leadership on Clean Energy Technologies*. https://bit.ly/3Bz8947.
[62] Knowles, M., H. Scott, and D. Baglee. The effect of driving style on electric vehicle performance, economy and perception. *International Journal of Electric and Hybrid Vehicles,* Vol. 4, No. 3, 2012, pp. 228-247.
[63] Mohammadnazar, A., R. Arvin, and A. J. Khattak. Classifying travelers' driving style using basic safety messages generated by connected vehicles: application of unsupervised machine learning. *Transportation research part C: emerging technologies,* Vol. 122, 2021, p. 102917.
[64] Mantouka, E. G., E. N. Barmpounakis, and E. I. Vlahogianni. Identifying driving safety profiles from smartphone data using unsupervised learning. *Safety Science,* Vol. 119, 2019, pp. 84-90.
[65] Zhang, K., S. Batterman, and F. Dion. Vehicle emissions in congestion: Comparison of work zone, rush hour and free-flow conditions. *Atmospheric Environment,* Vol. 45, No. 11, 2011, pp. 1929-1939.
[66] Salem, O., S. Pirzadeh, S. Ghorai, and A. Abdel-Rahim. Improving Sustainability of Work-zones by Implementing Lean Construction Techniques.In *International Conference on Architecture and Civil Engineering*, 2014.
[67] Qiao, F., J. Jia, L. Yu, Q. Li, and D. Zhai. Drivers' smart assistance system based on radio frequency identification: Enhanced safety and reduced emissions in work zones. *Transportation Research Record,* Vol. 2458, No. 1, 2014, pp. 37-46.
[68] Liu, Z., A. Ivanco, and Z. Filipi. Naturalistic drive cycle synthesis for pickup trucks. *Journal of safety research,* Vol. 54, 2015, pp. 109. e129-115.
[69] Li, Q., F. Qiao, and L. Yu. Vehicle emission implications of drivers' smart advisory system for traffic operations in work zones. *Journal of the Air & Waste Management Association,* Vol. 66, No. 5, 2016, pp. 446-455.
[70] Zhou, X., S. Tanvir, H. Lei, J. Taylor, B. Liu, N. M. Rouphail, and H. C. Frey. Integrating a simplified emission estimation model and mesoscopic dynamic traffic simulator to efficiently evaluate emission impacts of traffic management strategies. *Transportation Research Part D: Transport and Environment,* Vol. 37, 2015, pp. 123-136.

[71] Farzaneh, R., T. Ramani, M. Venugopal, S. Vallamsundar, G. Pesti, J. Crawford, A. Birt, C. Gu, M. Askariyeh, and G. Valdez. Air Quality Benefits of Nighttime Construction in Texas Non-Attainment Counties.In, 2017.
[72] Thomas, S. *Modeling of freeway air quality during recurring and nonrecurring congestion events*. Purdue University, 2007.
[73] Barth, M., and K. Boriboonsomsin. Real-world carbon dioxide impacts of traffic congestion. *Transportation Research Record,* Vol. 2058, No. 1, 2008, pp. 163-171.
[74] Bigazzi, A., and M. Figliozzi. An analysis of the relative efficiency of freeway congestion mitigation as an emissions reduction strategy.In *90th Annual Meeting of the Transportation Research Board*, Transportation Research Board Washington, DC, 2011. pp. 23-27.
[75] Qi, Y., A. Padiath, Q. Zhao, and L. Yu. Development of operating mode distributions for different types of roadways under different congestion levels for vehicle emission assessment using MOVES. *Journal of the Air & Waste Management Association,* Vol. 66, No. 10, 2016, pp. 1003-1011.
[76] Papson, A., S. Hartley, and K.-L. Kuo. Analysis of emissions at congested and uncongested intersections with motor vehicle emission simulation 2010. *Transportation Research Record,* Vol. 2270, No. 1, 2012, pp. 124-131.
[77] Sun, Y., H. Xu, J. Wu, E. Hajj, and X. Geng. Data Processing Framework for Driving Cycle Development with Naturalistic Driving Study Data.In *96th Annual Meeting of the Transportation Research Board, Washington, DC*, 2017. pp. 2645-2606.
[78] LeBlanc, D. J., M. Sivak, and S. Bogard. Using naturalistic driving data to assess variations in fuel efficiency among individual drivers.In, University of Michigan, Ann Arbor, Transportation Research Institute, 2010.
[79] Tanvir, S., R. Chase, and N. Rouphail. Heterogeneity and Consistency of Eco-Driving Metrics Using Naturalistic Driving Data.In *96thAnnual Meeting of the Transportation Research Board, Washington, DC*, 2017.
[80] Hankey, J. M., M. A. Perez, and J. A. McClafferty. Description of the SHRP 2 naturalistic database and the crash, near-crash, and baseline data sets.In, Virginia Tech Transportation Institute, 2016.
[81] Wali, B., A. J. Khattak, and T. Karnowski. The relationship between driving volatility in time to collision and crash-injury severity in a naturalistic driving environment. *Analytic methods in accident research,* Vol. 28, 2020, p. 100136.
[82] Khattak, A. J., and B. Wali. Analysis of volatility in driving regimes extracted from basic safety messages transmitted between connected vehicles. *Transportation research part C: emerging technologies,* Vol. 84, 2017, pp. 48-73.
[83] Khattak, Z. H., B. L. Smith, H. Park, and M. D. Fontaine. Cooperative lane control application for fully connected and automated vehicles at multilane freeways. *Transportation research part C: emerging technologies,* Vol. 111, 2020, pp. 294-317.
[84] Kassambara, A. *Practical guide to cluster analysis in R: Unsupervised machine learning*. Sthda, 2017.
[85] Gentleman, R., and V. J. Carey. Unsupervised machine learning.In *Bioconductor case studies*, Springer, 2008. pp. 137-157.
[86] Murtagh, F., and P. Contreras. Algorithms for hierarchical clustering: an overview. *Wiley Interdisciplinary Reviews: Data Mining and Knowledge Discovery,* Vol. 2, No. 1, 2012, pp. 86-97.
[87] Moawad, A., P. Sharer, and A. Rousseau. Light-duty vehicle fuel consumption displacement potential up to 2045.In, Argonne National Lab.(ANL), Argonne, IL (United States), 2013.
[88] Song, Y.-y., E.-j. Yao, T. Zuo, and Z.-f. Lang. Emissions and fuel consumption modeling for evaluating environmental effectiveness of ITS strategies. *Discrete Dynamics in Nature and Society,* Vol. 2013, 2013.

[89] Frey, H. C., N. M. Rouphail, H. Zhai, T. L. Farias, and G. A. Gonçalves. Comparing real-world fuel consumption for diesel-and hydrogen-fueled transit buses and implication for emissions. *Transportation Research Part D: Transport and Environment,* Vol. 12, No. 4, 2007, pp. 281-291.
[90] Frey, H., A. Unal, J. Chen, S. Li, and C. Xuan. Methodology for developing modal emission rates for EPA's multi-scale motor vehicle & equipment emission system. *Ann Arbor, Michigan: US Environmental Protection Agency*, 2002.
[91] Fitzpatrick, K. *Design speed, operating speed, and posted speed practices*. Transportation Research Board, 2003.
[92] Srinivasan, R., D. Carter, and K. Bauer. Safety performance function decision guide: SPF calibration vs SPF development. *Federal Highway Administration–Office of Safety Report*, 2013.
[93] National Center for Statistics and Analysis. Traffic Safety Facts 2008: A Compilation of Motor Vehicle Crash Data from the Fatality Analysis Reporting System and the General Estimates System In, Washington, DC: National Highway Traffic Safety Administration., 2008.
[94] Saito, M., B. K. Brimley, and G. G. Schultz. Transportation safety data and analysis: Volume 2, Calibration of the highway safety manual and development of new safety performance functions.In, Utah. Dept. of Transportation. Research Division, 2011.
[95] Srinivasan, R., and D. Carter. Development of safety performance functions for North Carolina.In, North Carolina. Dept. of Transportation. Research and Analysis Group, 2011.
[96] Kweon, Y.-J., and I.-K. Lim. Development of safety performance functions for multilane highway and freeway segments maintained by the Virginia Department of Transportation.In, 2014.
[97] Mehta, G., and Y. Lou. Safety performance function calibration and development for the State of Alabama: Two-lane two-way rural roads and four-lane divided highways.In *92nd Annual Meeting of the Transportation Research Board, Washington, DC*, 2013.
[98] Khattak, A., N. Ahmad, A. Mohammadnazar, I. MahdiNia, B. Wali, and R. Arvin. HIGHWAY SAFETY MANUAL SAFETY PERFORMANCE FUNCTIONS & ROADWAY CALIBRATION FACTORS: ROADWAY SEGMENTS PHASE 2, PART. 2020.
[99] Green, E. R., C. L. Blackden, and M. A. Fields. Development of a Spatial Database for Intersections in Kentucky.In, Kentucky Transportation Center, 2016.
[100] Donnell, E., V. Gayah, and P. Jovanis. Safety performance functions.In, Pennsylvania. Dept. of Transportation. Bureau of Planning and Research, 2014.
[101] Dixon, K., C. Monsere, F. Xie, and K. Gladhill. Calibrating the future highway safety manual predictive methods for Oregon state highways.In, Oregon. Dept. of Transportation. Research Section, 2012.
[102] Sun, C., P. Edara, H. Brown, J. Berry, B. Claros, and X. Yu. Missouri Highway Safety Manual Recalibration.In, Missouri. Dept. of Transportation. Construction and Materials Division, 2018.
[103] Tegge, R. A., J.-H. Jo, and Y. Ouyang. Development and application of safety performance functions for Illinois.In, Development of Safety Performance Functions for Illinois 2010.
[104] Storm, R., and V. Richfield. Phase I-II of the Minnesota Highway Safety Manual Calibration.In, Minnesota Department of Transportation, 2014.
[105] Shin, H., Y.-J. Lee, and S. Dadvar. The development of local calibration factors for implementing the highway safety manual in Maryland.In, Maryland. State Highway Administration, 2014.
[106] Lubliner, H., C. Bornheimer, S. Schrock, M.-H. Wang, and E. Fitzsimmons. Evaluation of interactive highway safety design model crash prediction tools for two-lane rural roads on Kansas Department of Transportation projects.In, Kansas. Dept. of Transportation, 2014.
[107] *Highway Safety Manual*. American Association of State Highway and Transportation (AASHTO), Washington, DC, 2010.

[108] Jovanis, P. P., and H.-L. Chang. Modeling the relationship of accidents to miles traveled. *Transportation research record,* Vol. 1068, 1986, pp. 42-51.
[109] Joshua, S. C., and N. J. Garber. Estimating truck accident rate and involvements using linear and Poisson regression models. *Transportation planning and Technology,* Vol. 15, No. 1, 1990, pp. 41-58.
[110] Lord, D., and F. Mannering. The statistical analysis of crash-frequency data: a review and assessment of methodological alternatives. *Transportation research part A: policy and practice,* Vol. 44, No. 5, 2010, pp. 291-305.
[111] Bonneson, J. A., and P. T. McCoy. Estimation of safety at two-way stop-controlled intersections on rural highways. *Transportation research record,* Vol. 1399, 1993, pp. 83-89.
[112] Poch, M., and F. Mannering. Negative binomial analysis of intersection-accident frequencies. *Journal of transportation engineering,* Vol. 122, No. 2, 1996, pp. 105-113.
[113] Persaud, B., and T. Nguyen. Disaggregate safety performance models for signalized intersections on Ontario provincial roads. *Transportation research record,* Vol. 1635, No. 1, 1998, pp. 113-120.
[114] El-Basyouny, K., and T. Sayed. Comparison of two negative binomial regression techniques in developing accident prediction models. *Transportation research record,* Vol. 1950, No. 1, 2006, pp. 9-16.
[115] Lord, D. Modeling motor vehicle crashes using Poisson-gamma models: Examining the effects of low sample mean values and small sample size on the estimation of the fixed dispersion parameter. *Accident Analysis & Prevention,* Vol. 38, No. 4, 2006, pp. 751-766.
[116] Lord, D., and L. F. Miranda-Moreno. Effects of low sample mean values and small sample size on the estimation of the fixed dispersion parameter of Poisson-gamma models for modeling motor vehicle crashes: A Bayesian perspective. *Safety Science,* Vol. 46, No. 5, 2008, pp. 751-770.
[117] Miaou, S.-P., R. Bligh, and D. Lord. DEVELOPING MEDIAN BARRIER INSTALLATION GUIDELINES: ABenefit/COST ANALYSIS USING TEXAS DATA.In *Presented at the 84th Transportation Research Board's Annual Meeting*, 2005.
[118] Lord, D., S. P. Washington, and J. N. Ivan. Poisson, Poisson-gamma and zero-inflated regression models of motor vehicle crashes: balancing statistical fit and theory. *Accident Analysis & Prevention,* Vol. 37, No. 1, 2005, pp. 35-46.
[119] Kumara, S., and H. C. Chin. Modeling accident occurrence at signalized tee intersections with special emphasis on excess zeros. *Traffic injury prevention,* Vol. 4, No. 1, 2003, pp. 53-57.
[120] Shirani-Bidabadi, N., N. Mallipaddi, K. Haleem, and M. Anderson. Developing bicycle-vehicle crash-specific safety performance functions in Alabama using different techniques. *Accident Analysis & Prevention,* Vol. 146, 2020, p. 105735.
[121] Daniels, S., T. Brijs, E. Nuyts, and G. Wets. Explaining variation in safety performance of roundabouts. *Accident Analysis & Prevention,* Vol. 42, No. 2, 2010, pp. 393-402.
[122] Li, X., D. Lord, and Y. Zhang. Development of accident modification factors for rural frontage road segments in Texas using generalized additive models. *Journal of transportation engineering,* Vol. 137, No. 1, 2011, pp. 74-83.
[123] Malyshkina, N. V., F. L. Mannering, and A. P. Tarko. Markov switching negative binomial models: an application to vehicle accident frequencies. *Accident Analysis & Prevention,* Vol. 41, No. 2, 2009, pp. 217-226.
[124] Chen, E., and A. P. Tarko. Modeling safety of highway work zones with random parameters and random effects models. *Analytic methods in accident research,* Vol. 1, 2014, pp. 86-95.
[125] Mokhtarimousavi, S., J. C. Anderson, A. Azizinamini, and M. Hadi. Factors affecting injury severity in vehicle-pedestrian crashes: a day-of-week analysis using random parameter ordered response models and artificial neural networks. *International journal of transportation science and technology,* Vol. 9, No. 2, 2020, pp. 100-115.

[126] Khoda Bakhshi, A., and M. M. Ahmed. Practical advantage of crossed random intercepts under Bayesian hierarchical modeling to tackle unobserved heterogeneity in clustering critical versus non-critical crashes. *Accident Analysis & Prevention,* Vol. 149, 2021, p. 105855.
[127] Mohammadnazar, A., I. Mahdinia, N. Ahmad, A. J. Khattak, and J. Liu. Understanding how relationships between crash frequency and correlates vary for multilane rural highways: Estimating geographically and temporally weighted regression models. *Accident Analysis & Prevention,* Vol. 157, 2021, p. 106146.
[128] Lord, D., and B. N. Persaud. Accident prediction models with and without trend: application of the generalized estimating equations procedure. *Transportation research record,* Vol. 1717, No. 1, 2000, pp. 102-108.
[129] Abdel-Aty, M., and X. Wang. Crash estimation at signalized intersections along corridors: analyzing spatial effect and identifying significant factors. *Transportation research record,* Vol. 1953, No. 1, 2006, pp. 98-111.
[130] Wang, X., and M. Abdel-Aty. Temporal and spatial analyses of rear-end crashes at signalized intersections. *Accident Analysis & Prevention,* Vol. 38, No. 6, 2006, pp. 1137-1150.
[131] Guo, F., X. Wang, and M. A. Abdel-Aty. Modeling signalized intersection safety with corridor-level spatial correlations. *Accident Analysis & Prevention,* Vol. 42, No. 1, 2010, pp. 84-92.
[132] Song, J. J., M. Ghosh, S. Miaou, and B. Mallick. Bayesian multivariate spatial models for roadway traffic crash mapping. *Journal of multivariate analysis,* Vol. 97, No. 1, 2006, pp. 246-273.
[133] Aguero-Valverde, J., and P. P. Jovanis. Analysis of road crash frequency with spatial models. *Transportation research record,* Vol. 2061, No. 1, 2008, pp. 55-63.
[134] El-Basyouny, K., and T. Sayed. Urban arterial accident prediction models with spatial effects. *Transportation research record,* Vol. 2102, No. 1, 2009, pp. 27-33.
[135] Xie, K., X. Wang, K. Ozbay, and H. Yang. Crash frequency modeling for signalized intersections in a high-density urban road network. *Analytic methods in accident research,* Vol. 2, 2014, pp. 39-51.
[136] Choi, E.-H. Crash factors in intersection-related crashes: An on-scene perspective.In, 2010.
[137] Wali, B., A. J. Khattak, H. Bozdogan, and M. Kamrani. How is driving volatility related to intersection safety? A Bayesian heterogeneity-based analysis of instrumented vehicles data. *Transportation research part C: emerging technologies,* Vol. 92, 2018, pp. 504-524.
[138] Kamrani, M., B. Wali, and A. J. Khattak. Can data generated by connected vehicles enhance safety?: Proactive approach to intersection safety management. *Transportation research record,* Vol. 2659, No. 1, 2017, pp. 80-90.
[139] Besag, J., J. York, and A. Mollié. Bayesian image restoration, with two applications in spatial statistics. *Annals of the institute of statistical mathematics,* Vol. 43, No. 1, 1991, pp. 1-20.
[140] Carriquiry, A. L., and M. Pawlovich. From empirical Bayes to full Bayes: methods for analyzing traffic safety data. 2004.
[141] Andrieu, C., N. De Freitas, A. Doucet, and M. I. Jordan. An introduction to MCMC for machine learning. *Machine learning,* Vol. 50, No. 1, 2003, pp. 5-43.
[142] Murphy, K. P. *Machine learning: a probabilistic perspective*. MIT press, 2012.
[143] Xie, K., X. Wang, H. Huang, and X. Chen. Corridor-level signalized intersection safety analysis in Shanghai, China using Bayesian hierarchical models. *Accident Analysis & Prevention,* Vol. 50, 2013, pp. 25-33.
[144] Cheng, W., G. S. Gill, Y. Zhang, T. Vo, F. Wen, and Y. Li. Exploring the modeling and site-ranking performance of Bayesian spatiotemporal crash frequency models with mixture components. *Accident Analysis & Prevention,* Vol. 135, 2020, p. 105357.
[145] Gelman, A., J. B. Carlin, H. S. Stern, D. B. Dunson, A. Vehtari, and D. B. Rubin. *Bayesian data analysis*. CRC press, 2013.

[146] Brooks, S. P., and A. Gelman. General methods for monitoring convergence of iterative simulations. *Journal of computational and graphical statistics,* Vol. 7, No. 4, 1998, pp. 434-455.
[147] Bozdogan, H. Model selection and Akaike's information criterion (AIC): The general theory and its analytical extensions. *Psychometrika,* Vol. 52, No. 3, 1987, pp. 345-370.
[148] Spiegelhalter, D. J., N. G. Best, B. P. Carlin, and A. Van Der Linde. Bayesian measures of model complexity and fit. *Journal of the royal statistical society: Series b (statistical methodology),* Vol. 64, No. 4, 2002, pp. 583-639.
[149] Burnham, K. P., and D. R. Anderson. Practical use of the information-theoretic approach.In *Model selection and inference*, Springer, 1998. pp. 75-117.
[150] Geisser, S., and W. F. Eddy. A predictive approach to model selection. *Journal of the American Statistical Association,* Vol. 74, No. 365, 1979, pp. 153-160.
[151] Kass, R. E., and A. E. Raftery. Bayes factors. *Journal of the American Statistical Association,* Vol. 90, No. 430, 1995, pp. 773-795.
[152] Hunter, M., E. Saldivar-Carranza, J. Desai, J. K. Mathew, H. Li, and D. M. Bullock. A Proactive Approach to Evaluating Intersection Safety Using Hard-Braking Data. *Journal of Big Data Analytics in Transportation*, 2021, pp. 1-14.
[153] Bagdadi, O. Assessing safety critical braking events in naturalistic driving studies. *Transportation research part F: traffic psychology and behaviour,* Vol. 16, 2013, pp. 117-126.
[154] Potts, I. B., K. M. Bauer, D. J. Torbic, and J. F. Ringert. Safety of channelized right-turn lanes for motor vehicles and pedestrians. *Transportation research record,* Vol. 2398, No. 1, 2013, pp. 93-100.
[155] Harwood, D. W., K. M. Bauer, I. B. Potts, D. J. Torbic, K. R. Richard, E. R. Rabbani, E. Hauer, L. Elefteriadou, and M. S. Griffith. Safety effectiveness of intersection left-and right-turn lanes. *Transportation research record,* Vol. 1840, No. 1, 2003, pp. 131-139.
[156] Srinivasan, R., F. Council, C. Lyon, F. Gross, N. Lefler, and B. Persaud. Safety effectiveness of selected treatments at urban signalized intersections. *Transportation research record,* Vol. 2056, No. 1, 2008, pp. 70-76.
[157] Chen, L., C. Chen, and R. Ewing. Left-turn phase: Permissive, protected, or both? A quasi-experimental design in New York City. *Accident Analysis & Prevention,* Vol. 76, 2015, pp. 102-109.
[158] Zador, P. L. Right-turn-on-red laws and motor vehicle crashes: A review of the literature. *Accident Analysis & Prevention,* Vol. 16, No. 4, 1984, pp. 241-245.
[159] Zador, P., J. Moshman, and L. Marcus. Adoption of right turn on red: Effects on crashes at signalized intersections. *Accident Analysis & Prevention,* Vol. 14, No. 3, 1982, pp. 219-234.
[160] Hu, W., A. T. McCartt, and E. R. Teoh. Effects of red light camera enforcement on fatal crashes in large US cities. *Journal of safety research,* Vol. 42, No. 4, 2011, pp. 277-282.
[161] Ahmed, M. M., and M. Abdel-Aty. Evaluation and spatial analysis of automated red-light running enforcement cameras. *Transportation research part C: emerging technologies,* Vol. 50, 2015, pp. 130-140.
[162] Chrzan, S., M. Hamill, M. Wacht, and J. Brown. Connected Vehicle Pilot Deployment Program Phase 1, Outreach Plan–Tampa (THEA).In, United States. Department of Transportation. Intelligent Transportation …, 2016.
[163] Galgano, S., M. Talas, K. Opie, M. Marsico, A. Weeks, Y. Wang, D. Benevelli, R. Rausch, K. Ozbay, and S. Muthuswamy. Connected Vehicle Pilot Deployment Program phase 1: performance measurement and evaluation support plan: New York City.In, United States. Joint Program Office for Intelligent Transportation Systems, 2016.
[164] Zou, W., X. Wang, and D. Zhang. Truck crash severity in New York city: an investigation of the spatial and the time of day effects. *Accident Analysis & Prevention,* Vol. 99, 2017, pp. 249-261.
[165] Zhu, X., and S. Srinivasan. Modeling occupant-level injury severity: An application to large-truck crashes. *Accident Analysis & Prevention,* Vol. 43, No. 4, 2011, pp. 1427-1437.

[166] Lee, C., and X. Li. Analysis of injury severity of drivers involved in single-and two-vehicle crashes on highways in Ontario. *Accident Analysis & Prevention,* Vol. 71, 2014, pp. 286-295.
[167] Dong, C., S. H. Richards, B. Huang, and X. Jiang. Identifying the factors contributing to the severity of truck-involved crashes. *International journal of injury control and safety promotion,* Vol. 22, No. 2, 2015, pp. 116-126.
[168] Dong, C., Q. Dong, B. Huang, W. Hu, and S. S. Nambisan. Estimating factors contributing to frequency and severity of large truck–involved crashes. *Journal of Transportation Engineering, Part A: Systems,* Vol. 143, No. 8, 2017, p. 04017032.
[169] Chang, L.-Y., and F. Mannering. Analysis of injury severity and vehicle occupancy in truck- and non-truck-involved accidents. *Accident Analysis & Prevention,* Vol. 31, No. 5, 1999, pp. 579-592.
[170] Khattak, A. J., R. J. Schneider, and F. Targa. Risk factors in large truck rollovers and injury severity: analysis of single-vehicle collisions. *Transportation Research Record,* Vol. 40, 2003.
[171] Golob, T. F., and A. C. Regan. Traffic conditions and truck accidents on urban freeways. 2004.
[172] Khattak, A. J., and F. Targa. Injury severity and total harm in truck-involved work zone crashes. *Transportation Research Record,* Vol. 1877, No. 1, 2004, pp. 106-116.
[173] Pahukula, J., S. Hernandez, and A. Unnikrishnan. A time of day analysis of crashes involving large trucks in urban areas. *Accident Analysis & Prevention,* Vol. 75, 2015, pp. 155-163.
[174] Teoh, E. R., D. L. Carter, S. Smith, and A. T. McCartt. Crash risk factors for interstate large trucks in North Carolina. *Journal of safety research,* Vol. 62, 2017, pp. 13-21.
[175] McKnight, A. J., and G. T. Bahouth. Analysis of large truck rollover crashes. *Traffic injury prevention,* Vol. 10, No. 5, 2009, pp. 421-426.
[176] Krull, K. A., A. J. Khattak, and F. M. Council. Injury effects of rollovers and events sequence in single-vehicle crashes. *Transportation Research Record,* Vol. 1717, No. 1, 2000, pp. 46-54.
[177] Deutermann, W. Characteristics of fatal rollover crashes.In, National Center for Statistics and Analysis, Research and Development, 2002.
[178] Azimi, G., A. Rahimi, H. Asgari, and X. Jin. Severity analysis for large truck rollover crashes using a random parameter ordered logit model. *Accident Analysis & Prevention,* Vol. 135, 2020, p. 105355.
[179] Al-Bdairi, N. S. S., and S. Hernandez. An empirical analysis of run-off-road injury severity crashes involving large trucks. *Accident Analysis & Prevention,* Vol. 102, 2017, pp. 93-100.
[180] Duncan, C. S., A. J. Khattak, and F. M. Council. Applying the ordered probit model to injury severity in truck-passenger car rear-end collisions. *Transportation Research Record,* Vol. 1635, No. 1, 1998, pp. 63-71.
[181] Zhu, X., and S. Srinivasan. A comprehensive analysis of factors influencing the injury severity of large-truck crashes. *Accident Analysis & Prevention,* Vol. 43, No. 1, 2011, pp. 49-57.
[182] Jiang, X., B. Huang, X. Yan, R. L. Zaretzki, and S. Richards. Two-vehicle injury severity models based on integration of pavement management and traffic engineering factors. *Traffic injury prevention,* Vol. 14, No. 5, 2013, pp. 544-553.
[183] Osman, M., R. Paleti, S. Mishra, and M. M. Golias. Analysis of injury severity of large truck crashes in work zones. *Accident Analysis & Prevention,* Vol. 97, 2016, pp. 261-273.
[184] Daniel, J., C. Tsai, and S. Chien. Factors in truck crashes on roadways with intersections. *Transportation Research Record,* Vol. 1818, No. 1, 2002, pp. 54-59.
[185] Mannering, F. L., V. Shankar, and C. R. Bhat. Unobserved heterogeneity and the statistical analysis of highway accident data. *Analytic methods in accident research,* Vol. 11, 2016, pp. 1-16.

[186] da Silva, A. R., and T. C. V. Rodrigues. Geographically weighted negative binomial regression—incorporating overdispersion. *Statistics and Computing,* Vol. 24, No. 5, 2014, pp. 769-783.
[187] Liu, J., A. Hainen, X. Li, Q. Nie, and S. Nambisan. Pedestrian injury severity in motor vehicle crashes: an integrated spatio-temporal modeling approach. *Accident Analysis and Prevention,* Vol. 132, 2019, p. 105272.
[188] Fotheringham, A. S., C. Brunsdon, and M. Charlton. *Geographically weighted regression: the analysis of spatially varying relationships*. John Wiley & Sons, 2003.
[189] Long, J. S. Regression models for categorical and limited dependent variables (Vol. 7). *Advanced quantitative techniques in the social sciences*, 1997.
[190] Burnham, K. P., and D. R. Anderson. Multimodel inference: understanding AIC and BIC in model selection. *Sociological methods & research,* Vol. 33, No. 2, 2004, pp. 261-304.
[191] Islam, M. S., J. N. Ivan, N. E. Lownes, R. A. Ammar, and S. Rajasekaran. Developing safety performance function for freeways by considering interactions between speed limit and geometric variables. *Transportation Research Record,* Vol. 2435, No. 1, 2014, pp. 72-81.
[192] Liu, J., A. J. Khattak, and B. Wali. Do safety performance functions used for predicting crash frequency vary across space? Applying geographically weighted regressions to account for spatial heterogeneity. *Accident Analysis & Prevention,* Vol. 109, 2017, pp. 132-142.
[193] Kim, K., I. M. Brunner, and E. Y. Yamashita. Influence of land use, population, employment, and economic activity on accidents. *Transportation Research Record,* Vol. 1953, No. 1, 2006, pp. 56-64.
[194] Hoffman, M. R. Two-Way, Left-Tum Lanes Work! In Traffic Engineering. *Institute of Transportation Engineers, Washington, D.C.,* Vol. 44, No. 11, 1974, pp. 24-27.
[195] Knuiman, M. W., F. M. Council, and D. W. Reinfurt. Association of median width and highway accident rates (with discussion and closure). *Transportation Research Record,* Vol. 1401, 1993, pp. 70-82.
[196] Wali, B., A. J. Khattak, J. Waters, D. Chimba, and X. Li. Development of safety performance functions: incorporating unobserved heterogeneity and functional form analysis. *Transportation Research Record,* Vol. 2672, No. 30, 2018, pp. 9-20.
[197] Khan, M., A. Abdel-Rahim, and C. J. P. Williams. Potential crash reduction benefits of shoulder rumble strips in two-lane rural highways. *Accident Analysis & Prevention,* Vol. 75, 2015, pp. 35-42.
[198] Milton, J., and F. J. T. Mannering. The relationship among highway geometrics, traffic-related elements and motor-vehicle accident frequencies. Vol. 25, No. 4, 1998, pp. 395-413.
[199] Lee, J., K. Chung, and S. Kang. Evaluating and addressing the effects of regression to the mean phenomenon in estimating collision frequencies on urban high collision concentration locations. *Accident Analysis & Prevention,* Vol. 97, 2016, pp. 49-56.
[200] Oluwajana, S. D. Development of Hotzone Identification Models for Simultaneous Crime and Collision Reduction. 2018.
[201] Wang, C., M. A. Quddus, and S. G. Ison. Predicting accident frequency at their severity levels and its application in site ranking using a two-stage mixed multivariate model. *Accident Analysis & Prevention,* Vol. 43, No. 6, 2011, pp. 1979-1990.
[202] Anarkooli, A. J., B. Persaud, M. Hosseinpour, and T. Saleem. Comparison of univariate and two-stage approaches for estimating crash frequency by severity—Case study for horizontal curves on two-lane rural roads. *Accident Analysis & Prevention,* Vol. 129, 2019, pp. 382-389.
[203] Ma, J., K. M. Kockelman, and P. Damien. A multivariate Poisson-lognormal regression model for prediction of crash counts by severity, using Bayesian methods. *Accident Analysis & Prevention,* Vol. 40, No. 3, 2008, pp. 964-975.
[204] Safety Performance Functions for Intersections.In, Colorado Department of Transportation, 2009.

[205] Savolainen, P. T., T. Gates, D. Lord, S. Geedipally, E. Rista, T. Barrette, B. J. Russo, and R. Hamzeie. Michigan urban trunkline intersections safety performance functions (SPFs) development and support.In, Michigan. Dept. of Transportation. Office of Research Administration, 2015.
[206] Dixon, K., C. M. Monsere, F. Xie, and K. Gladhill. Calibrating the HSM Predictive Methods for Oregon Highways.In, Oregon Department of Transportation and Oregon Transportation Research and Education Consortium, 2012.
[207] Srinivasan, S., P. Haas, N. S. Dhakar, R. Hormel, D. Torbic, and D. Harwood. Development and calibration of highway safety manual equations for Florida conditions.In, University of Florida. Transportation Research Center, 2011.
[208] Storm, R., and V. Richfield. Phase I-II of the Minnesota Highway Safety Manual Calibration In, Minnesota Department of Transportation 2014.
[209] Xiao Qin, P., and K. Vachal. Evaluating Local and Tribal Rural Road Design with the Interactive Highway Safety Design Model (IHSDM).In, 2013.
[210] Troyer, D., K. Bradbury, and C. Juliano. Strength of the variable: calculating and evaluating safety performance function calibration factors for the state of Ohio. *Transportation Research Record,* Vol. 2515, No. 1, 2015, pp. 86-93.
[211] Shankar, V., and S. Madanat. Methods for Identifying High Collision Concentrations for Identifying Potential Safety Improvements: Development of Safety Performance Functions for California.In, 2015.
[212] Farid, A., M. Abdel-Aty, J. Lee, N. Eluru, and J.-H. Wang. Exploring the transferability of safety performance functions. *Accident Analysis & Prevention,* Vol. 94, 2016, pp. 143-152.
[213] Chen, Y., B. Persaud, and E. Sacchi. Improving transferability of safety performance functions by Bayesian model averaging. *Transportation Research Record,* Vol. 2280, No. 1, 2012, pp. 162-172.
[214] Kaaf, K. A., and M. Abdel-Aty. Transferability and calibration of Highway Safety Manual performance functions and development of new models for urban four-lane divided roads in Riyadh, Saudi Arabia. *Transportation Research Record,* Vol. 2515, No. 1, 2015, pp. 70-77.
[215] Sacchi, E., B. Persaud, and M. Bassani. Assessing international transferability of highway safety manual crash prediction algorithm and its components. *Transportation Research Record,* Vol. 2279, No. 1, 2012, pp. 90-98.
[216] Makaiwi, M. Modeling crash frequency and severity using historical traffic and weather data: truck involved crashes on I-80 in Iowa. 2006.
[217] Abdulhafedh, A. Crash frequency analysis. *Journal of transportation technologies,* Vol. 6, No. 04, 2016, p. 169.
[218] ---. Road crash prediction models: different statistical modeling approaches. *Journal of transportation technologies,* Vol. 7, No. 02, 2017, p. 190.
[219] Shirani-Bidabadi, N., M. Doustmohammadi, K. Haleem, and M. Anderson. Safety investigation of nonmotorized crashes in the City of Huntsville, Alabama, using count regression models.In *Transportation Research Board 100th Annual Meeting*, Washington DC, 2018.
[220] R. Gehrke, S., B. Sadeghinasr, Q. Wang, and T. G.Reardon. Patterns and Predictors of Dockless Bikeshare Trip Generation and Duration in Boston's Suburbs. *Case Studies on Transport Policy*, 2021.
[221] Malyshkina, N. V., and F. L. Mannering. Markov switching multinomial logit model: an application to accident-injury severities. *Accident Analysis & Prevention,* Vol. 41, No. 4, 2009, pp. 829-838.
[222] Xie, Y., and Y. Zhang. Crash frequency analysis with generalized additive models. *Transportation Research Record,* Vol. 2061, No. 1, 2008, pp. 39-45.
[223] Li, X., D. Lord, Y. Zhang, and Y. Xie. Predicting motor vehicle crashes using support vector machine models. *Accident Analysis & Prevention,* Vol. 40, No. 4, 2008, pp. 1611-1618.

[224] Malyshkina, N. V., and F. L. Mannering. Empirical assessment of the impact of highway design exceptions on the frequency and severity of vehicle accidents. *Accident Analysis & Prevention,* Vol. 42, No. 1, 2010, pp. 131-139.
[225] Park, B.-J., and D. Lord. Application of finite mixture models for vehicle crash data analysis. *Accident Analysis & Prevention,* Vol. 41, No. 4, 2009, pp. 683-691.
[226] Mohammadnazar, A., I. Mahdinia, R. Arvin, and A. J. Khattak. Exploring the Effects of Physical Condition and Driving Errors of At-fault Drivers on Injury Severity of Large Truck Angle Crashes.In *Transportation Research Board 100th Annual Meeting*, Washington DC, 2021.
[227] Wali, B., N. Ahmad, A. J Khattak, and A. Mohammadnazar. Developing Safety Performance Functions for Rural Multilane Highways in Tennessee: Accounting for Unobserved Heterogeneity.In *Transportation Research Board 100th Annual Meeting*, Washington DC, 2020.
[228] Huang, Y., X. Wang, and D. Patton. Examining spatial relationships between crashes and the built environment: A geographically weighted regression approach. *Journal of transport geography,* Vol. 69, 2018, pp. 221-233.
[229] Hadayeghi, A., A. S. Shalaby, and B. N. Persaud. Development of planning level transportation safety tools using Geographically Weighted Poisson Regression. *Accident Analysis & Prevention,* Vol. 42, No. 2, 2010, pp. 676-688.
[230] Zheng, L., R. M. Robinson, A. Khattak, and X. Wang. All Accidents are Not Equal: Using Geographically Weighted Regressions Models to Assess and Forecast Accident Impacts.In *3rd International Conference on Road Safety and Simulation, Indianapolis, USA. Transportation Research Board*, 2011. pp. 14-16.
[231] Martin, J.-L. Relationship between crash rate and hourly traffic flow on interurban motorways. *Accident Analysis & Prevention,* Vol. 34, No. 5, 2002, pp. 619-629.
[232] Wang, X., M. Abdel-Aty, and P. A. Brady. Crash estimation at signalized intersections: significant factors and temporal effect. *Transportation Research Record,* Vol. 1953, No. 1, 2006, pp. 10-20.
[233] Liu, C., and A. Sharma. Using the multivariate spatio-temporal Bayesian model to analyze traffic crashes by severity. *Analytic methods in accident research,* Vol. 17, 2018, pp. 14-31.
[234] Ma, X., S. Chen, and F. Chen. Multivariate space-time modeling of crash frequencies by injury severity levels. *Analytic Methods in Accident Research,* Vol. 15, 2017, pp. 29-40.
[235] Mannering, F. Temporal instability and the analysis of highway accident data. *Analytic methods in accident research,* Vol. 17, 2018, pp. 1-13.
[236] Zaloshnja, E., and T. R. Miller. Costs of large truck-involved crashes in the United States. *Accident Analysis & Prevention,* Vol. 36, No. 5, 2004, pp. 801-808.
[237] Federal Motor Carrier Safety Administration. Unit costs of medium and heavy truck crashes.In, Washington, DC: US Department of Transportation., 2008.
[238] Occupational Safety and Health Administration. Trucking Industry Hazards.In, 2020.
[239] National Center for Statistics and Analysis. Traffic Safety Facts, Summary of Motor Vehicle Crashes, 2015 Data.In, Washington, DC: National Highway Traffic Safety Administration., 2020
[240] ---. Traffic Safety Facts, Police-Reported Motor Vehicle Traffic Crashes in 2018.In, Washington, DC: National Highway Traffic Safety Administration., 2020.
[241] Large Truck Crash Facts.In, Federal Motor Carrier Safety Administration, 2020.
[242] *The Large Truck Crash Causation Study.* U.S. Department of Transportation Federal Motor Carrier Safety Administration, Washington, D.C. . http://www.fmcsa.dot.gov/safety/research-and-analysis/large-truck-crash-causation-study-analysis-brief. Accessed May 21, 2008.
[243] Schneider, W. H., and P. T. Savolainen. Comparison of severity of motorcyclist injury by crash types. *Transportation Research Record,* Vol. 2265, No. 1, 2011, pp. 70-80.

[244] Moudon, A. V., L. Lin, J. Jiao, P. Hurvitz, and P. Reeves. The risk of pedestrian injury and fatality in collisions with motor vehicles, a social ecological study of state routes and city streets in King County, Washington. *Accident Analysis & Prevention,* Vol. 43, No. 1, 2011, pp. 11-24.
[245] Mergia, W. Y., D. Eustace, D. Chimba, and M. Qumsiyeh. Exploring factors contributing to injury severity at freeway merging and diverging locations in Ohio. *Accident Analysis & Prevention,* Vol. 55, 2013, pp. 202-210.
[246] Quddus, M. A., C. Wang, and S. G. Ison. Road traffic congestion and crash severity: econometric analysis using ordered response models. *Journal of Transportation Engineering,* Vol. 136, No. 5, 2010, pp. 424-435.
[247] Klop, J. R., and A. J. Khattak. Factors influencing bicycle crash severity on two-lane, undivided roadways in North Carolina. *Transportation Research Record,* Vol. 1674, No. 1, 1999, pp. 78-85.
[248] Behnood, A., and F. L. Mannering. An empirical assessment of the effects of economic recessions on pedestrian-injury crashes using mixed and latent-class models. *Analytic methods in accident research,* Vol. 12, 2016, pp. 1-17.
[249] Ahmadi, A., A. Jahangiri, V. Berardi, and S. G. Machiani. Crash severity analysis of rear-end crashes in California using statistical and machine learning classification methods. *Journal of Transportation Safety & Security,* Vol. 12, No. 4, 2020, pp. 522-546.
[250] Molan, A. M., M. Moomen, and K. Ksaibati. Investigating the effect of geometric dimensions of median traffic barriers on crashes: Crash analysis of interstate roads in Wyoming using actual crash datasets. *Journal of safety research,* Vol. 71, 2019, pp. 163-171.
[251] Xin, C., R. Guo, Z. Wang, Q. Lu, and P.-S. Lin. The effects of neighborhood characteristics and the built environment on pedestrian injury severity: a random parameters generalized ordered probability model with heterogeneity in means and variances. *Analytic methods in accident research,* Vol. 16, 2017, pp. 117-132.
[252] Washington, S. P., M. G. Karlaftis, and F. Mannering. *Statistical and econometric methods for transportation data analysis*. Chapman and Hall/CRC, 2010.
[253] Mannering, F. L., and C. R. Bhat. Analytic methods in accident research: Methodological frontier and future directions. *Analytic methods in accident research,* Vol. 1, 2014, pp. 1-22.
[254] Ye, F. Investigating the effects of underreporting of crash data on three commonly used traffic crash severity models.In, Ph. D. Dissertation. Zachry Department of Civil Engineering, Texas A&M …, 2011.
[255] Greene, W. H. *Econometric analysis*. Pearson Education India, 2003.
[256] Hanna, R. The contribution of medical conditions to passenger vehicle crashes.In, 2009.
[257] Laberge-Nadeau, C., G. Dionne, U. Maag, D. Desjardins, C. Vanasse, and J.-M. Ékoé. Medical conditions and the severity of commercial motor vehicle drivers' road accidents. *Accident Analysis & Prevention,* Vol. 28, No. 1, 1996, pp. 43-51.
[258] Laberge-Nadeau, C., G. Dionne, J.-M. Ékoé, P. Hamet, D. Desjardins, S. Messier, and U. Maag. Impact of diabetes on crash risks of truck-permit holders and commercial drivers. *Diabetes Care,* Vol. 23, No. 5, 2000, pp. 612-617.
[259] Ronna, B. B., M. S. Thiese, U. Ott, A. Effiong, M. Murtaugh, J. Kapellusch, A. Garg, and K. Hegmann. The association between cardiovascular disease risk factors and motor vehicle crashes among professional truck drivers. *Journal of occupational environmental medicine/American College of Occupational Environmental Medicine,* Vol. 58, No. 8, 2016, p. 828.
[260] Songer, T. J., and R. R. Dorsey. High risk characteristics for motor vehicle crashes in persons with diabetes by age.In *Annual Proceedings/Association for the Advancement of Automotive Medicine, No. 50*, Association for the Advancement of Automotive Medicine, 2006. p. 335.

[261] Dobbs, B. M., E. P. Wodzin, and M. Vegega. Medical conditions and driving: a review of the literature (1960-2000).In, National Highway Traffic Safety Administration, National Highway Traffic Safety Administration, 2005.
[262] Khorashadi, A., D. Niemeier, V. Shankar, and F. Mannering. Differences in rural and urban driver-injury severities in accidents involving large-trucks: an exploratory analysis. *Accident Analysis & Prevention,* Vol. 37, No. 5, 2005, pp. 910-921.
[263] Chang, L.-Y., and J.-T. Chien. Analysis of driver injury severity in truck-involved accidents using a non-parametric classification tree model. *Safety science,* Vol. 51, No. 1, 2013, pp. 17-22.
[264] Laude, J. R., and M. T. Fillmore. Simulated driving performance under alcohol: effects on driver-risk versus driver-skill. *Drug and alcohol dependence,* Vol. 154, 2015, pp. 271-277.
[265] Penning, R., J. L. Veldstra, A. P. Daamen, B. Olivier, and J. C. Verster. Drugs of abuse, driving and traffic safety. *Current drug abuse reviews,* Vol. 3, No. 1, 2010, pp. 23-32.
[266] Bunn, T. L., S. Slavova, T. Struttmann, and S. Browning. Sleepiness/fatigue and distraction/inattention as factors for fatal versus nonfatal commercial motor vehicle driver injuries. *Accident Analysis & Prevention,* Vol. 37, No. 5, 2005, pp. 862-869.
[267] Hao, W., C. Kamga, X. Yang, J. Ma, E. Thorson, M. Zhong, and C. Wu. Driver injury severity study for truck involved accidents at highway-rail grade crossings in the United States. *Transportation research part F: traffic psychology behaviour,* Vol. 43, 2016, pp. 379-386.
[268] Williamson, A., D. A. Lombardi, S. Folkard, J. Stutts, T. K. Courtney, and J. L. Connor. The link between fatigue and safety. *Accident Analysis & Prevention,* Vol. 43, No. 2, 2011, pp. 498-515.
[269] McCartt, A. T., J. W. Rohrbaugh, M. C. Hammer, and S. Z. Fuller. Factors associated with falling asleep at the wheel among long-distance truck drivers. *Accident Analysis & Prevention,* Vol. 32, No. 4, 2000, pp. 493-504.
[270] Chen, F., S. J. A. A. Chen, and Prevention. Injury severities of truck drivers in single-and multi-vehicle accidents on rural highways. Vol. 43, No. 5, 2011, pp. 1677-1688.
[271] National Center for Statistics and Analysis. Traffic Safety Facts, Speeding.In, Washington, DC: National Highway Traffic Safety Administration., 2019.
[272] Peng, Y., and L. N. Boyle. Commercial driver factors in run-off-road crashes. *Transportation Research Record,* Vol. 2281, No. 1, 2012, pp. 128-132.
[273] Ahmed, M. M., R. Franke, K. Ksaibati, and D. S. Shinstine. Effects of truck traffic on crash injury severity on rural highways in Wyoming using Bayesian binary logit models. *Accident Analysis & Prevention,* Vol. 117, 2018, pp. 106-113.
[274] National Transportation Safety Board. Wrong-Way Driving- Highway Special Investigation Report.In, 2012.
[275] Chen, F., and S. Chen. Injury severities of truck drivers in single-and multi-vehicle accidents on rural highways. *Accident Analysis & Prevention,* Vol. 43, No. 5, 2011, pp. 1677-1688.
[276] Behnood, A., and F. J. A. m. i. a. r. Mannering. Time-of-day variations and temporal instability of factors affecting injury severities in large-truck crashes. Vol. 23, 2019, p. 100102.
[277] Stuster, J. *Aggressive driving enforcement: evaluations of two demonstration programs*. US Department of Transportation, National Highway Traffic Safety Administration, 2004.
[278] Lemp, J. D., K. M. Kockelman, and A. Unnikrishnan. Analysis of large truck crash severity using heteroskedastic ordered probit models. *Accident Analysis & Prevention,* Vol. 43, No. 1, 2011, pp. 370-380.
[279] Federal Motor Carrier Safety Administration. *DOT Medical Exam and Commercial Motor Vehicle Certification*, 2019.
[280] ---. *Summary of Hours of Service Regulations*, 2020.

[281] Jovanis, P. P., S.-W. Park, K.-Y. Chen, and F. Gross. On the relationship of crash risk and driver hours of service.In *2005 International Truck and Bus Safety and Security Symposium, Alexandria, VA*, 2005.
[282] Chen, C., and Y. Xie. The impacts of multiple rest-break periods on commercial truck driver's crash risk. *Journal of safety research,* Vol. 48, 2014, pp. 87-93.
[283] European Commission. *Driving time and rest periods*, 2020.
[284] Jo, J., S. J. Lee, J. Kim, H. G. Jung, and K. R. Park. Vision-based method for detecting driver drowsiness and distraction in driver monitoring system. *Optical Engineering,* Vol. 50, No. 12, 2011, p. 127202.

VITA

Amin Mohammadnazar was born in Tehran and raised in Isfahan, Iran. In 2014, he graduated from the Isfahan University Technology, Iran, with a BS in Civil Engineering. In 2017, Amin graduated with his Master's degree in Transportation Engineering from Iran University of Science and Technology, Iran. His thesis was titled "A Probabilistic Model for Pedestrian Gap Acceptance Behavior at Uncontrolled Midblock Crosswalks." He joined the University of Tennessee, Knoxville in 2018 to pursue his Ph.D. in Civil and Environmental Engineering-Transportation and Master in Statistics. In 2021, he received a doctoral degree in Civil Engineering with a concentration in Transportation Engineering. As a Ph.D. student, Amin received several scholarships and awards including the Lifesavers Scholarship, TSITE Student Paper Competition Award, HSIS Excellence in Highway Safety Data paper competition award, and Graduate Student Senate Travel Award. His research covers a wide range of topics related to traffic safety, driving behavior, connected and automated vehicles, fuel economy, and geospatial modeling. Specifically, his research focuses on harnessing emerging data sources such as CAV data and naturalistic driving data and integrating them with conventional safety to analyze driving behavior.